OFFICE OF CIVILIAN RADIOACTIVE WASTE MANAGEMENT
SPECIAL INSTRUCTION SHEET

1. QA: QA

Complete Only Applicable Items

This is a placeholder page for records that cannot be scanned.

2. Record Date	3. Accession Number
09/28/2001	MOL.20011015.0020
4. Author Name(s)	5. Author Organization
LELAND MONTIERTH	N/A

6. Title/Description
INTACT AND DEGRADED MODE CRITICALITY CALCULATIONS FOR THE CODISPOSAL OF FORT SAINT VRAIN HTGR SPENT NUCLEAR FUEL IN A WASTE PACKAGE

7. Document Number(s)	8. Version Designator
CAL-EDC-NU-000007	REV. 00

9. Document Type	10. Medium
REPORT	OPTIC/PAPER

11. Access Control Code
PUB

12. Traceability Designator
DC# 28746

13. Comments
THIS IS A ONE-OF-A-KIND DOCUMENT DUE TO THE GRAY SHADED AREAS ENCLOSED AND CAN BE LOCATED THROUGH THE RPC.

OFFICE OF CIVILIAN RADIOACTIVE WASTE MANAGEMENT
CALCULATION COVER SHEET

1. QA: QA
Page: 1 Of: ~~70~~ 71 9/28/01

2. Calculation Title

Intact and Degraded Mode Criticality Calculations for the Codisposal of Fort Saint Vrain HTGR Spent Nuclear Fuel in a Waste Package

3. Document Identifier (including Revision Number)

CAL-EDC-NU-000007 REV 00

4. Total Attachments	5. Attachment Numbers – Number of pages in each
2	I-Compact Disc, II-14

	Print Name	Signature	Date
6. Originator	Leland Montierth	Leland Montierth	9/28/01
7. Checker	John Scaglione	John Scaglione	9/28/01
8. Lead	Abdelhalim A. Alsaed	Abdelhalim A. Alsaed	9/28/01

9. Remarks

MCNP input and output files are included in Attachment I on compact disk. Attachment II is a list of each file's attributes on the compact disk.

Revision History

10. Revision No.	11. Description of Revision
00	Initial issue

CONTENTS

Page

1. PURPOSE 6
2. METHOD 6
3. ASSUMPTIONS 7
4. USE OF COMPUTER SOFTWARE AND MODELS 9
   - 4.1 SOFTWARE 9
     - 4.1.1 MCNP 9
   - 4.2 MODELS 9
5. CALCULATION 10
   - 5.1 WASTE PACKAGE COMPONENTS DESCRIPTION 11
     - 5.1.1 FSV Spent Nuclear Fuel 11
     - 5.1.2 Description of DOE SNF Canister 15
     - 5.1.3 High-Level Waste Glass Pour Canister 15
     - 5.1.4 Waste Package Description 15
   - 5.2 MATERIALS DESCRIPTION 18
   - 5.3 FORMULAS 22
   - 5.4 INTACT MODE CRITICALITY CALCULATIONS 23
     - 5.4.1 FSV Fuel Compositions and Other Modeling Details 23
   - 5.5 DEGRADED MODE 25
     - 5.5.1 Waste Form Degrades Within the Intact SNF Canister 26
       - 5.5.1.1 Intact C Block with Some Degradation of the Fuel Compacts 26
       - 5.5.1.2 Degraded C Block with Intact Fuel Compacts 29
       - 5.5.1.3 Degraded C Block and Degraded Fuel Compacts 32
     - 5.5.2 Internal Components of the Waste Package Degraded (Outside SNF Canister) 32
       - 5.5.2.1 Intact SNF Canister with Contents Either Intact or Degraded 33
       - 5.5.2.2 Degraded SNF Canister with Non-reacted Pre-breach Clay 33
     - 5.5.3 All Components Degrade at the Same Time 37
6. RESULTS 39
   - 6.1 INTACT MODE 39
     - 6.1.1 Comparison of FSV Fuel Compositions and Other Modeling Details 39
   - 6.2 DEGRADED MODE 42
     - 6.2.1 Inner Component of the SNF Canister Degrades First 42
       - 6.2.1.1 Partial Degradation of Fuel Compacts Before the C Block 43
       - 6.2.1.2 C Block Degrades Before the Fuel Compacts 48
       - 6.2.1.3 C Blocks and Fuel Compacts Degrade Before SNF Canister 52
     - 6.2.2 Outer Components of the WP Degrade (Outside SNF Canister) 54

CONTENTS (Continued)

Page

6.2.2.1 Intact SNF Canister with Contents Either Intact or Degraded Surrounded by Pre-breach Clay in the WP 54
6.2.2.2 Intact and Degraded Fuel Components Surrounded by Products of Degraded SNF Canister with Non-reacted Pre-breach Clay 56
6.2.3 Waste Package Components Degrade at the Same Time 65

7. REFERENCES 68
7.1 DOCUMENTS CITED 68
7.2 CODES, STANDARDS, REGULATIONS, AND PROCEDURES 69
7.3 SOURCE DATA 70

8. ATTACHMENTS 71

FIGURES

Page

1. Cross-section of Standard FSV Fuel Element 12
2. Cross-sectional Sketch of a FSV Element in the DOE SNF Canister. 16
3. Cross-sectional View of 5-HLW/DOE Spent Fuel-Long Codisposal WP 17
4. Cross-sectional View of Intact SNF Canister Inside the WP 24
5. Fuel Assembly where Fissile Material is in Solution in the Lower Half of the Coolant/Void Channels of the Assembly 27
6. A Portion of the Fuel from the Assembly is in the Bottom of the SNF Canister 28
7. Similar Case to that Shown in Figure 6 but the Assembly is Rotated 30° 29
8. Tilting of the Canister Simulated by Removing Fuel From the Upper Portion of the Assembly and Redepositing At Canister End 29
9. Assembly Has Broken into 6 Pieces, Each Separated by a 1 cm Gap 30
10. C Assembly Block Has Broken into Rubble and the Fuel Compacts Remain Axially Aligned Comprising "Fuel Pins" 31
11. An Alternative Configuration of "Fuel Pins" than that Shown in Figure 10 31
12. Contents of SNF Canister Have Degraded Forming Separate Layers of Fuel, Carbon and Water Inside the Canister 32
13. Cross-sectional View of an Intact SNF Canister Centered in Clay Formed from the Degradation of the Contents of the WP 33
14. Intact Assembly Surrounded by Clay in the WP 34
15. Intact Assembly Surrounded by Goethite Trapped in Pre-breach Clay in the WP 35
16. Loose "Fuel Pins" at the bottom of the WP Surrounded by a Mixture of Goethite, Carbon, Water and Pre-breach Clay 36
17. Cylinder of Loose "Fuel Pins" Surrounded by Goethite, Carbon, and Water Trapped in the Pre-breach Clay in the WP 36
18. Layers of Completely Degraded Fuel Compacts, Goethite, Carbon, and Pre-breach Clay in the WP 37
19. "Fuel Pin" Configurations Investigated in Table 20 51

TABLES

Page

1. Composition of Fuel w/ High Fissile Loads and "As Modeled" Assemblies 14
2. Composition and Density of Stainless Steel 304L 18
3. Composition and Density of Carbon Block 18
4. Composition and Density of Savannah River Site High-Level Waste Glass 18
5. Composition and Density of Stainless Steel 316L 19
6. Composition and Density of Alloy 22 19
7. Composition and Density of Carbon Steel 516 Grade 70 20
8. Composition and Density of Dry Tuff 20
9. Pre-Breach Clay Compositions[a,b] 20
10. Post-Breach Clay Compositions 21
11. Alternative Post-Breach Clay Composition 21
12. Comparison of Actual FSV Fuel Assemblies with the "As Modeled" Assembly and Other Modeling Details 40
13. Amount of Water Saturation of Voids in the Fuel Compacts and C Fuel Block 40
14. Variations in Positioning of the Various Components in the WP and Other Results 42
15. Dissolved Fuel Redistributed in Coolant/Void Channels of Fuel Assembly 43
16. Degraded Fuel from an End Assembly Re-deposits at Bottom of SNF Canister 45
17. Degraded Fuel from the Entire Length of the Assemblies Re-deposits at Bottom of SNF Canister 46
18. Simulated Tilting of the SNF Canister Fills Volume at End of Stack or Between Assemblies with Fuel 47
19. Intact Fuel Compacts with C Block Broken into Pieces 48
20. Fuel Compacts form "Fuel Pins" in Rubble from Degraded C Blocks 48
21. Results for Completely Degraded Fuel Assemblies with no Mixing of Degraded Materials in Intact SNF Canister 52
22. Results for Completely Degraded Fuel Assemblies with Mixed Degraded Materials in Intact SNF Canister 53
23. Intact SNF Canister Surrounded by Pre-Breach Clay 55
24. Intact Assemblies Surrounded by Goethite and Pre-Breach Clay in the WP 57
25. Fuel Compacts Form "Pins" Piled at the Bottom of the WP Surrounded by Layers of C Rubble, Goethite and Pre-breach Clay 59
26. Fuel Compacts Form Circular or Hexagonal Array of "Pins" Surrounded by Layers of C Rubble, Goethite and Pre-breach Clay in the WP 61
27. Completely Degraded Fuel Compacts, C Rubble, Goethite and Pre-breach Clay Form Layers in the WP 63
28. A Portion of the Fuel Compacts Remain with the Post-breach Clay 65
29. Results for Post-breach Clay where the Contents of the WP are Completely Degraded and Mixed 67

1. PURPOSE

The objective of these calculations is to perform intact and degraded mode criticality evaluations of the Department of Energy's (DOE) Fort Saint Vrain (FSV) commercial High Temperature Gas Reactor (HTGR) spent nuclear fuel. This analysis evaluates codisposal in a 5-Defense High-Level Waste (5-DHLW/DOE SNF) Long Waste Package (WP) (CRWMS M&O 2000c, Attachment V), which is to be placed in a potential monitored geologic repository (MGR). The scope of this calculation is limited to the determination of the effective neutron multiplication factor (k_{eff}) for both intact and degraded mode internal configurations of the codisposal waste package.

These calculations will support the analysis that will be performed to demonstrate the technical viability for disposing of graphite based (FSV) spent nuclear fuel in the potential MGR.

These calculations are associated with the waste package design and is performed in accordance with the *Technical Work Plan For: Department of Energy Spent Nuclear Fuel Work Packages* (Civilian Radioctive Waste Management System Management and Operating Contractor [CRWMS M&O 2000a]). This document is prepared in accordance with the Administrative Procedures AP-3.12Q, *Calculations,* and AP-3.15Q, *Managing Technical Products Inputs*.

2. METHOD

The method to perform the criticality calculations consists of using MCNP Version 4B2 (CRWMS M&O 1998a, CRWMS M&O 1998b) to calculate the effective neutron multiplication factor of the codisposal waste package. The calculations are performed using the continuous-energy cross section libraries, which are part of the qualified code system MCNP 4B2 (CRWMS M&O 1998a, CRWMS M&O 1998b). All calculations are performed with a most reactive fissile concentration that bounds the beginning-of-life (BOL) and end-of-life (EOL) FSV fuels.

The control of the electronic management of data was accomplished in accordance with methods specified in the technical work plan (CRWMS M&O 2000a).

3. ASSUMPTIONS

3.1 For the degraded mode criticality calculations, it is assumed that the iron in the stainless steel degrades to goethite (FeOOH) rather than hematite (Fe_2O_3). The basis of this assumption is that it is conservative to consider goethite rather than hematite since hydrogen (a moderator) is a component of goethite. All the other constituents of stainless steel are neglected since they are neutron absorbers, and hence their absence provides a conservative (higher) value for the k_{eff} of the system. This assumption is used throughout Section 5.

3.2 Ba-138 cross sections are used instead of Ba-137 cross sections in the MCNP input since the cross sections of Ba-137 are not available in the Waste Package Project cross section libraries. The basis of this assumption is that it is conservative since the thermal neutron capture cross section and the resonance integral of Ba-137 (5.1 and 4 barn, respectively [Parrington et al. 1996, p. 34]) are greater than the thermal neutron capture cross section and the resonance integral of Ba-138 (0.43 and 0.3 barn, respectively [Parrington et al. 1996, p. 34]). This assumption is used throughout Section 5.

3.3 A most reactive fissile concentration is used for the FSV fuel that is shown (Table 12) to bound fuel compositions for actual fuel assemblies. These selected fuel compositions use the larger fissile masses from either the beginning-of-life (BOL) or end-of-life (EOL), neglect any U-238, and use EOL values for Th-232. The basis of this assumption is that the selected compositions are conservative since they maximize the fissile isotope content while minimizing the effect of neutron absorbers. Therefore, the fuel composition used for the FSV fuel is even more conservative since it bounds these actual (conservative) compositions. This assumption is used throughout Section 5.

3.4 The length of the fuel in the fuel assemblies is assumed to be the same as the length of the assemblies rather than the actual length of the fuel holes, which is slightly smaller. This gives a larger void fraction and thus the potential for more water in the fuel. The basis of this assumption is that using this length is conservative since it is shown (Table 13) that it is more reactive to have more water in the fuel, i.e., this gives a larger value of k_{eff} for the system. This assumption is used throughout Section 5.

3.5 Al cross sections are used instead of Zn cross sections in the MCNP input since the cross sections of Zn are not available in the Waste Package Project cross-section libraries. The basis of this assumption is that it is conservative since the thermal neutron capture cross section and the resonance integral of Zn (Parrington et al., 1996, p. 24) are greater than the thermal neutron capture cross section and the resonance integral of Al (Parrington et al., 1996, p. 21). This assumption is used throughout Section 5.

3.6 It is assumed that the density of the SRS HLW glass is 2.85 g/cm^3. The density of glass may vary between 2.56 and 2.75 g/cm^3 (Plodinec and Marra 1994, p. 22). The rationale for this assumption is that height glass density provides conservative isotope mass.

3.7 It is assumed that the chemical composition provided in CRWMS M&O (1999, p. 7) is representative of HLW glass. The rational for this assumption is that similar chemical composition are provided for projected HLW glass to be produced at Savannah River Site (Fowler et al. 1995, p. 4).

4. USE OF COMPUTER SOFTWARE AND MODELS

4.1 SOFTWARE

4.1.1 MCNP

The MCNP code is used to calculate the k_{eff} of the codisposal waste package. The software specifications are as follow:

- Software name: MCNP
- Software version/revision number: Version 4B2LV
- Software tracking number (computer software configuration item [CSCI]): 30033 V4B2LV
- Computer type: Hewlett Packard (HP) 9000 Series Workstations
- Computer processing unit number: Software is installed on the INEEL workstation "bigdog" whose INEEL Tag number is 336829

The input and output files for the various MCNP calculations are documented in Attachment I, (Attachment II gives the list of the files on Attachment I). The calculation files described in Sections 5 and 6 are such that an independent repetition of the software use may be performed.

The MCNP software used is: (a) appropriate for the application of research reactor k_{eff} calculations, (b) used only within the range of validation as documented in CRWMS M&O (1998a), (c) obtained from the Software Configuration Management in accordance with appropriate procedures.

4.2 MODELS

None used.

5. CALCULATION

This section describes the calculations performed to calculate the k_{eff} of an intact and a degraded waste package containing high-level waste material and FSV spent nuclear fuel. Section 5.1 describes the waste package. Section 5.2 gives the composition of the materials used in this calculation. The basic formulas used in this calculation are listed in Section 5.3. The different intact configurations of a waste package are outlined in Section 5.4. Section 5.5 describes calculations performed to characterize the degraded configurations of a waste package. The MCNP input and output files developed for this section are presented in Attachment I. The spreadsheet used to prepare the MCNP input files is given in Attachment I, file "fsv_cals.xls." The results of the calculations are presented in Section 6.

The Savannah River Site high-level waste glass degraded (pre-breach) compositions are from CRWMS M&O (2000b) and BSC (2001). The composition from CRWMS M&O (2000b) is for the Shippingport LWBR fuel. Since these fuels (Shippingport and FSV) share the same WP externals, i.e., components external to the SNF canister, the pre-breach compositions would be the same. The Savannah River Site high-level waste glass composition and density are from CRWMS M&O (1999a) and Stout and Leider (1991), respectively. The Savannah River Site high-level waste glass canister dimensions are from Taylor (1997). This information is unqualified and is therefore considered to-be-verified.

Avogadro's number is from Parrington et al. (1996). Atomic weights are from Parrington et al. (1996) and Audi and Wapstra (1995).

The description of the FSV fuel is from the *Fort Saint Vrain HTGR (Th/U carbide) Fuel Characteristics for Disposal Criticality Analysis* report (Taylor 2001). All fuel-related information is from this reference unless otherwise noted.

The tuff composition and the tuff density are taken from a previous calculation (CRWMS M&O 2001, Attachment II, spreadsheet "Tuff Composition.xls").

This calculation is based in part on unqualified information such as that in Taylor (2001). However, the unqualified information is only used to determine the bounding values and items that are important to safety for the fuel group. The fuel group is identified by the National Spent Nuclear Fuel Program, and a 'representative' fuel type within that group is used to establish limits, e.g. burnup, fissile content, weights, dimensions. Therefore, the input values used to evaluate the codisposal viability of FSV spent nuclear fuel do not constitute information that has to be qualified prior to use of any results from this calculation for input into documents supporting procurement, fabrication, or construction. They merely establish the bounds for acceptance. Since the input values are not relied upon directly to address radiological safety and waste isolation issues, nor do the design inputs affect a system characteristic that is critical for satisfactory performance, the information does not need to be controlled as to-be-verified.

The number of digits in the values cited herein may be the result of a calculation or may reflect the input from another source; consequently, the number of digits should not be interpreted as an indication of accuracy.

The metric units used in this document are calculated using the English units as given in Taylor (2001). The differences that might exist between the metric units calculated and the metric units cited in Taylor (2001) have no effect on the calculation and should not be interpreted as an indication of accuracy.

5.1 WASTE PACKAGE COMPONENTS DESCRIPTION

5.1.1 FSV Spent Nuclear Fuel

FSV fuel consists of small particles (spheres of the order of 0.5 mm diameter.) of uranium carbide. The particles are coated with multiple, thin layers of pyrolytic carbon (pyrocarbon) and silicon carbide, which serve as tiny pressure vessels to contain fission products and the Th/U carbide matrix. In the FSV fuel elements, the coated particles are bound in a carbonized matrix, which form fuel pins or 'compacts' that are loaded into large hexagonal graphite prisms. The large graphite prisms (or blocks) are the physical forms that will be loaded into the SNF standard canisters.

The FSV fuel element is hexagonal in cross-section with dimensions of 360.60 mm (14.172 in.) across flats by 792.988 mm (31.22 in.) high (Taylor 2001, p. 12). The active fuel is contained in an array of small-diameter holes, which are parallel with the coolant channels, and occupy alternating positions in a triangular array within the graphite structure. The fuel holes, 12.70 mm (0.50 in.) in diameter, are drilled from the top face of the element to within about 7.62 mm (0.3 in.) of the bottom face, and cemented graphite plugs 12.7 mm (0.5 in.) long seal the tops of the fuel holes. The fuel compacts, 12.5 mm (0.49 in.) in diameter, containing the coated fuel particles are stacked within the holes. The fuel holes and coolant channels are distributed in a triangular array with a pitch spacing of about 18.796 mm (0.74 in.) (Taylor 2001, pp. 12-13), which gives a unit cell pitch of 3.2556 cm. A cross-sectional view of the FSV assembly is shown in Figure 1. (Note that the terms fuel assembly and fuel element are used interchangeably in this report.)

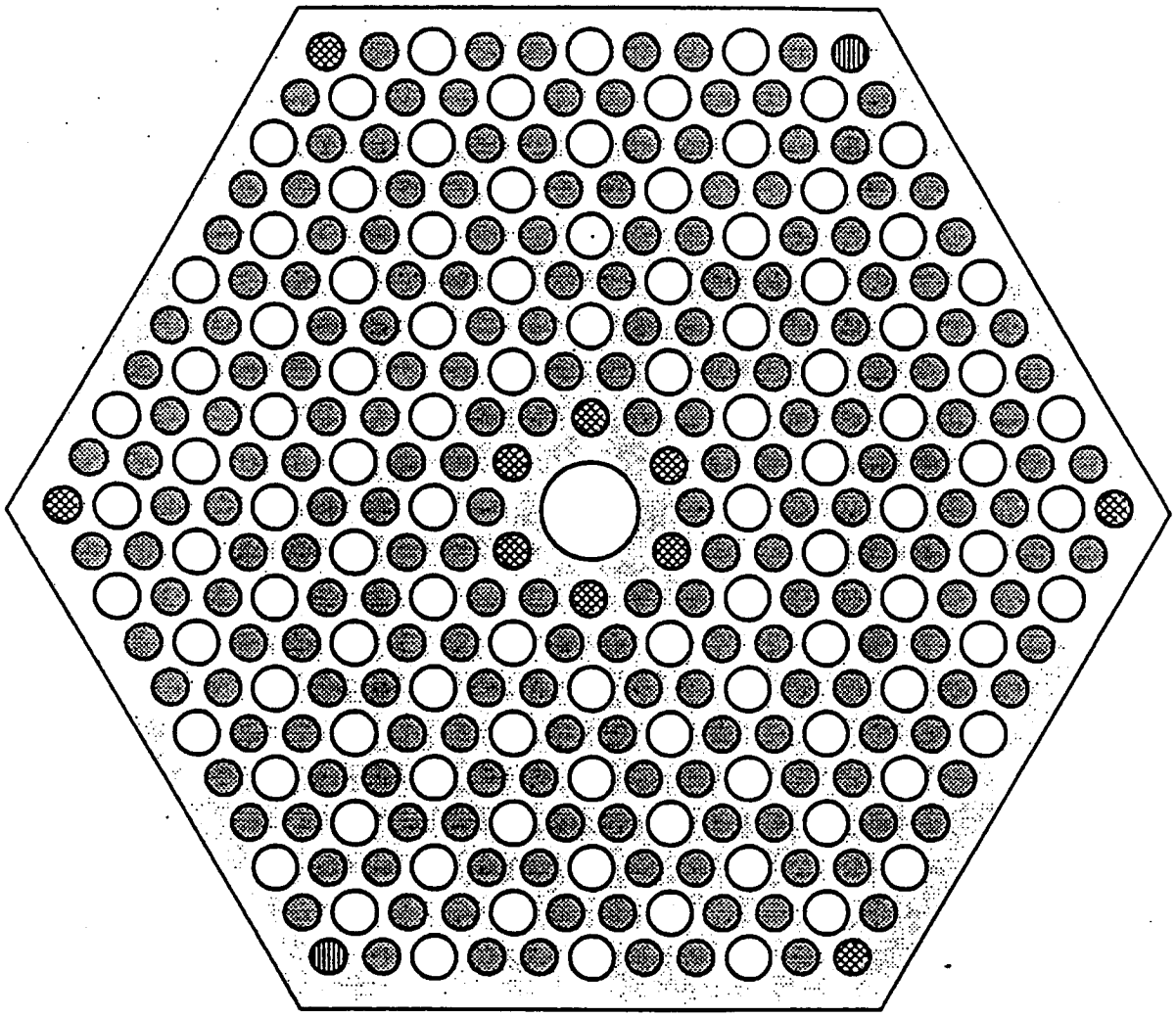

Figure 1. Cross-section of Standard FSV Fuel Element

(Taylor 2001, p. 16)

There are four main types of FSV fuel elements: standard elements, control elements, bottom control elements, and neutron source elements with the neutron sources removed (Taylor 2001, p.11). All four types are made of graphite and have the same external dimensions but differ in weight, number of coolant holes, fuel holes, and neutron source holes. No metallic components are present in the fuel elements.

The standard elements have 12.7 mm (0.5 in.) diameter holes in each of their six corners for possible insertion of burnable poison rods. The burnable poison rods are 50.8 mm (2.00 in) long and 11.43 mm (0.45 in.) in diameter, and are made of boron carbide particles in a carbon matrix. They are added as required and did not always completely fill the hole; no credit was taken for their presence in any of the calculations.

The fuel blocks are made of nuclear grade graphite, type H-327 (needle-coke graphite) or type H-451 (near-isotropic graphite). The densities of types H-327 and H-451 are 1.72 and 1.75 g/ cm^3, respectively (Taylor 2001, p.13). Using these densities and a reported amorphous carbon density (maximum) of 2.1 g/cm^3 (Taylor 2001, p. 17), the porosity of the fuel blocks is calculated to be 16.67% and 18.10% for the H-451 and H-327 materials, respectively. A calculated value for the total void space within the fuel channels is found to be 50.76% (Taylor 2001, p.17).

As discussed in Taylor (2001, pp. 18-20), due to the different reported maximum fissile loadings reported and since the EOL fuel contains ^{233}U, four different most reactive fuel concentrations are considered. Each of the four fuel concentrations is modeled in MCNP, but the fourth item was the basis for all calculations after it was shown to be most reactive. These are repeated here on a per element basis.

1. BOL ^{235}U = 1256.61 gm, EOL ^{233}U = 135.79 gm (from Public Service of Colorado [PSC] database) (Taylor 2001, Appendix B)
2. BOL ^{235}U = 1172.0 gm, EOL ^{233}U = 239.63 gm (from PSC database); there should be a 'defacto' ^{238}U composition of at least 73.8 gm (from adjacent U group loading in database) since ^{235}U was never available in the 100% enrichments inferred in the PSC database
3. BOL ^{235}U = 1168 gm, EOL ^{233}U = 248.95 gm (from PSC database); use a 'defacto' ^{238}U composition of at least 73.8 gm
4. Total U = 1485.0 gm @ 93.15 % enrichment (from FSV specification); use 1485.0 gm BOL ^{235}U as maximum case and EOL $^{233}U + ^{238}U$ = 0.0 gm

The chemical composition for a typical fuel compact other than U and Th is 0.8 g Si (as SiC) and 4.1 g carbide (matrix and coating). (Taylor 2001, p.23)

When combined, these fissile masses and masses per fuel compact give the compositions used for the different fuel elements which are summarized in Table 1 (these values are calculated in Attachment I, spreadsheet "fsv_cals.xls," sheet "Intact"). Some values, as indicated in the table, are at beginning-of-life (BOL) while others are at end-of-life (EOL). Also given in the following table is a composite depiction of both reported (proceeding 'four fuel concentrations and 'Taylor

2001, Appendix B) and calculated values for compositions used in a degradation scenario where the C matrix binder material is neglected.

Table 1. Composition of Fuel w/ High Fissile Loads and "As Modeled" Assemblies

Element/Isotope	Fuel Element 1-4242	Fuel Element 1-1426	Fuel Element 1-0466	[c] Proposed Fuel Composition (as Modeled in MCNP)
U-235 (BOL) (g)	1256.61	1172	1168	1485
Th (EOL) (g)	10855.82	11084.9	11079.42	10789.97
Si (g)	2504	2504	2504	2504
C (total) (g)	27306.6	27165.2	27174.8	[a] 27221.0
U-233 (EOL) (g)	135.79	239.63	248.95	-
Pu-239 (EOL) (g)	2.39	2.39	2.23	[d] 2.59
[b] Density (g/cm^3)	1.9874	1.9876	1.9876	1.9911

NOTES:
[a] Total C content is 17170.5 g if C matrix binder is neglected.
[b] Densities calculated in Attachment I, spreadsheet "fsv_cals.xls," sheet "Intact."
[c] Fuel void fractions of 51.5% and 50.0% are used when the fuel length is modeled as being the same as the assembly length and being its actual length, respectively, Attachment I, spreadsheet "fsv_cals.xls," sheet "Intact."
[d] Maximum EOL Pu-239 content for any FSV assembly, see Taylor (2001, Appendix B).

Post-irradiation destructive examination was conducted on selected fuel compacts from a single fuel element, 1-0743. The fuel element experienced a burnup of 6.2% fissile and 0.3% fertile (from U-233 during the transmutation of Th-232); this represents an unaccounted for conservatism in the MCNP calculations. The analysis reported ~ 0.3% of the fissile and 0.2% of the fertile microspheres were failed. These failures were due to manufacturing defects such as no coating, cracks, thin coatings, etc. About 3% of the compacts were broken; the disassembly process most likely broke the majority of them. (Taylor 2001, p.24) The failure percentages reported formed a basis for establishing the quantity of fissile material mobility in a degraded waste package.

No credit is taken for the fuel burnup, i.e., fuel is assumed to be fresh (non-irradiated). A fuel void fraction of 51.1% is used except where the fuel is modeled as having its actual length (see Table 1). Unless otherwise specified, the C blocks are type H-327 and the WP is reflected by water.

5.1.2 Description of DOE SNF Canister

The description of the 15-ft DOE SNF canister (also referred to as the 18-in.-diameter DOE SNF canister) is taken from DOE (1999, p. 5, A-2, and A-3). The DOE SNF canister is a right circular cylinder made of stainless steel pipe (Type 316L or UNS S31603) with an outside diameter of 457.2 mm (18 in.) and a wall thickness of 9.525 mm (0.375 in.). A nominal internal length of the DOE SNF canister used for fuel loading is 411.7086 cm (162.09 in.); minimum length dimension is 411.5 cm (162.0 in.) (DOE 1999, Appendix A, Dwg. 507692). (Note that this nominal length is insignificantly different from the minimum length.) The top and bottom carbon steel (Carbon Steel 516 Grade 70) impact plates are 50.8 mm (2.0 in.) thick at the centers. Dished heads seal the ends of the DOE SNF canister. The DOE SNF canister pipe extends several inches beyond the dished heads on each end to give a maximum external length of 456.9968 cm (179.92 in.).

The 15-foot canister is capable of a maximum load of five fuel elements stacked axially. Taking into consideration the small axial and radial gaps between the assemblies and the canister and, the interlocking features of FSV fuel elements, no canister internals are needed within the package. A cross-sectional view of a FSV fuel element stack inside the DOE SNF canister is shown in Figure 2.

5.1.3 High-Level Waste Glass Pour Canister

There is no long Savannah River Site high-level waste (HLW) glass canister. Therefore, the expected Hanford 15-foot high-level waste glass canister is used in the FSV waste package. Since the specific composition of the Hanford high-level waste glass has not yet been specified, it was assumed to be the same as the Savannah River Site glass composition. The Hanford 15-foot high-level waste glass canister is a 4,572 mm long stainless steel Type 304L canister with an outer diameter of 610 mm (24.00 in.) (Taylor, 1997). The wall thickness is 10.5 mm. These parameters are the same as the SRS canister, except that it is longer. The maximum loaded canister weight is 4,200 kg and the fill volume is 87%. (Taylor, 1997)

5.1.4 Waste Package Description

The codisposal waste package contains five HLW glass pour canisters spaced radially around an 18 in. DOE SNF canister, see Figure 3 (CRWMS M&O 2000c, pp. 30-32 and Attachment V). The waste package barrier materials are typical of those used for commercial spent nuclear fuel waste containers. The inner barrier shell is composed of 50 mm of Stainless Steel 316 (SA-240 S31600) and serves as a corrosion allowance material. The outer barrier shell is composed of 25 mm of Nickel Alloy (Alloy 22, SB-575 N06022) and serves as a corrosion resistant material. The outside diameter of the waste container is 2030 mm and the outer length is 5217 mm. The inner barrier lids are 105 mm thick and the outer barrier lids are 25 mm thick. There is a 30 mm thick closure lid gap between the upper inner and outer barrier lids. Note that some of the details concerning the lids are simplified, e.g., a 1 cm flat closure lid and 3 cm gap are neglected for the upper lid.

The DOE SNF canister is placed in a 31.75 mm (1.25-in.) -thick carbon steel (ASME SA 516 K02700) support tube with a 565 mm (22.244 in.) nominal outer diameter. The support tube is connected to the inside wall of the codisposal WP by web-like carbon steel (ASME SA 516 K02700) support plates that form five emplacement positions for the HLW glass pour canisters equally spaced in angle about the center support tube. The support tube and plates are 4607 mm (181.3780 in.) long.

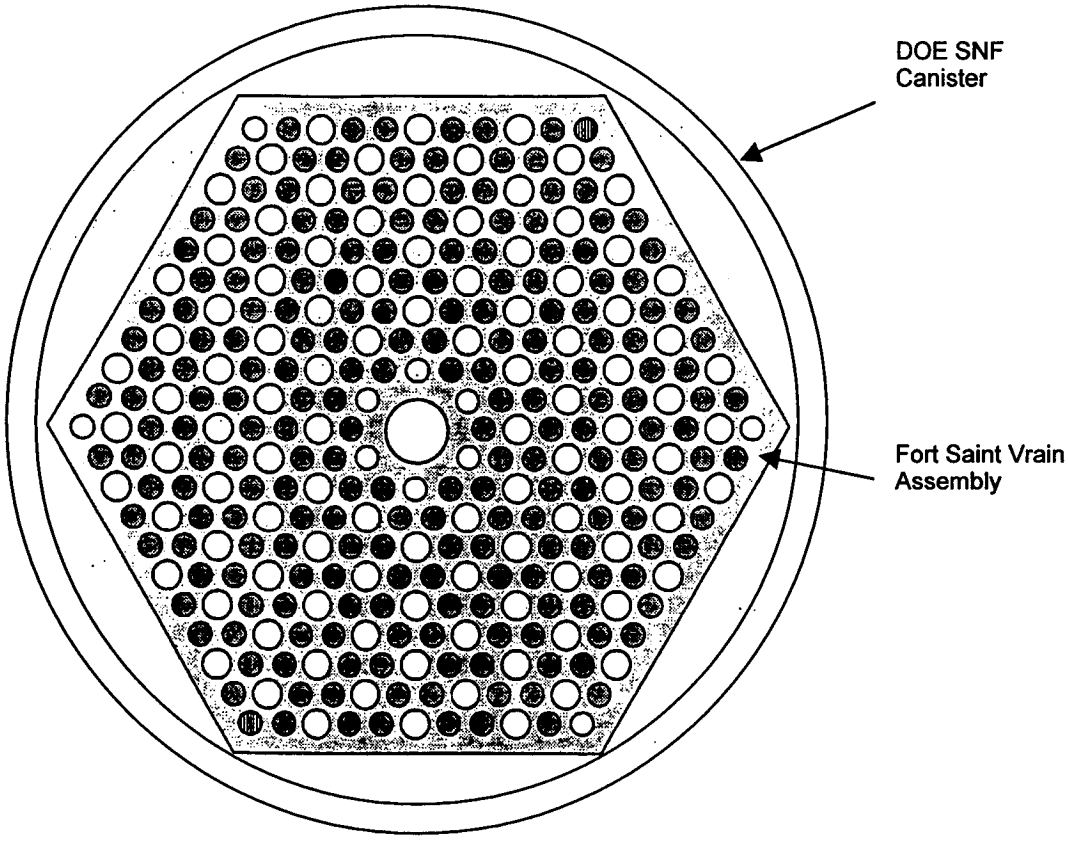

Figure 2. Cross-sectional Sketch of a FSV Element in the DOE SNF Canister.

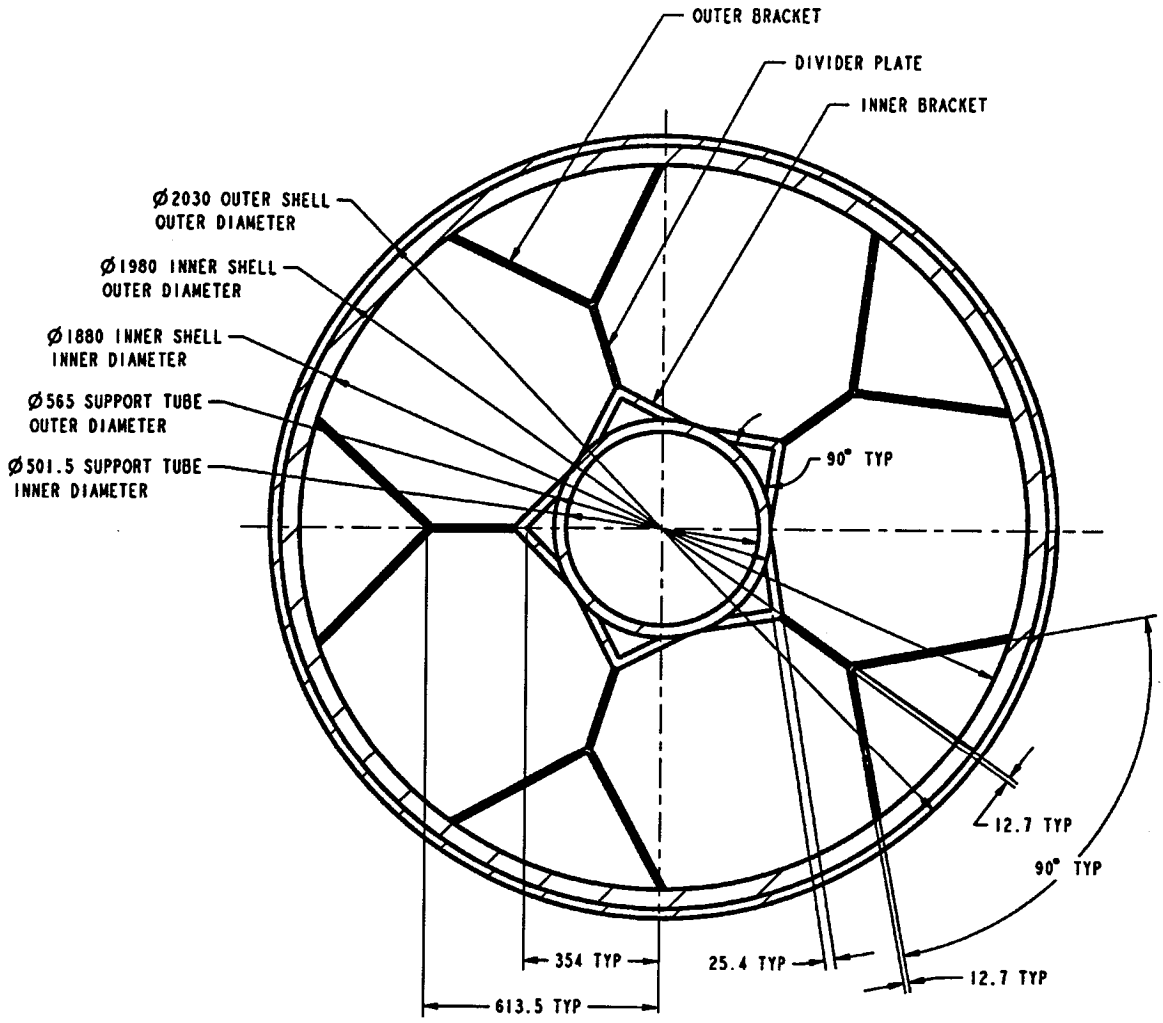

NOTE: TYP = typical; dimensions in mm

Figure 3. Cross-sectional View of 5-HLW/DOE Spent Fuel-Long Codisposal WP

(CRWMS M&O 2000c, Attachment V, p. V-1)

5.2 MATERIALS DESCRIPTION

Tables 2 through 11 give the composition of the materials used in this calculation. The number densities used in the inputs are calculated in Attachment I, spreadsheet "fsv_cals.xls."

Table 2. Composition and Density of Stainless Steel 304L

Element	Composition (wt %)[a]	Value Used (wt %)
C	0.030 (max)	0.030
Mn	2.000 (max)	2.000
P	0.045 (max)	0.045
S	0.030 (max)	0.030
Si	0.750 (max)	0.750
Cr	18-20	19.000
Ni	8-12	10.000
N	0.100 (max)	0.100
Fe	Balance	68.045
Density [b] = 7.94 g/cm^3		

NOTES: [a] ASTM A 240/A 240M-99b, p. 2.
[b] ASTM G 1-90, Table X1.1.

Table 3. Composition and Density of Carbon Block

Element	Composition (wt %)	Value Used (wt %)
C	100	100
Density = 1.75 and 1.72 g/cm^3 for Types H-451 and H-327, respectively Void fraction=0.1667 and 0.1810 for Types H-451 and H-327, respectively		

NOTE: Void fractions [=1 - (density / (theoretical density))] are calculated in Attachment I, spreadsheet "fsv_cals.xls," sheet "Intact."

Table 4. Composition and Density of Savannah River Site High-Level Waste Glass

Element / Isotope	Composition[a] (wt %)	Element / Isotope	Composition[a] (wt %)
O	4.4770E+01	Ni	7.3490E-01
U-234	3.2794E-04	Pb	6.0961E-02
U-235	4.3514E-03	Si	2.1888E+01
U-236	1.0415E-03	Th	1.8559E-01
U-238	1.8666E+00	Ti	5.9676E-01
Pu-238	5.1819E-03	Zn[d]	6.4636E-02
Pu-239	1.2412E-02	B-10	5.9176E-01
Pu-240	2.2773E-03	B-11	2.6189E+00
Pu-241	9.6857E-04	Li-6	9.5955E-02
Pu-242	1.9168E-04	Li-7	1.3804E+00
Cs-133	4.0948E-02	F	3.1852E-02
Cs-135	5.1615E-03	Cu	1.5264E-01
Ba-137[c]	1.1267E-01	Fe	7.3907E+00
Al	2.3318E+00	K	2.9887E+00

Element / Isotope	Composition[a] (wt %)	Element / Isotope	Composition[a] (wt %)
S	1.2945E-01	Mg	8.2475E-01
Ca	6.6188E-01	Mn	1.5577E+00
P	1.4059E-02	Na	8.6284E+00
Cr	8.2567E-02	Cl	1.1591E-01
Ag	5.0282E-02	—	—
Density[b] at 25 °C = 2.85 g/cm^3			

NOTES: [a] CRWMS 1999a, p. 7.
[b] Stout and Leider 1991, p. 2.2.1.1-4.
[c] See Assumption 3.2.
[d] See Assumption 3.5

Table 5. Composition and Density of Stainless Steel 316L

Element	Composition [a] (wt %)	Value Used
C	0.03 (max)	0.0300
N	0.10 (max)	0.1000
Si	1.00 (max)	1.0000
P	0.045 (max)	0.0450
S	0.03 (max)	0.0300
Cr	16-18	17.0000
Mn	2.00 (max)	2.0000
Ni	10-14	12.0000
Mo	2-3	2.5000
Fe	Balance	65.2950
Density[b] = 7.98 g/cm^3		

NOTES: [a] ASTM A 276-91a, p. 2.
[b] ASTM G 1-90, Table X1.1.

Table 6. Composition and Density of Alloy 22

Element	Composition (wt %)	Value Used
C	0.015 (max)	0.015
Mn	0.50 (max)	0.5
Si	0.08 (max)	0.08
Cr	20-22.5	21.25
Mo	12.5-14.5	13.5
Co	2.50 (max)	2.5
W	2.5-3.5	3.0
V	0.35 (max)	0.35
Fe	2.0-6.0	4.0
P	0.02 (max)	0.02
S	0.02 (max)	0.02
Ni	Balance	54.765
Density = 8.69 g/cm^3		

SOURCE: DTN: MO0003RIB00071.000

Table 7. Composition and Density of Carbon Steel 516 Grade 70

Element	Composition (wt %)	Value Used
C	0.28	0.30
Mn	0.85-1.20	1.025
P	0.035 (max)	0.035
S	0.035 (max)	0.035
Si	0.15-0.40	0.275
Fe	Balance	98.33
Density = 7.85 g/cm^3		

SOURCE: DTN: MO0003RIB00072.000

Table 8. Composition and Density of Dry Tuff

Mineral	Composition (wt %)	Element	Composition (wt %)
SiO_2	76.83	Si	0.359
Al_2O_3	12.74	Al	0.067
FeO	0.84	Fe	0.007
MgO	0.25	Mg	0.002
CaO	0.56	Ca	0.004
Na_2O	3.59	Na	0.027
K_2O	4.93	K	0.041
TiO_2	0.1	Ti	0.001
P_2O_5	0.02	P	0.0001
MnO	0.07	Mn	0.001
—	—	H	0.000
—	—	O	0.492
Density=2.245 g/cm^3			

NOTE: CRWMS M&O (2001, Attachment II spreadsheet "Tuff composition.xls")

Table 9. Pre-Breach Clay Compositions[a,b]

Element	Mass of Element after 59473 Years of Emplacement[c] (kg)	Mass of Element after 53241 Years of Emplacement (kg)
O	1.55E+04	9.67E+03
H	8.07E+01	7.14E+01
Fe	1.98E+04	1.07E+04
Al	3.46E+02	3.36E+02
Ba	[d] 2.16E+01	[d] 2.15E+01
Ca	1.69E+02	8.11E+01
F	2.60E+00	1.04E+00
P	1.27E+01	[d] 5.09E+00
K	1.62E+01	0.00E+00
Mg	5.81E+01	9.05E+01
Mn	4.46E+02	1.67E+02
Na	1.39E+01	0.00E+00
Ni	1.85E+03	[d] 3.87E+02
Si	4.47E+03	3.42E+03
Cr	8.14E+00	8.10E+00
U	2.69E+02	0.00E+00

Total (kg)	4.31E+04	2.50E+04
Density (g/cm^3)	4.23[e]	3.88

NOTES: [a].Clay is formed from DHLW glass degradation.
[b] BSC 2001, p. 56 and CRWMS M&O 2000b, p. 41
[c] Composition same as used for Shippingport LWBR, (CRWMS M&O 2000b, p. 41).
[d] Values vary by one digit in least significant decimal place since masses are calculated from number of moles in reference using isotopic rather than elemental atomic masses.
[e] Value listed in reference is 4.235 which is insignificantly different from value used.

Table 10. Post-Breach Clay Compositions

Element	Mass of Element after 72689 Years of Emplacement (kg)	Mass of Element after 378240 Years of Emplacement (kg)
O	9.93E+03	1.24E+04
Al	3.35E+02	3.35E+02
Ba	2.14E+01	2.13E+01
Ca	6.58E+01	7.02E+01
Cr	8.09E+00	8.08E+00
F	5.51E-01	0.00E+00
Fe	1.13E+04	1.65E+04
H	6.94E+01	7.10E+01
C	0.00E+00	0.00E+00
P	5.41E+00	8.80E+00
Mg	9.93E+01	9.99E+01
Mn	1.82E+02	3.43E+02
Mo	1.60E+01	2.51E+01
Ni	4.18E+02	4.10E+02
Si	3.43E+03	3.53E+03
Th	3.23E+00	5.39E+01
U-235	4.48E-01	7.25E+00
Total (kg)	2.59E+04	3.39E+04
Density (g/cm^3)	3.98	4.16
Remaining Mass of Fuel Compacts (kg)	1.974E+02	0

SOURCE: BSC 2001, p. 59 and Attachment III, file fm2t1011.6o.

Table 11. Alternative Post-Breach Clay Composition

Element	Mass of Element after 74818 Years of Emplacement (kg)
O	9.96E+03
Al	3.35E+02
B	0.00E+00
Ba	2.14E+01
Ca	6.58E+01
Cr	8.09E+00
F	4.80E-01
Fe	1.13E+04
H	6.94E+01
P	5.44E+00
Mg	9.93E+01

Mn	1.84E+02
Mo	1.77E+01
Ni	4.19E+02
Si	3.43E+03
Th	5.39E-01
U-235	7.18E-02
Total (kg)	2.59E+04
Density (g/cm^3)	3.92
Remaining Mass of Fuel Compacts (kg)	0

NOTES: BSC 2001, p. 62 and file fm2i1021.6o.

5.3 FORMULAS

The basic equation used to calculate the number density values for materials composed of one or more elements/isotopes is shown below. It is used in the spreadsheet included in Attachment I, and in the cases described throughout Section 5:

$$N_i = (m_i / m) * \rho * N_a / M_i = (V_i / V) * \rho_i * N_a / M_i = (af)_i * \rho * N_a / M$$

where: N_i is the number density in atoms/(barn*cm) of the ith element/isotope
m_i is the mass in grams of the ith element/isotope in the material
m is the mass in grams of the material; note that $m=\Sigma m_i$
N_a is the Avogadro's number (6.022 E+23 atoms/mole, Parrington et al. 1996, p. 59)
M_i is the atomic mass in g/mole of the ith element (Parrington et al., 1996)/isotope (Audi and Wapstra, 1995)
M is the atomic mass in g/mole of the material
V_i is the volume in cm^3 of the ith element/isotope in the material
V is the volume in cm^3 of the material; note that $V=\Sigma V_i$
ρ_i is the density of the ith element/isotope
ρ is the *density* of the material; note that $\rho=\Sigma\rho_i*(V_i/V)$
$(af)_i$ is the atom fraction of the ith isotope of the element; note that $M=\Sigma(af)_i M_i$

Volumes of cylinder segments (volume = area of circle segment × length of the cylinder) are also calculated throughout Attachment I. The following equation uses an iterative approach, given a specified volume, to solve for the height (h) inside the package. These calculations are based on the equation for the segment of a circle shown below (Beyer 1987, p. 125):

$$\text{Area of a segment of a circle} = \left(R^2 \cos^{-1}\left(\frac{R-h}{R}\right) - (R-h)\sqrt{2Rh-h^2} \right)$$

where: R is the cylinder radius, and
h is the height of the segment.

Alternatively, the height of the displaced volume in a degraded waste package can be calculated with the following parametric formula, that provides a relationship between the area of the segment and the angle θ.

$$\text{Area of a segment of a circle} = R^2\left(\theta - \frac{1}{2}\sin(2\theta)\right)$$

where $h=R^*[1-\cos(\theta)]$ and $0 \le \theta \le \pi$.

5.4 INTACT MODE CRITICALITY CALCULATIONS

In this section, the intact mode of the DOE SNF canister is analyzed. These configurations represent a waste package, which has been breached allowing inflow of water, but the internal components of the waste package are as-loaded, i.e., intact. For most of the calculations the waste package is reflected by water. For the remaining cases (as identified in the comments column of the various 'intact case' tables), the waste package uses a reflective boundary condition (BC) that acts as a mirror for neutrons, i.e., there is no neutron leakage. Use of this reflective boundary condition is conservative since no neutrons leak (escape) from the system. The C block is type H-327 unless otherwise specified. The SNF canister is loaded with 5 FSV fuel assemblies that are axially aligned. Variations of the intact configurations are examined to identify the configuration that results in the highest calculated k_{eff} value within the range of possible conditions.

5.4.1 FSV Fuel Compositions and Other Modeling Details

In this section, k_{eff} for the fuel composition of three actual fuel assemblies is compared with the proposed fuel composition given in Table 1. These actual compositions are a conservative combination of BOL and EOL values as described in Section 5.1.1. A cross-sectional view of the WP is shown in Figure 4. The WP is shown in a horizontal storage position where the effect of gravity on the HLW and SNF canisters is evident, with the FSV assembly centered in the SNF canister. The WP inside components can shift in position, though not significantly, during the loading, transportation and ultimate storage of the WP. Note that there is no basket structure in the SNF canister, and the WP is water reflected.

Modeling of the end structure of the DOE SNF canister incorporated both the impact plate and the dished head as a single piece that serves as a reflector. The curved gap between the two pieces is conservatively modeled as filled with iron.

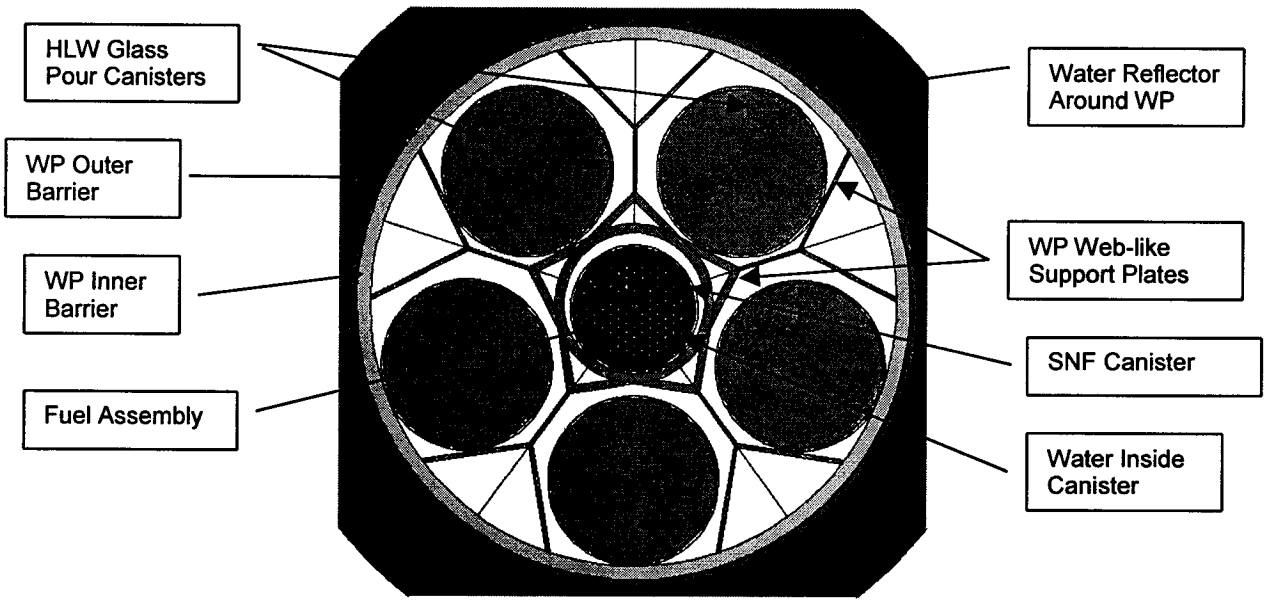

Figure 4. Cross-sectional View of Intact SNF Canister Inside the WP

In the base case, shown in Figure 4, the voids in the fuel and C block are completely filled with water, the fuel length is assumed to be the same as the assembly length and the SNF canister is completely flooded. The fuel composition is given in Table 1 under the column entitled, "As Modeled in MCNP". A comparison is made of k_{eff} for the different fuel compositions given in this table. The purpose of this comparison is to demonstrate that the fuel composition used in the MCNP code is equally or more reactive than the actual fuel assemblies that are assumed to contain the larger amounts of BOL (^{235}U) and EOL (^{233}U and ^{239}Pu) for each fissile isotope and EOL fertile (^{232}Th). For the base case composition, material variations are made that include comparing the two different types of graphite that compose the assembly block, the significance of the Pu in the fuel composition and the effect of whether the outer poison positions of the assembly contain either water or graphite. The amount of thorium in the fuel is reduced (arbitrarily) by 5% to show the sensitivity of the results to thorium content. Other modeling details such as whether the fuel has the same length as the assembly (neglecting the plugs at the end of the fuel holes) or the slightly smaller length of the actual fuel holes and reflector boundary conditions are investigated. These results are shown in Table 12.

Using the base case portrayed in Figure 4, the next set of cases studies whether the intact assembly is over or under moderated. This is accomplished by assuming the voids in the fuel and graphite assembly block contain varying amounts of water (including no water). If the voids are completely filled with water then this is considered to be 100% saturated. Though unphysical, cases where the saturation is greater than 100% are considered since they illustrate the trend of increasing moderation in the fuel assembly. These results are presented in Table 13.

The first six cases for the intact results, given in Table 14, compares the effect of repositioning the various components in the WP. As previously stated, an example of configuration repositioning is seen in Figure 4 where all components in the WP except the assembly have shifted downward due to the effect of gravity, as compared to their as-loaded position (vertical) where the components would be in a more centered position. Repositioning of the components in the WP is done to determine the reactivity in a horizontal waste package orientation. The next two cases investigates the effect of water rather than void in the WP, i.e., whether the WP is flooded or dry. Finally, in the last four cases the number of fuel assemblies stacked in the SNF canister is varied for the base case conditions to determine whether the stack of 5 assemblies is "neutronically" infinite in length.

5.5 DEGRADED MODE

The criticality calculations conducted for the degraded cases are discussed in the following sections. Several configurations are considered. Detailed descriptions of these configurations are given on pages 27 through 37 of CRWMS M&O (1999b). In Section 5.5.1, configurations are analyzed resulting from the degradation scenarios in which the waste form (FSV Reactor fuel) degrades inside the SNF canister (CRWMS M&O 1999b, pp. 27-29). In Section 5.5.2, configurations resulting from the degradation of the high-level waste glass are investigated (see Attachment I, spreadsheet "fsv_cals.xls," sheet "WP" for detailed description of cases) for sensitivity to changing WP parameters. Configurations where all the internal components of the waste package have degraded are discussed in Section 5.5.3 (see Attachment I, spreadsheet "fsv_cals.xls" sheet "Post-breach" for detailed description of cases), also for sensitivity to changing WP parameters. In configurations resulting from a flow through the waste package, it has been shown (BSC 2001, p. 64) that the fissile material will likely be flushed out of the waste package. As the amount of fissile material decreases, the risk of internal criticality is diminished.

As for the intact cases, in most of the calculations the waste package is reflected by water, with the remaining cases (as identified in the tables in Section 6.2), the waste package is either reflected by tuff or the outer surfaces have a reflective BC. Use of this reflective boundary condition is conservative. The C block used in the degraded cases is type H-327 unless noted otherwise.

In these cases, the terms "fraction of water" or "percent of water" refer to a volume fraction or to a percentage of volume, respectively. For the degraded cases, the voids in the graphite from the C blocks and the fuel are always represented as saturated with water; therefore, any more water that may be mixed with these materials is labeled as additional water. The percentages listed for the other components of the degradation products are volume fractions unless noted otherwise. The SNF canister is almost always considered to be flooded and for those cases where the SNF canister is intact, the waste package is dry because, as shown in Table 14, that is the most reactive configuration.

5.5.1 Waste Form Degrades Within the Intact SNF Canister

In this section, cases are investigated where the spent fuel degrades while still in the intact SNF canister. This corresponds to scenario IP-1A from YMP (2000, pp.3-13 and 3-14) and from CRWMS M&O 1999b, p. 27).

5.5.1.1 Intact C Block with Some Degradation of the Fuel Compacts

In this scenario the C blocks are intact, but some portion of the fuel compacts have degraded. This degradation is due to either some amount of the fissile material in the fuel having dissolved into solution and re-entering the fuel assembly, or some portion of the fuel compact has fallen out of the C block and is now at the bottom of the canister. In the former case, where the fissile material has dissolved, only the uranium is assumed to dissolve and is redistributed in the coolant and void (c/v) channels of the fuel assembly. This is a conservative assumption since the uranium would redistribute in all the water throughout the entire canister and not just inside the assembly. The conservative fuel compositions listed in Table 1 that are based on the three actual fuel assemblies are compared with the proposed fuel composition for one of the more reactive cases. Variations are also considered where the water level in the canister is such that only a portion of the assembly is submerged and the dissolved fissile material only fills the portion of the assembly below the water level. This situation is shown in Figure 5 where the water level is such that half of the assembly is submerged and dissolved fissile material fills the c/v channels below the water level. This case is unphysical, but conservative, in the sense that water is assumed to fill the c/v channels above the water level. Water fills the remainder of the canister and assemblies for all cases except those where the canister is only partially filled with water. These results are shown in Table 15.

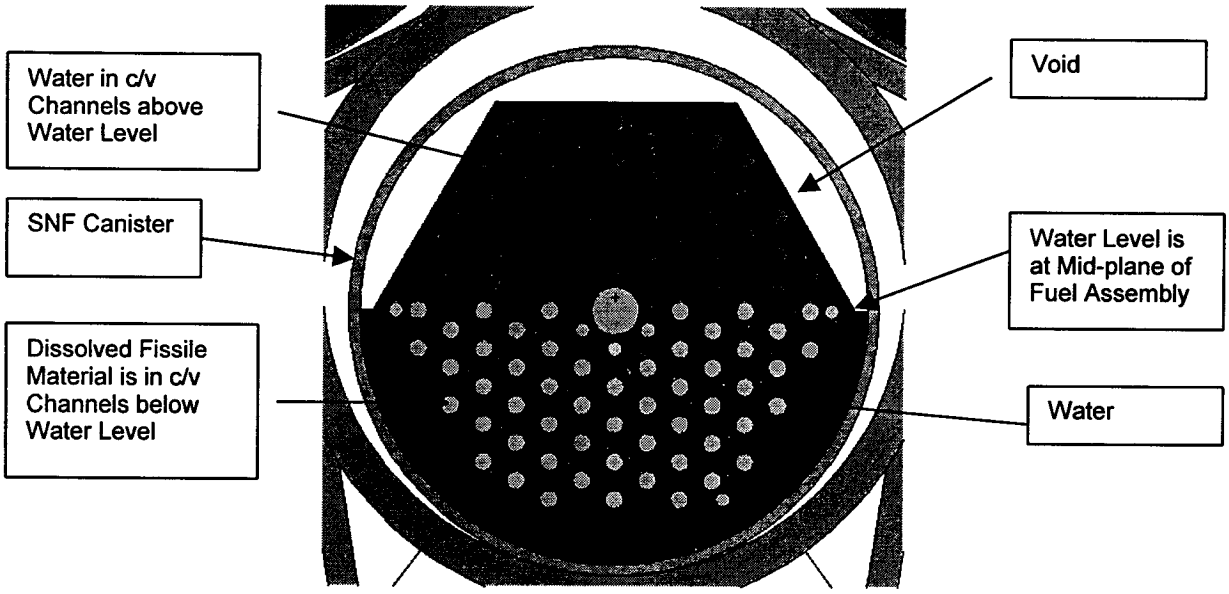

Figure 5. Fuel Assembly where Fissile Material is in Solution in the Lower Half of the Coolant/Void Channels of the Assembly

For the scenario where some portion of the fuel compact is removed from the fuel assembly and redistributed at the bottom of the canister, the fuel is assumed to be removed either from the outer end of an end assembly (first or last assembly in the canister) or to be removed uniformly from all assemblies in the canister. For those cases where the fuel is uniformly removed from the fuel compacts of all assemblies in the canister, the fuel remaining in the assemblies is modeled as having either a smaller diameter or is homogenized with the appropriate volume of water so as to completely fill the fuel hole. The binder material in the fuel compacts (carbon matrix) that holds the fuel particles together is neglected for the re-deposited (displaced) fuel at the bottom of the canister, i.e., the re-deposited fuel is composed of only fuel particles. (See footnote "a" at the bottom of Table 1). This situation is shown in Figure 6 where the fuel has been removed from the assemblies and re-deposited at the bottom of the canister. In this case the assembly is shown to be oriented with a corner of the assembly pointed downward. Figure 7 shows the assembly rotated 30° in a more stable position with a flat side of the assembly pointing downward and with fuel and water in the space directly below the assembly. Water fills the remainder of the canister and assemblies for all cases. The results where fuel is removed from the end assembly are shown in Table 16. The results for the fuel being uniformly removed from all fuel assemblies are shown in Table 17. The fuel remaining in the fuel tubes can now be modeled in one of at least two ways. The first would be to homogenize the remaining fuel with water to completely fill the fuel tubes, while the second would be to fill the annulus between the remaining fuel and C block with water. Since some degradation of the canister is possible (forming goethite, FeOOH), cases are also considered where goethite is mixed with the re-deposited fuel.

A variation of the cases just described is done to simulate the effect of tilting of the DOE canister inside the WP. This could result from fuel spilling out of an assembly and filling an open volume in the SNF canister. For these cases the fuel consists of homogenized fuel compacts mixed with water. The fuel could be redistributed from an end assembly of the stack into the volume between the assembly and the end of the canister. To make this volume as large as possible the stack of assemblies is positioned so that the assembly at the opposite end of the volume is touching its end of the canister. The fuel that fills this volume is assumed to come from either the upper cross-sectional portion of an end assembly, i.e., above the center row of fuel as seen in the first frame of Figure 8, or from the entire cross-section of an end assembly. Only enough fuel is removed from the last assembly to fill the desired portion of the existing void space between the end assembly and impact plate (only one end). The void in the fuel holes (due to removing fuel) is either filled by water or is filled by axially homogenizing the remaining fuel with water over the entire length of the fuel holes. Cases are also investigated where the volume is formed by separating the second and third assemblies in the stack, i.e., the end assemblies are touching their respective ends of the canister and the volume occurs within the stack. The volume percentage of water in the displaced fuel is also varied as shown in Table 18. Any unoccupied volumes in the canister are filled with water as shown in the second frame of Figure 8 which is a cross-sectional view of the canister between the end of the fuel stack and the canister end. In this case the canister is only half filled with the fuel mixture. The results for these tilted cases are given in Table 18.

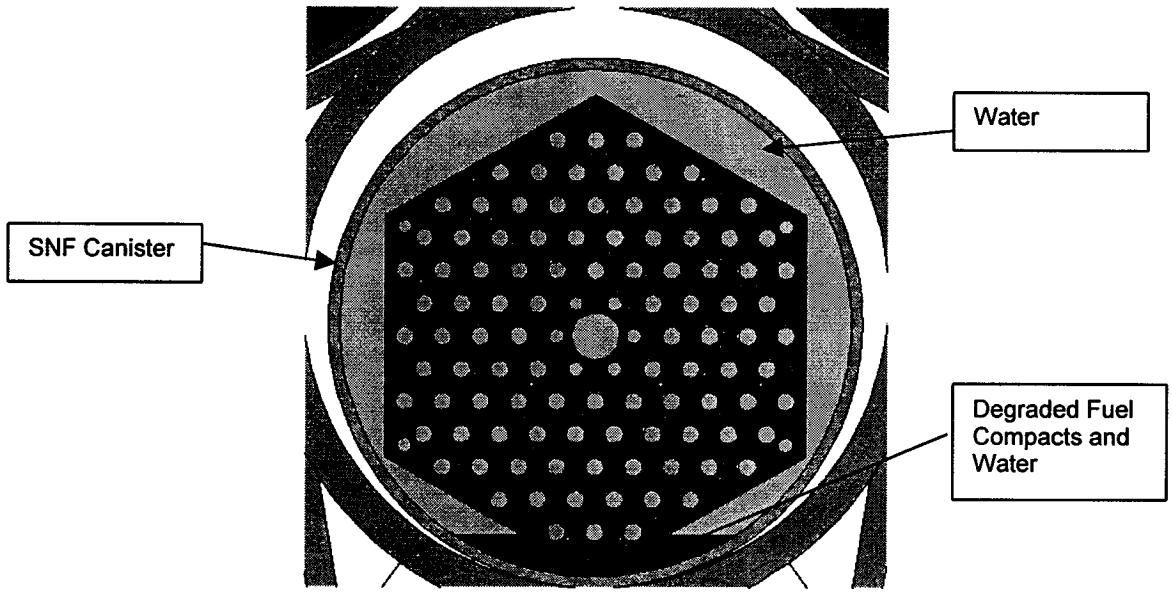

Figure 6. A Portion of the Fuel from the Assembly is in the Bottom of the SNF Canister

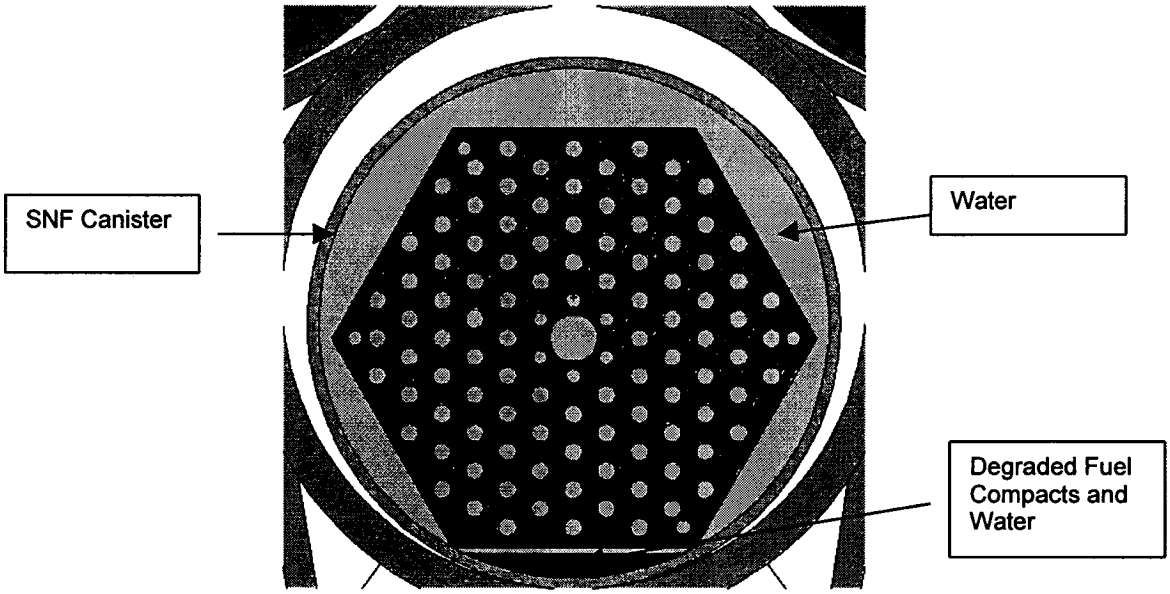

Figure 7. Similar Case to that Shown in Figure 6 but the Assembly is Rotated 30°

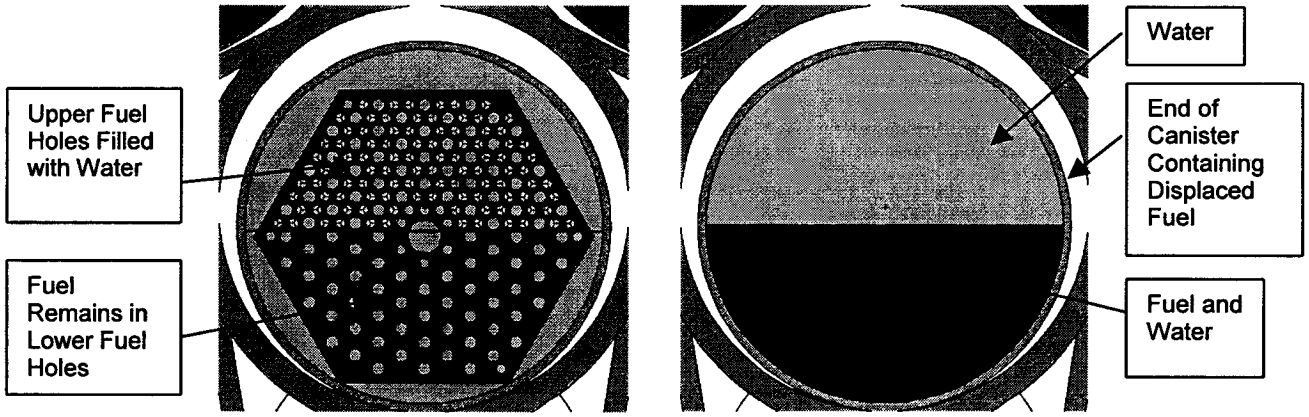

Figure 8. Tilting of the Canister Simulated by Removing Fuel From the Upper Portion of the Assembly and Redepositing At Canister End

For all cases that deal with the scenarios in this section, it is important to note that since the 5 assemblies in the canister are essentially infinitely long (based on unchanging k_{eff} values as shown in Table 14), any redistribution of fuel from the end of a fuel assembly to the bottom of the canister can have a significant effect on the reactivity of the system if this process increases the linear loading of fissile material over a 'localized' portion in the canister.

5.5.1.2 Degraded C Block with Intact Fuel Compacts

In the cases in Table 19, the fuel compacts are intact and the C blocks have degraded. Cases are treated for various degrees of degradation ranging from where the block has broken into a few

pieces all the way to where the block has completely rubblized. For the cases where the block has broken into pieces, the separation between pieces is varied between 0.0 and 1.0 cm. This separation is achieved by moving each piece the same distance in the radial direction from the center of the assembly. An example of an assembly that has broken into 6 pieces each separated by a 1 cm gap is shown in Figure 9.

For the cases where the block is treated as rubble, the fuel compacts are assumed to remain axially aligned and radially separated so as to form fictitious "fuel pins" which are surrounded by the carbon from the assembly mixed with water. In these cases the radial separation (pitch) between "fuel pins" is varied from touching to just greater than that for the intact assembly. Figure 10 shows a configuration of these "fuel pins" in the SNF canister. In this configuration the "fuel pins" have settled into the canister and uniformly fill the canister to about the same level. This is the more probable end state of the degradation process than that shown in Figure 11 where the "fuel pins" form a pile heaped at the center of the canister. This latter configuration (Figure 11) is shown to be the more reactive of the two in Section 6.2.1.2. The effect of varying the volume fraction of water in the rubble is investigated. Cases are also presented where the axial separation between the fuel compacts in the "fuel pins" is varied. For these cases, the number of fuel compacts for each fuel hole is assumed to be 16 and their lengths are changed to 4.956175 cm (rather than the stated length of 4.9276 cm), this gives the same number of compacts per "fuel pin" and simplifies the geometry. For this scenario any unoccupied space in the canister is filled with water. Results for these cases are shown in Table 20.

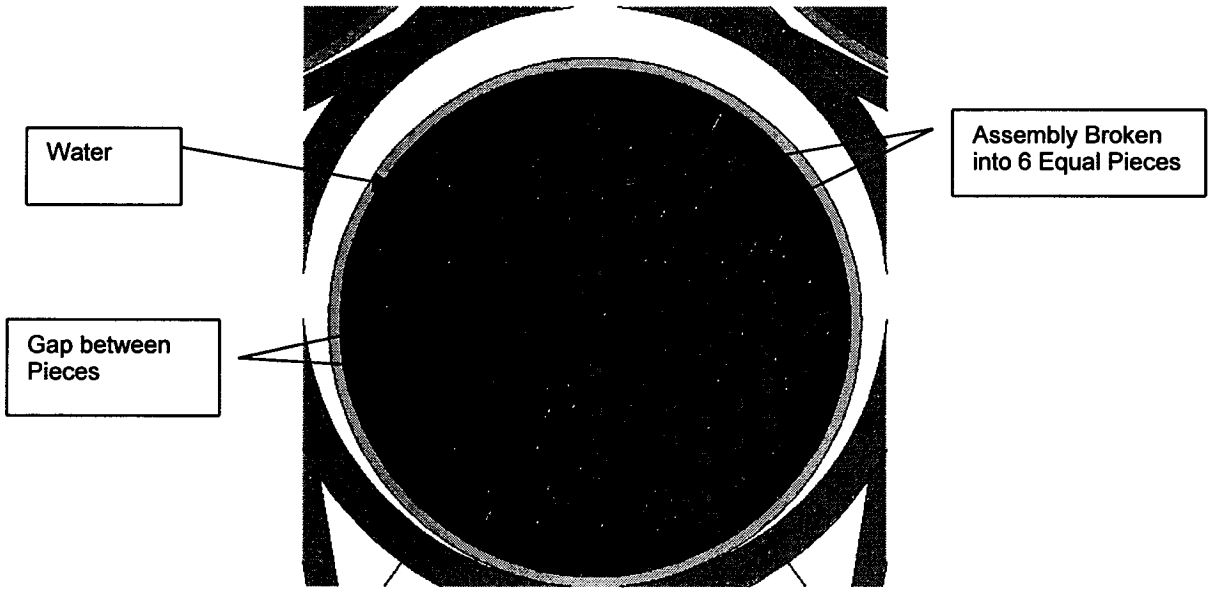

Figure 9. Assembly Has Broken into 6 Pieces, Each Separated by a 1 cm Gap

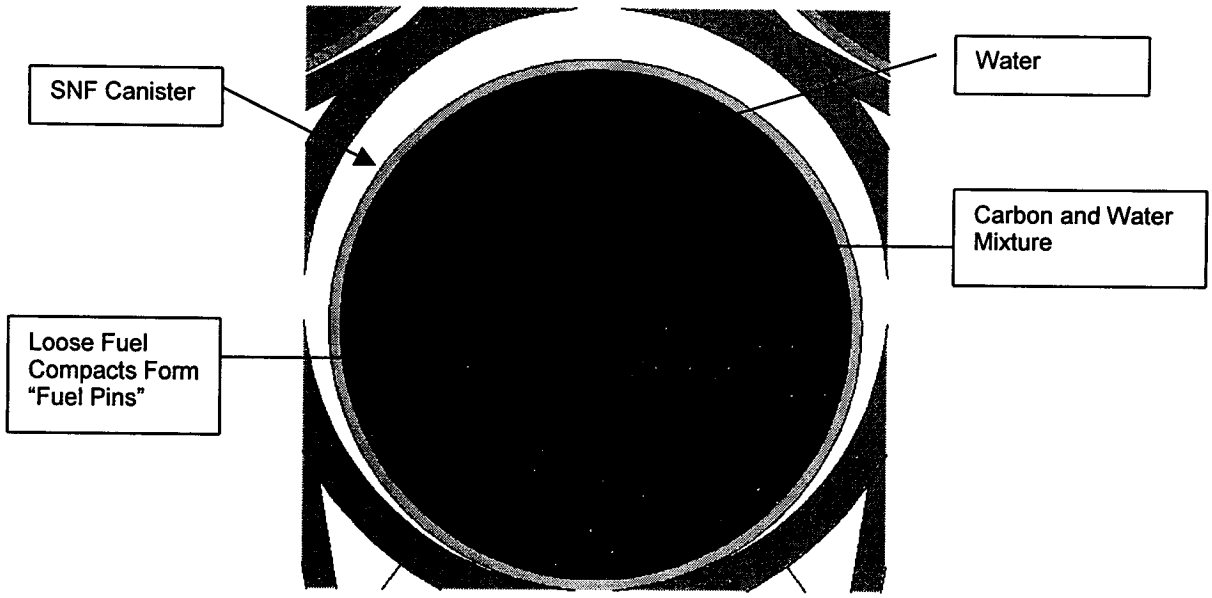

Figure 10. C Assembly Block Has Broken into Rubble and the Fuel Compacts Remain Axially Aligned Comprising "Fuel Pins"

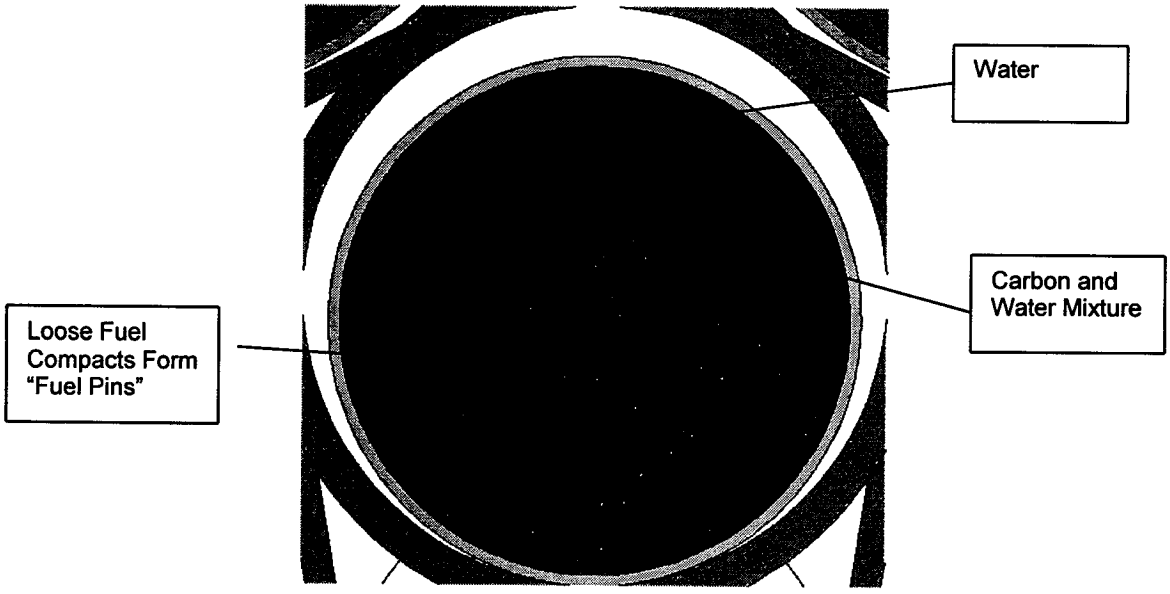

Figure 11. An Alternative Configuration of "Fuel Pins" than that Shown in Figure 10

5.5.1.3 Degraded C Block and Degraded Fuel Compacts

In this scenario both the C block and the fuel compacts have degraded to rubble. These degraded materials would in general mix together, but cases are presented where these are treated as layers of separate material. Such a case is shown in Figure 12 where the remnants of the fuel compacts mixed with carbon from the assembly block and water are below a layer of carbon and water. A set of cases where the carbon from the assembly block is neglected and another set where the fuel and varying amounts of carbon are mixed together are investigated. When mixed together the materials are treated as homogeneous. The volume percent of additional water in the material is varied from 0 to the point where the volume of the canister is completely filled with material. In all cases the degradation materials are assumed fully saturated with water as was done for the intact cases. Any unoccupied space in the canister is filled with water. Unless indicated otherwise, the C block used for these results is type H-451. These cases are presented in Tables 21 and 22.

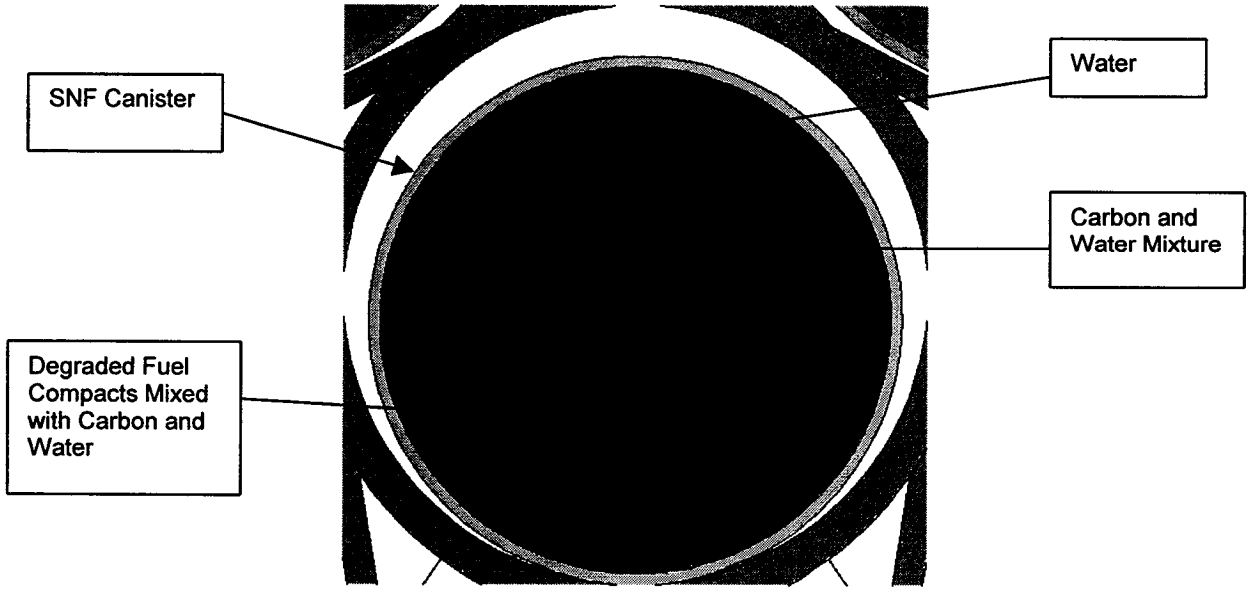

Figure 12. Contents of SNF Canister Have Degraded Forming Separate Layers of Fuel, Carbon and Water Inside the Canister

5.5.2 Internal Components of the Waste Package Degraded (Outside SNF Canister)

This section describes configurations resulting from the scenario IP-3 (YMP 2000, p. 3-13). The internal components of the waste package outside the SNF canister are completely degraded, including the inner barrier shell of the WP. The compositions of the slurry resulting from this degradation are given in CRWMS M&O (2000b, p. 41) and BSC (2001, p. 56) and are referred to as the pre-breach clay (Table 9). The amount of water mixed in this clay varies. There is U-238 present in the slurry from the degraded glass, but it is conservative to neglect it in these calculations since it is a neutron absorber. The cases in this section can be further divided into 2 categories depending upon whether the SNF canister is treated as being intact or degraded. In

the first category, described in Section 5.5.2.1, the SNF canister is intact and its contents can either be intact, partially or completely degraded. In the second category, described in Section 5.5.2.2, the SNF canister has degraded, but the canister and its contents have not chemically reacted with the pre-breach clay.

5.5.2.1 Intact SNF Canister with Contents Either Intact or Degraded

The SNF canister configurations studied include intact and degraded cases and are derived from the most reactive cases identified in the previous Sections (5.4 and 5.5.1). For the cases given in Table 23, the intact canister containing the intact or degraded fuel is surrounded by pre-breach clay. The location of the SNF canister in the clay is varied along the vertical axis centerline. The composition of the clay with various volume fractions of water is determined in Attachment I, spreadsheet "fsv_calcs.xls," sheet "WP". Figure 13 shows a configuration where a SNF canister containing an intact fuel assembly (see Section 5.4.1) is centered in the clay formed from the degraded contents of the waste package.

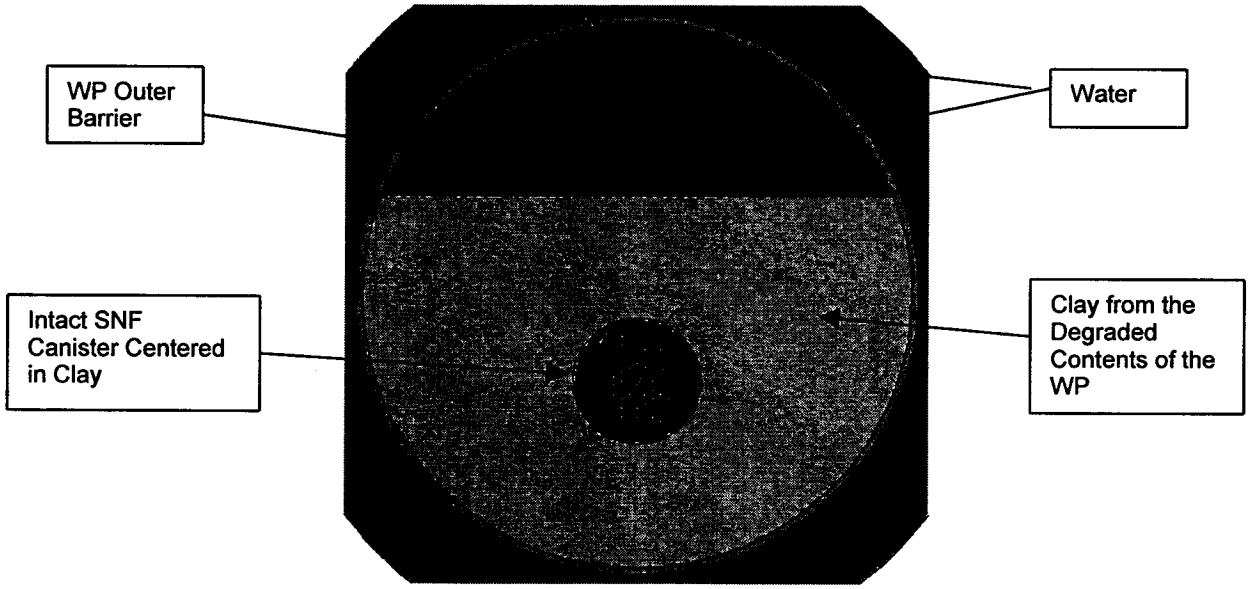

Figure 13. Cross-sectional View of an Intact SNF Canister Centered in Clay Formed from the Degradation of the Contents of the WP

5.5.2.2 Degraded SNF Canister with Non-reacted Pre-breach Clay

For these configurations the SNF canister has degraded to goethite, but the fuel assembly may be intact, partially or fully degraded. The fuel component and the goethite formed from the canister walls have not chemically reacted with each other or the pre-breach clay. The configurations in this section are similar to those in Sections 5.4 and 5.5.1, but now pre-breach clay and goethite, either mixed together or forming separate layers, can surround or be mixed with the fuel component from the assembly. The positioning of these configurations in the WP is varied, and

any unoccupied space in the WP is filled with water. The results of these cases can be found in Tables 24 through 27.

5.5.2.2.1 Intact Assembly with Degraded Canister and Degraded Contents of WP

In these configurations, the fuel assembly is intact and surrounded by pre-breach clay and goethite, either mixed together or in separate layers. These products would tend to mix together, but are treated as being unmixed in separate layers. The volume fraction of water in the materials is also varied. When mixed together, the composition of the mixture is varied to determine the reactivity of the configuration. Also, the water volume fraction of the materials in the various layers is varied to find a most reactive case. For most cases the c/v channels of the assembly are filled with water, but for some of the more reactive cases identified, a mixture of clay and water fills the c/v channels of the assembly. This type of configuration is shown in Figure 14 (goethite at the bottom of the WP is not portrayed in the figure). The location of the fuel assemblies is also varied from the bottom to the top of the clay layer while axial alignment is maintained.

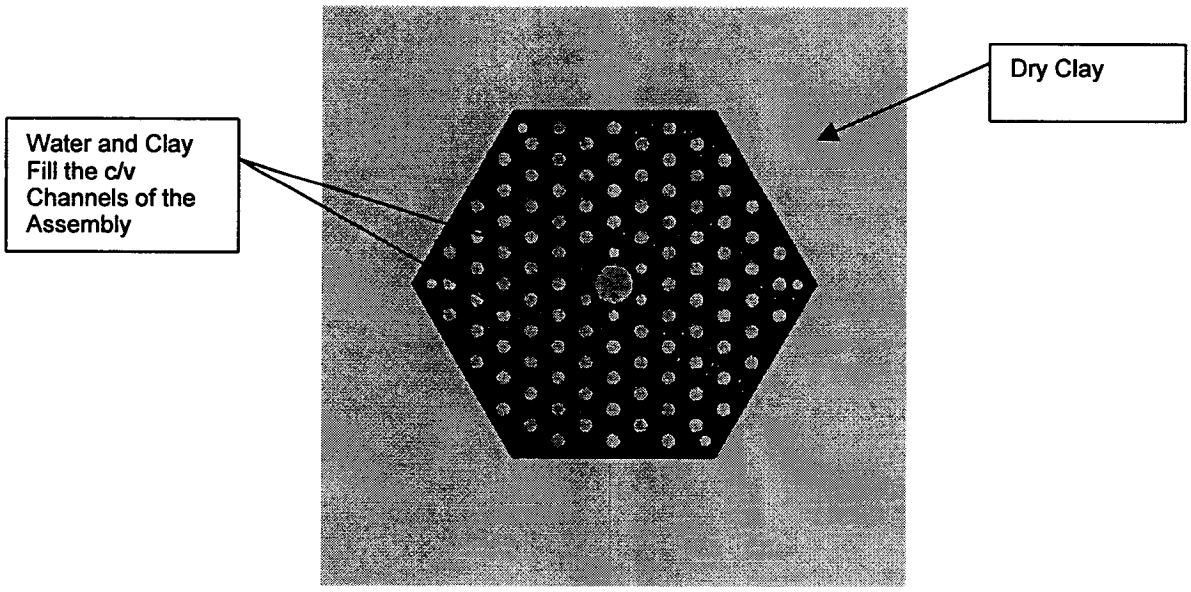

Figure 14. Intact Assembly Surrounded by Clay in the WP

Another configuration is shown in Figure 15 where goethite surrounds the intact assembly that in turn is surrounded by clay. This configuration could occur if the canister degrades to goethite after it is trapped in the clay formed from the degraded contents of the WP. Several variations of this case are investigated by changing the volume fraction of water in the goethite surrounding the assembly, varying the volume fraction of goethite in the c/v channels and by assuming the goethite forms a hexagonal shaped layer around the fuel assembly. The results for these cases are given in Table 24.

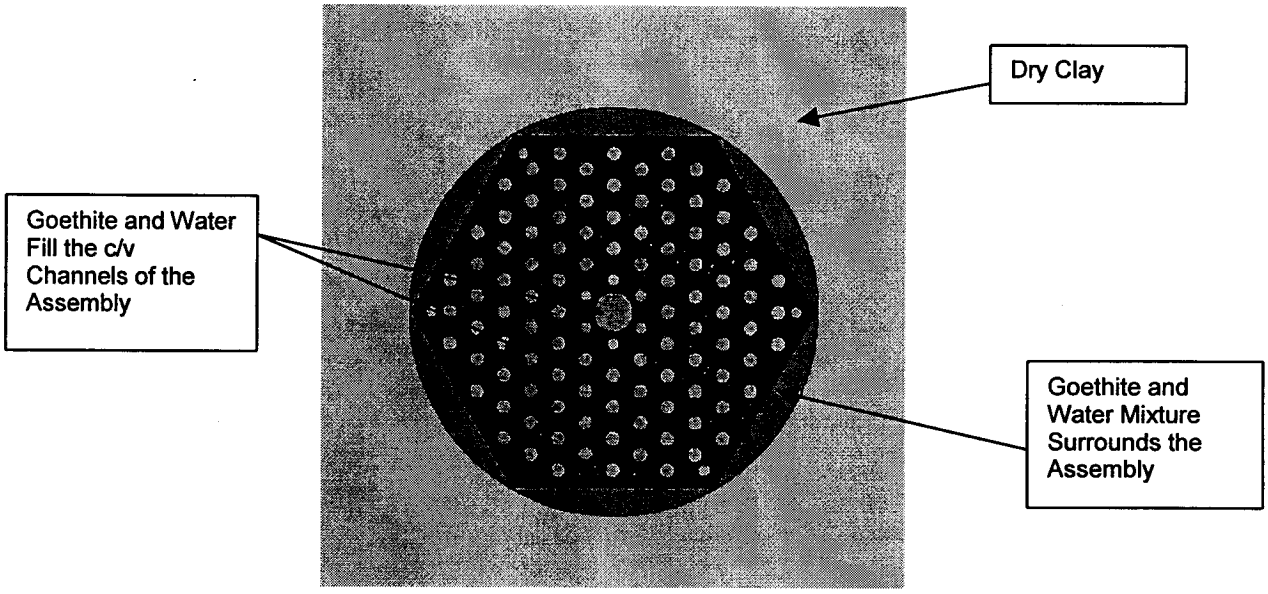

Figure 15. Intact Assembly Surrounded by Goethite Trapped in Pre-breach Clay in the WP

5.5.2.2.2 Intact Fuel Compacts with Degraded C Assembly Block, SNF Canister and Contents of WP

These cases are similar to those presented in Section 5.5.1.2, but the C block has been degraded to rubble and the fuel compacts are assumed to remain axially aligned and form "fuel pins" in the WP. Variations of these materials (goethite, clay, and carbon) and water volume fraction for the layers surrounding the fuel are investigated. The pitch of the "fuel pins" is also varied. An example of this type of configuration is shown in Figure 16. The loose "pins" are heaped at the bottom of the WP and are surrounded by a mixture of goethite, carbon, water and clay. For these cases the average pitch of the array of "pins" is chosen to be the same as that of the intact assembly, 1.8796 cm. The results of these cases are presented in Table 25.

Configurations similar to those in Section 5.5.2.2.1 where the pins surrounded by goethite and carbon have been trapped in the clay layer are also investigated. These configurations could occur if the assemblies become trapped in degraded material and then degrade without significant relocation of the "fuel pins", i.e., the pins either maintain or only slightly depart from their intact positions. An example configuration is shown in Figure 17 where the pins form an array with a circular cross-section (henceforth referred to as a "circular" array) with an average pitch equal to that of the intact assembly, 1.8796 cm. Here a mixture of goethite, carbon and water surrounds the pins that are positioned in the pre-breach clay layer. Different compositions, volume fractions of water and pitches are investigated. Also cases are considered where the "fuel pins" are assumed to be in the same position as in the intact assembly and are surrounded by goethite. The surrounding goethite forms a hexagonal shaped layer around the C rubble mixture that in turn is surrounded by the pre-breach clay. The volume fraction of additional water in the surrounding carbon is varied. All of these cases are shown in Table 26.

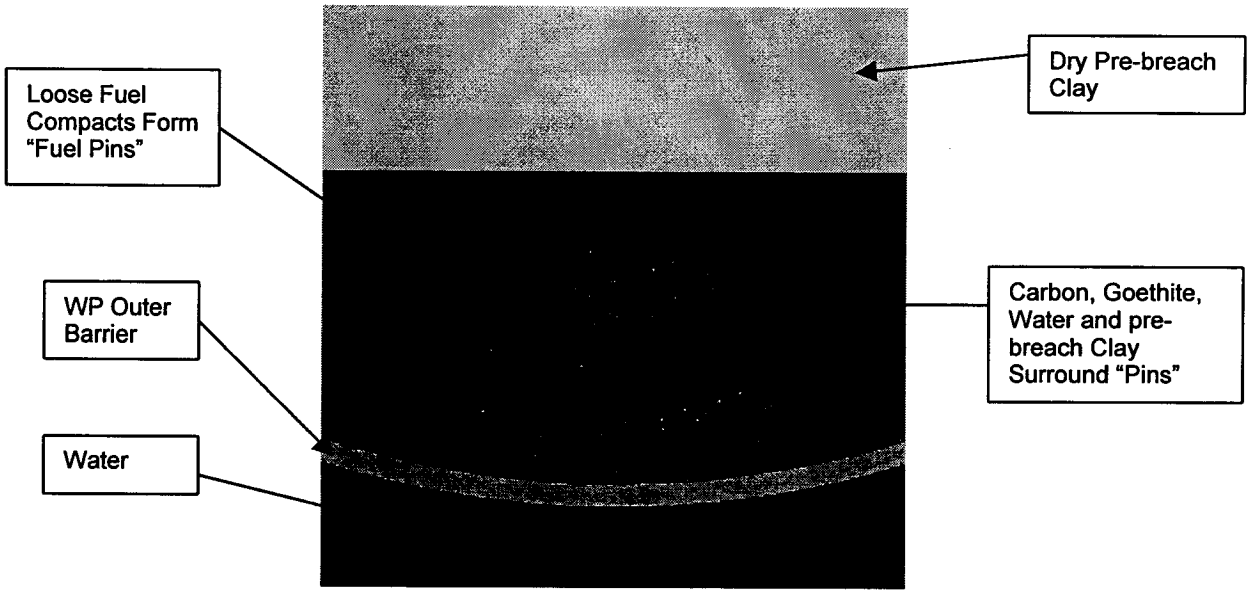

Figure 16. Loose "Fuel Pins" at the bottom of the WP Surrounded by a Mixture of Goethite, Carbon, Water and Pre-breach Clay

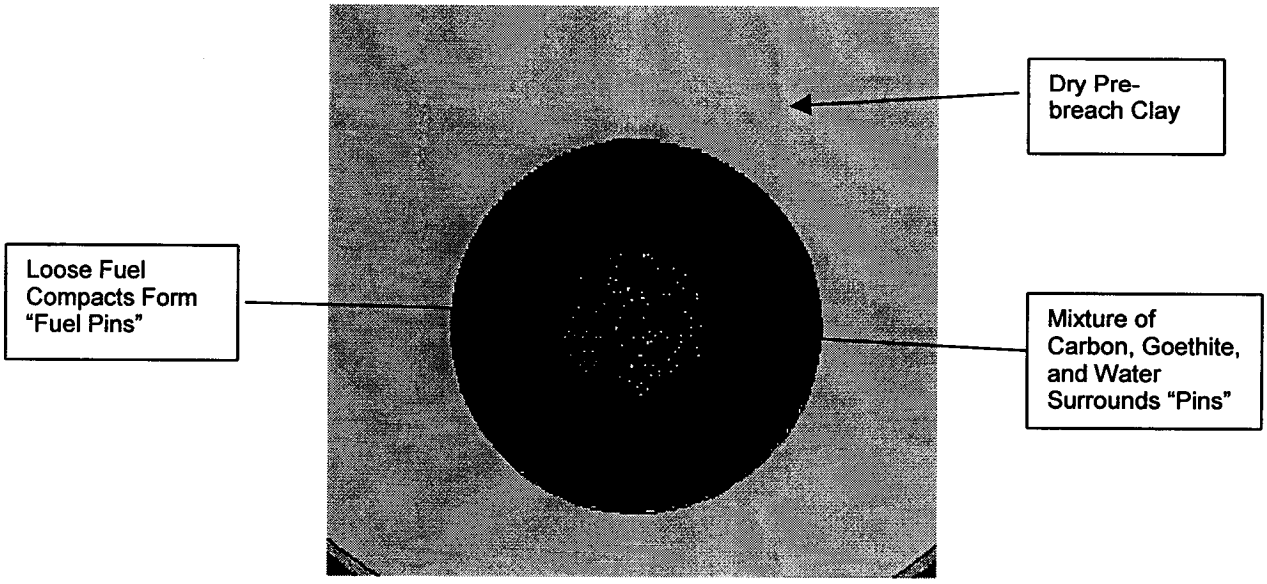

Figure 17. Cylinder of Loose "Fuel Pins" Surrounded by Goethite, Carbon, and Water Trapped in the Pre-breach Clay in the WP

5.5.2.2.3 Degraded Fuel Compacts, C Assembly Block, SNF Canister and Contents of WP

These configurations are similar to those in Section 5.5.1.3, but now the fuel can be mixed with goethite and clay in addition to carbon and water in the WP. These materials can form their own separate layers or be mixed together homogeneously in any combination to form layers. These layers can also contain water in various amounts. The voids in the fuel and C rubble are

assumed fully saturated with water with the same volume fraction as the intact fuel assembly, thus any added water listed in the table is in addition to the 'fully saturated' water condition. Figure 18 shows a somewhat improbable example of these materials forming different layers in the WP. Degraded fuel compacts mixed with water and carbon from the assembly form the bottom layer which is covered by layers of carbon, goethite, pre-breach clay and a top layer of water. A configuration with these materials mostly mixed together would seem more realistic. These cases are shown in Table 27.

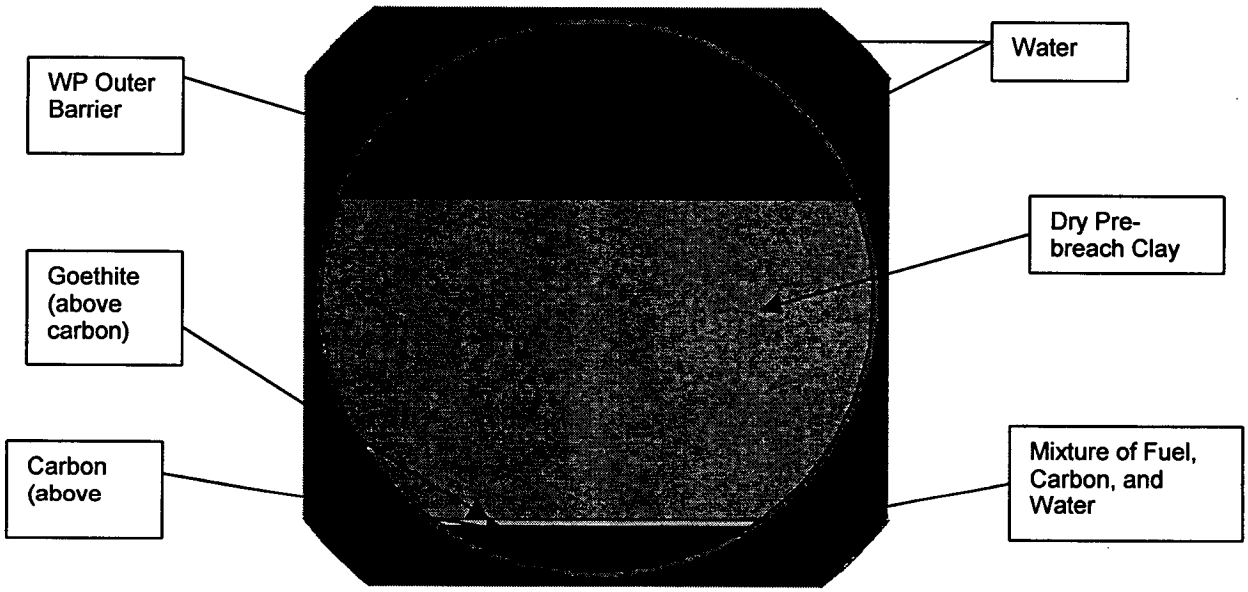

Figure 18. Layers of Completely Degraded Fuel Compacts, Goethite, Carbon, and Pre-breach Clay in the WP

5.5.3 All Components Degrade at the Same Time

These configurations represent the final stage of degradation for the two previous scenarios, Sections 5.5.1 and 5.5.2 (where the waste form degrades before/after the internal components of the waste package). The composition of the clay resulting from the degradation of all components inside the waste package is given in Tables 10 and/or 11, and comes from BSC (2001, pp. 59 and 62). This clay is referred to as post-breach clay. Typically by the time this clay forms, the fuel would be completely degraded and reacted with the other components in the WP, but for the composition given in Table 10 at the earlier time (72689 years) some portion of the fuel remains. In this instance the degradation rate for the fuel compacts is assumed to be very slow relative to the degradation rates for the other components. Cases for this clay must include separate layers of fuel and clay as well as mixed layers. Table 10 also gives a clay composition at a later time (378240 years) where all the fuel has degraded and becomes part of the clay. Compositions for the clay, fuel and/or water mixed in various proportions are determined in Attachment I, spreadsheet "fsv_cals.xls" sheet "Post-breach." Table 11 gives a post-breach clay composition for an alternative EQ3/6 case as shown in BSC (2001, p. 62). For the latter two compositions, sufficient time has passed for all the components of the waste

package to have degraded, chemically reacted, and formed post-breach clay. The amount of water in the clay is varied to determine the most reactive compositions. The clay is homogenized with varying amounts of water, and any remaining space in the WP is filled with water. The percentage of water homogenized in the clay is increased until the entire volume available in the waste package is filled with the clay mixture. These results are presented in Tables 28 and 29.

6. RESULTS

This calculation documents various intact and degraded mode configurations of the FSV HTGR fuel codisposal waste package. Sections 6.1 and 6.2 present the k_{eff} for the intact and the degraded configurations, respectively. The k_{eff} results represent the average collision, absorption, and track length estimator from the MCNP calculations. The standard deviation (σ) represents the standard deviation of k_{eff} about the average combined collision, absorption, and track length estimate due to Monte Carlo calculation statistics. The average energy of a neutron causing fission (AENCF) is the energy per source particle lost to fission divided by the weight per source neutron lost to fission from the "problem summary section" of the MCNP output. The MCNP input and output files developed for this calculation are included in ASCII format in Attachment I. (The output file name is derived by appending ".o" to the input file name.) The H/X ratio is the ratio of moles of hydrogen to moles of fissile materials (only U-235 unless noted otherwise). For intact fuel compacts the ratio is determined on the basis of a unit cell. For the fuel assembly, the most common unit cell is hexagonal, centered on a 0.625 in. diameter c/v channel, includes the equivalent of 2 fuel holes with graphite filling the remainder of the cell. For loose fuel compacts, the ratio is the simple average of the values of H/X for square and hexagonal unit cells since the fuel compacts are in an irregular array.

This document may be affected by technical product input information that requires confirmation. Any changes to the document that may occur as a result of completing the confirmation activities will be reflected in subsequent revisions. The status of the technical product information quality may be confirmed by review of the DIRS database.

For convenience in referencing cases within a given table, groups of cases may be referred to as a 'set', where the MCNP model for that set of cases examined variation(s) to a single parameter. These sets will be denoted by a preceding header within each table.

6.1 INTACT MODE

This section gives the results of the calculations described in Section 5.4. Unless noted otherwise, any void in the SNF canister is filled with water, whereas any space not occupied by glass canisters or structural material in the WP is treated as void.

6.1.1 Comparison of FSV Fuel Compositions and Other Modeling Details

Table 12 presents the results of the calculations described in Section 5.4.1. The first four cases in this table compare the compositions given in Table 1 to demonstrate that the fuel composition used in the MCNP code is conservative. The "base case" uses this composition while the other 3 cases represent actual fuel elements with conservative compositions shown in Table 1.

The next set of cases in Table 12 investigates the sensitivity of the base case to modeling details. In the first case, cs1aL.o, the fuel holes are modeled with their actual length rather than being the same length as the fuel assembly. The next case, cs1_ref.o, the water reflector around the WP is

replaced with a reflective boundary condition (BC). In the next two cases the 2 outer poison holes are modeled as filled with water rather than C, with one case having a water reflector around the WP (case cs1-ph.o) and the other an outer reflective BC (case cs1-ph_ref.o). In the second to last case, cs1noPu.o, the EOL plutonium is neglected in the fuel compacts. The other type of carbon block, type H-451, is used in the next to last case. None of these cases show a statistically significant change in results from the base case. Finally, in the last case the amount of thorium in the fuel is arbitrarily reduced by 5%. This gives about a 0.5% increase in k_{eff} and shows the sensitivity of the system to the presence of thorium.

Table 12. Comparison of Actual FSV Fuel Assemblies with the "As Modeled" Assembly and Other Modeling Details

Output File Name	$k_{eff} \pm \sigma$	$k_{eff} + 2\sigma$	AENCF (keV)	H/X Ratio	Comment
Fuel Composition Comparison, see Table 1					
cs1.o	0.9131 ± 0.0009	0.9149	6.751	602.7	Base case
cmp1.o	0.9017 ± 0.0009	0.9035	6.896	[a]642.3	Element 1-4242
cmp2.o	0.9094 ± 0.0009	0.9112	7.008	[a]633.1	Element 1-1426
cmp3.o	0.9090 ± 0.0010	0.9109	7.156	[a]630.7	Element 1-0466
Comparison of Modeling Details (case 'cs1.o' variants).					
cs1aL.o	0.9126 ± 0.0009	0.9144	6.947	642.3	Base case but actual fuel length modeled
cs1_ref.o	0.9143 ± 0.0009	0.9162	6.811	602.7	Base case but reflective BC
cs1-ph.o	0.9150 ± 0.0008	0.9167	6.898	602.7	Base case but water replaces C in poison holes
cs1-ph_ref.o	0.9159 ± 0.0009	0.9176	6.678	602.7	Case cs1-ph.o but reflective BC
cs1noPu.o	0.9139 ± 0.0009	0.9158	6.622	602.7	No (EOL) Pu in fuel
cs1othrC.o	0.9140 ± 0.0008	0.9157	6.876	593.0	Base case, but uses other type of (saturated) C block (H-451)
cs1-th.05.o	0.9178 ± 0.0009	0.9196	6.5861	602.7	Base case but 5% of the Th is neglected

NOTE: [a] Calculation of H/X ratio includes contribution from U-233.

For the results shown in Table 13, the percent saturation is varied in the fuel compacts and in the C fuel block. The first case in this table is the base case, repeated from Table 12, i.e., 100% saturated voids in the fuel and C block, while the last case of Table 13 is for a completely dry (0% saturated) assembly. Saturation values greater than 100% are not physically possible, but are considered here in order to show the trend of increasing water content. Examination of this table shows that the FSV fuel assemblies are clearly under-moderated, and the effect of no water in the fuel and graphite block voids significantly reduces k_{eff}.

Table 13. Amount of Water Saturation of Voids in the Fuel Compacts and C Fuel Block

Output File Name	$k_{eff} \pm \sigma$	$k_{eff} + 2\sigma$	AENCF (keV)	H/X Ratio	% Void Saturation in Fuel Compacts	% Void Saturation in C Block
Amount of Void Saturation in Fuel Compacts is Varied						
cs1.o	0.9131 ± 0.0009	0.9149	6.751	602.7	100	100
cs1a.o	0.9124 ± 0.0010	0.9144	6.782	593.3	95	100

Output File Name	$k_{eff} \pm \sigma$	$k_{eff} + 2\sigma$	AENCF (keV)	H/X Ratio	% Void Saturation in Fuel Compacts	% Void Saturation in C Block
Amount of Void Saturation in Fuel Compacts is Varied						
cs1c.o	0.9076 ± 0.0010	0.9095	7.007	574.3	85	100
cs1e.o	0.9008 ± 0.0009	0.9026	7.184	555.4	75	100
cs1+a.o	0.9165 ± 0.0009	0.9182	6.619	612.2	105	100
cs1+b.o	0.9192 ± 0.0009	0.9210	6.573	621.7	110	100
cs1+c.o	0.9216 ± 0.0009	0.9234	6.502	640.6	120	100
Amount of Void Saturation in C Block is Varied						
cs1Ca.o	0.9123 ± 0.0010	0.9142	6.773	596.5	100	95
cs1Cb.o	0.9129 ± 0.0009	0.9147	6.746	590.4	100	90
cs1Cc.o	0.9116 ± 0.0009	0.9134	6.830	584.2	100	85
cs1+Ca.o	0.9135 ± 0.0009	0.9154	6.845	608.9	100	105
cs1+Cb.o	0.9179 ± 0.0009	0.9198	6.687	615.1	100	110
cs1+Cc.o	0.9194 ± 0.0009	0.9212	6.678	633.6	100	125
No Water in Voids of Fuel or C Block						
cs1drya.o	0.7775 ± 0.0010	0.7796	10.323	289.7	0	0

Cases with variations in the positioning of these components in the WP and other cases are presented in Table 14. In the first 6 cases, these components are either centered or in the downward position as indicated in the table (the base case from Table 12 is repeated). In all of these cases, empty spaces in the WP but outside the SNF canister are modeled as voids. In case cs1_c_ref.o the water reflector for case cs1_c.o is replaced with a reflective boundary condition (BC) for the outside surfaces of the WP. As seen, there is no statistical difference between water and a perfect reflector.

In the next two cases in the table, some or all of the voids outside the SNF canister (inside the WP) are flooded. These results identify the most reactive configurations with regard to positioning of the various components and flooding in the waste package. As seen, the dry waste package (external to the canister) is more reactive while variations in centering tend to be negligible. Unless otherwise specified, in the remaining cases of this report, the SNF canister is flooded while empty spaces in the WP (outside the canister) are modeled as voids.

Finally, the last 4 cases in the table are for a SNF canister containing a reduced number of FSV assemblies. Values of k_{eff} are statistically unchanged for a canister containing at least 3 assemblies. Axially stacking more assemblies does not make the canister more reactive, i.e., the fuel is essentially infinitely long for these cases. The values of k_{eff} are reduced by slightly more than 1% and 5% for 2 and 1 assemblies, respectively.

Table 14. Variations in Positioning of the Various Components in the WP and Other Results

File Name	$k_{eff} \pm \sigma$	$k_{eff} + 2\sigma$	AENCF (keV)	H/X Ratio	Comment
Positioning Study of the Various Components					
cs1.o	0.9131 ± 0.0009	0.9149	6.751	602.7	(base case) HLW canisters down; canister down; assembly centered
cs1_a.o	0.9128 ± 0.0009	0.9146	6.976	602.7	HLW canisters down; canister centered; assembly centered
cs1_b.o	0.9121 ± 0.0009	0.9139	6.949	602.7	HLW canisters down; canister down; assembly down
cs1_c.o	0.9150 ± 0.0010	0.9169	6.556	602.7	Case cs1_b.o but assembly rotated 30°
cs1_c_ref.o	0.9156 ± 0.0009	0.9173	6.839	602.7	Case cs1_c but reflective BC
cs2.o	0.9147 ± 0.0009	0.9165	6.926	602.7	HLW canisters centered; canister centered; assembly centered
Effect of Water in the WP (External to the SNF Canister)					
cs1+wa.o	0.9045 ± 0.0009	0.9063	6.705	602.7	Base case, but water fills support tube of WP
cs1+wb.o	0.9003 ± 0.0009	0.9021	6.710	602.7	Base case, but water fills entire WP
Investigation of Number of Assemblies per WP					
cs1-1.o	0.9127 ± 0.0009	0.9145	6.909	602.7	Base case, but canister contains 4 FSV assemblies
cs1-2.o	0.9114 ± 0.0009	0.9133	6.642	602.7	Base case, but canister contains 3 FSV assemblies
cs1-3.o	0.9011 ± 0.0009	0.9029	6.854	602.7	Base case, but canister contains 2 FSV assemblies
cs1-4.o	0.8673 ± 0.0009	0.8692	7.063	602.7	Base case, but canister contains 1 FSV assembly

6.2 DEGRADED MODE

This section gives the results of the calculations described in Section 5.5. Section 6.2.1 presents the results of the calculation where the inner component of the SNF canister (FSV fuel assembly) degrades before the high-level waste canisters, the SNF canister, and the waste package basket (see Sections 5.5.1). Section 6.2.2 gives the results for the calculation where the internal components of the waste package (but external to the DOE SNF canister) degrade first (see Section 5.5.2). Section 6.2.3 presents the results for a waste package with its internal components fully degraded (see Section 5.5.3).

6.2.1 Inner Component of the SNF Canister Degrades First

Values of k_{eff} for the cases where some portion of the fuel compacts degrade first while the C block remains intact are given in Section 6.2.1.1. Section 6.2.1.2 lists the results for the cases where the C blocks degrade first but the fuel compacts remain intact. Section 6.2.1.3 shows the results of the calculations described in Section 5.5.1.3 where both the C blocks and fuel compacts have degraded.

6.2.1.1 Partial Degradation of Fuel Compacts Before the C Block

In this section, cases are investigated where the C block remains intact but some portion of the fuel compacts has degraded (see Section 5.5.1.1). The fuel from the compacts is assumed to be either dissolved and redistributed in the coolant/voids channels or degraded and deposited at the bottom of the SNF canister. Tables 15 through 18 present the results.

In Table 15 values of k_{eff} are given for configurations where some fraction of the fuel, as indicated in the table, has dissolved and been redistributed in the coolant/void channels of the assembly. For the first 18 cases in the table (first two sets), the fuel is dissolved in the coolant/void channels and water fills the remainder of the canister. In the second set of cases, the fuel compositions based on the actual fuel assemblies are compared to the proposed fuel composition, see Table 1 for these compositions, for the case where 10% of the uranium has dissolved. The remaining cases in the table give variations of these cases, but the canister is only partially filled with water. For these cases the water level is adjusted to fill the canister up to the half-height (see Figure 5) and ¾-height of the assembly. Here the dissolved fuel fills those c/v channels below the water level while the c/v channels above the water level are either treated as void or filled with water. Completely filling the channels above the water level with water is clearly unphysical but conservative as seen in the table. Also note that k_{eff} decreases as the water level decreases in the canister.

Table 15. Dissolved Fuel Redistributed in Coolant/Void Channels of Fuel Assembly

File Name	$k_{eff} \pm \sigma$	$k_{eff} + 2\sigma$	AENCF (keV)	H/X Ratio	% of U Dissolved	Comments
Canister is Completely Filled with Water						
fl_2%.o	0.9246 ± 0.0009	0.9264	6.670	591.9	2	No fuel removed from assemblies
fl_2%a.o	0.9176 ± 0.0010	0.9195	6.563	603.8	2	Fuel uniformly removed from assemblies
fl_3%.o	0.9265 ± 0.0010	0.9284	6.694	586.7	3	No fuel removed from assemblies
fl_3%rf.o	0.9280 ± 0.0009	0.9299	6.752	586.7	3	Previous case but reflective BC
fl_3%a.o	0.9205 ± 0.0009	0.9223	6.683	604.3	3	Fuel uniformly removed from assemblies
fl_4%.o	0.9327 ± 0.0009	0.9345	6.844	581.5	4	No fuel removed from assemblies
fl_4%a.o	0.9190 ± 0.0009	0.9208	6.690	604.9	4	Fuel uniformly removed from assemblies
fl_5%.o	0.9379 ± 0.0009	0.9398	6.617	576.4	5	No fuel removed from assemblies
fl_5%a.o	0.9238 ± 0.0009	0.9256	6.479	605.4	5	Fuel uniformly removed from assemblies
fl_5%arf.o	0.9208 ± 0.0009	0.9226	6.487	605.4	5	Previous case but reflective BC
fl_10%.o	0.9569 ± 0.0009	0.9587	6.552	552.4	10	No fuel removed from assemblies

fl_10%a.o	0.9272 ± 0.0009	0.9291	6.535	608.1	10	Fuel uniformly removed from assemblies
	Conservative Compositions Shown in Table 1					
fal1_10%.o	0.9456 ± 0.0009	0.9473	6.925	[a]588.6	10	Element 1-4242; no fuel removed from assemblies
fal1_10%a.o	0.9133 ± 0.0009	0.9151	6.633	[a]648.0	10	Element 1-4242; fuel uniformly removed from assemblies
fal2_10%.o	0.9508 ± 0.0009	0.9526	6.934	[a]580.2	10	Element 1-1426; no fuel removed from assemblies
fal2_10%a.o	0.9232 ± 0.0010	0.9251	6.692	[a]638.8	10	Element 1-1426; fuel uniformly removed from assemblies
fal3_10%.o	0.9523 ± 0.0010	0.9543	7.028	[a]578.0	10	Element 1-0466; no fuel removed from assemblies
fal3_10%a.o	0.9222 ± 0.0009	0.9241	6.873	[a]636.3	10	Element 1-0466; fuel uniformly removed from assemblies
	Canister is Partially Filled with Water					
[b]thq+10%+w.o	0.9476 ± 0.0009	0.9494	6.859	541.9	10	No fuel removed from assemblies; water level at 3/4 assembly height
thq+10%.o	0.9320 ± 0.0009	0.9339	7.165	541.9	10	No fuel removed from assemblies; water level at 3/4 assembly height
[b]hlf_10%+w.o	0.9413 ± 0.0009	0.9431	6.943	518.5	10	No fuel removed from assemblies; water level at 1/2 assembly height
hlf_10%.o	0.8997 ± 0.0009	0.9015	7.947	518.5	10	No fuel removed from assemblies; water level at 1/2 assembly height

NOTES: [a] Calculation of H/X ratio includes contribution from U-233.
[b] Water fills coolant/void channels above water level in canister.

For the most conservative scenario, i.e., no fuel is removed from the intact assemblies, these results show that the interim criticality limit of 0.93 is exceeded when 4% or more additional uranium is added to the c/v channels. If fuel is uniformly removed from the assemblies, then 10% of the uranium can be redistributed into the channels. Both these amounts of uranium represent a significantly greater amount of fuel than the 0.3% failure rate mentioned in Section 5.1.1. Also note that as was shown in Table 12 for the intact base case, the proposed fuel composition is as or more reactive than the conservative fuel compositions.

Table 16 shows the results where a portion of fuel degrades, is removed from an end assembly in the assembly stack, and is re-deposited at the bottom of the canister along its entire length. This situation was shown in Figures 6 and 7. For the first seven of cases in Table 16, the amount of water in this degraded fuel is the same as that of the intact assembly. Additional water is added to the fuel to give different volume fractions of water for the remaining cases in the table. The

H/X ratio given in the table is for the re-deposited fuel, while the H/X ratio for the intact compacts is 602.7.

Table 16. Degraded Fuel from an End Assembly Re-deposits at Bottom of SNF Canister

File Name	$k_{eff} \pm \sigma$	$k_{eff} + 2\sigma$	AENCF (keV)	[a] H/X Ratio	% of Fuel Removed from Assemblies	% Additional Water in Degraded Fuel	Comment
bd.1.o	0.9244 ± 0.0010	0.9263	6.878	137.9	10	0	—
bd.15.o	0.9253 ± 0.0008	0.9270	7.110	137.9	15	0	—
bd.15rf.o	0.9279 ± 0.0009	0.9296	7.140	137.9	15	0	Previous case, but reflective BC
bd.197.o	0.9305 ± 0.0009	0.9323	7.137	137.9	19.7	0	chord below assembly just filled
bd.2.o	0.9305 ± 0.0010	0.9324	7.163	137.9	20	0	—
bdq.o	0.9326 ± 0.0008	0.9342	7.386	137.9	25	0	—
bdqp.o	0.9339 ± 0.0009	0.9357	7.005	137.9	25	0	assembly partially submerged
bd.1+w.1.o	0.9223 ± 0.0009	0.9240	7.105	167.9	10	10	Variation of case bd.1.o
bd.1+w.2.o	0.9238 ± 0.0010	0.9257	6.873	205.4	10	20	Variation of case bd.1.o
bd.1+w.3.o	0.9253 ± 0.0009	0.9271	6.838	253.6	10	30	Variation of case bd.1.o
bd.1+w.4.o	0.9259 ± 0.0009	0.9276	6.980	317.9	10	40	Variation of case bd.1.o
bd.1+w.4rf.o	0.9278 ± 0.0009	0.9296	6.916	317.9	10	40	Previous case, but reflective BC
bd.15+w.1.o	0.9281 ± 0.0009	0.9299	7.082	167.9	15	10	Variation of case bd.15.o
bd.15+w.2.o	0.9270 ± 0.0010	0.9290	7.275	205.4	15	20	Variation of case bd.15.o
bd.15+w.24.o	0.9293 ± 0.0009	0.9311	7.041	222.9	15	24	Variation of case bd.15.o
bd.15+w.24p.o	0.9302 ± 0.0009	0.9320	7.005	222.9	15	24	Previous case, but assembly rotated 30° and partially submerged (see Figure 6)

NOTE: [a] H/X ratio is for re-deposited fuel at bottom of canister.

A simple variation of the cases presented in Table 16 was performed where some portion of the fuel degrades, is removed uniformly from the entire length of the fuel assemblies and re-deposits at the bottom of the SNF canister. Results for these and other cases with different volume fractions of additional water in the degraded fuel are presented in Table 17. These results show that k_{eff} decreases as the amount of fuel removed from the fuel assembly (and redistributed at the bottom of the canister) increases.

The last 4 cases in Table 17 are variations of case alt.1+w.4h, with goethite mixed into the degraded fuel at the bottom of the SNF canister. The amount of goethite is given as a volume percent as stated in the table. Increasing the amount of goethite while maintaining the water

volume percent at 40% has a statistically negligible effect on the results. The H/X ratios for the assembly and the displaced fuel at the bottom of the canister are given in the table.

Table 17. Degraded Fuel from the Entire Length of the Assemblies Re-deposits at Bottom of SNF Canister

File Name	$k_{eff} \pm \sigma$	$k_{eff} + 2\sigma$	AENCF (keV)	H/X Ratio assembly /mixture	% of Fuel Removed from Assemblies	% Additional Water in Degraded Fuel	Comment
alt.1+w.4h.o	0.9011 ± 0.0008	0.9028	6.466	689.8 / 317.9	10	40	Homogenized fuel in assemblies
alt.1+w.4hrf.o	0.9021 ± 0.0009	0.9040	6.292	689.8 / 317.9	10	40	Previous case, but reflective BC
alt.15+w.24h.o	0.8886 ± 0.0009	0.8903	6.237	741.1 / 222.9	15	24	Homogenized fuel in assemblies
alt.197.o	0.8718 ± 0.0008	0.8734	6.469	795.3 / 137.9	19.7	0	Water fills annulus around fuel in assemblies
alt.197h.o	0.8775 ± 0.0009	0.8792	6.368	795.3 / 137.9	19.7	0	Homogenized fuel in assemblies
alt.25h.o	0.8642 ± 0.0008	0.8659	6.434	864.1 / 137.9	25	0	Homogenized fuel in assemblies
alt.25+w.2h.o	0.8682 ± 0.0009	0.8699	6.331	864.1 / 205.4	25	20	Homogenized fuel in assemblies
alt.5.o	0.7632 ± 0.0008	0.7649	7.859	1386.8 / 137.9	50	0	Water fills annulus around fuel in assemblies
alt.5h.o	0.7725 ± 0.0008	0.7741	7.593	1386.8 / 137.9	50	0	Homogenized fuel in assemblies
[a] alt.1+w.4h+g.02.o	0.8986 ± 0.0009	0.9004	6.469	689.8 / 328.1	10	40	Case alt.1+w.4h, but 2% goethite
[a] alt.1+w.4h+g.04.o	0.8986 ± 0.0009	0.9004	6.416	689.8 / 339.1	10	40	Case alt.1+w.4h, but 4% goethite
[a] alt.1+w.4h+g.1.o	0.9007 ± 0.0009	0.9024	6.597	689.8 / 377.2	10	40	Case alt.1+w.4h, but 10% goethite
[a] alt.1+w.4h+g.2.o	0.8991 ± 0.0008	0.9007	6.352	689.8 / 466.3	10	40	Case alt.1+w.4h, but 20% goethite

NOTE: [a] Goethite from degradation of the SNF canister is mixed with displaced fuel.

Table 18 presents the results of the calculation that simulates the tilting of the SNF canister. In the first nine cases, the fuel is removed from the upper portion (see the first frame of Figure 8) of an end assembly in the stack and is redistributed in the volume at the end of the stack between the last assembly and its end of the canister. The volume percent of water in the displaced fuel is varied, and sufficient fuel is removed from the end assembly so that 50% of the volume is filled with the fuel mixture. For the first seven cases, the volume that the removed fuel occupied in the end assembly is replaced with water. For the last two of the first nine cases, the remaining fuel in the end assembly is homogenized with water and axially redistributed so as to fill the entire length of the fuel holes. The tenth and eleventh cases are similar, but 100% of the volume at the end of the fuel stack is filled with the fuel mixture. Finally in the last cases in Table 18, the second and third assemblies of the stack are assumed to have separated forming the volume that is filled by displaced fuel. The first H/X ratio for each case in the table is for the displaced fuel

at the bottom of the canister, and the second ratio (if given) is for the homogenized fuel in the assembly. The H/X ratio for the unaffected fuel in the assembly is 602.7 (Table 12, base case).

Table 18. Simulated Tilting of the SNF Canister Fills Volume at End of Stack or Between Assemblies with Fuel

File Name	$k_{eff} \pm \sigma$	$k_{eff} + 2\sigma$	AENCF (keV)	[a] H/X Ratio	% Additional Water in Degraded Fuel	Comment
Fuel from Upper Portion of End Assembly Fills 50% of Volume at End of Assembly Stack						
tlt1a.o	0.9130 ± 0.0009	0.9148	6.685	242.1	12.4	Displaced fuel in assembly is replaced with water; upper portion of end assembly is emptied of fuel
tlt1a_.2.o	0.9146 ± 0.0009	0.9164	6.775	282.2	20.0	Displaced fuel in assembly is replaced with water
tlt1a_.3.o	0.9118 ± 0.0009	0.9137	6.963	348.4	30.0	Displaced fuel in assembly is replaced with water
tlt1a_.4.o	0.9147 ± 0.0010	0.9166	6.809	436.6	40.0	Displaced fuel in assembly is replaced with water
tlt1a_.4rf.o	0.9143 ± 0.0008	0.9159	6.899	436.6	40.0	Previous case but uses reflective BC
tlt1a_.5.o	0.9124 ± 0.0009	0.9143	6.866	560.2	50.0	Displaced fuel in assembly is replaced with water
tlt1a_.6.o	0.9129 ± 0.0009	0.9147	6.784	745.6	60.0	Displaced fuel in assembly is replaced with water
tlt1b_.2.o	0.9120 ± 0.0010	0.9140	6.781	282.2 / 8879.1	20.0	Remaining fuel is homogenized over length of end assembly
tlt1b_.4.o	0.9122 ± 0.0010	0.9141	6.777	436.6 / 2308.5	40.0	Remaining fuel is homogenized over length of end assembly
Fuel from End Assembly Fills 100% of Volume at End of Assembly Stack						
tlt2a.o	0.9114 ± 0.0010	0.9133	6.818	221.9	8.04	End assembly is emptied of fuel; displaced fuel in assembly is replaced with water
tlt2a_.4.o	0.9125 ± 0.0009	0.9143	6.802	436.6	40.0	Displaced fuel in assembly is replaced with water
tlt2b_.4.o	0.9142 ± 0.0009	0.9160	6.702	436.6 / 2074.7	40.0	Remaining fuel is homogenized over length of end assembly
Fuel from Upper Portion of Assembly Fills Volume Between Second and Third Assemblies of Stack						
tlt1sh_.4.o	0.9105 ± 0.0010	0.9124	7.239	436.6 / 2308.5	40.0	Fuel fills 50% of volume; remaining fuel is homogenized over length of assembly
tlt2sh_.4.o	1.0014 ± 0.0010	1.0034	7.548	436.6 / 2074.7	40.0	Fuel fills 100% of volume; remaining fuel is homogenized over length of assembly

NOTE: [a] The first H/X value is for the displaced fuel, while the second value of H/X (if given) is for the homogenized portion of the fuel assembly.

6.2.1.2 C Block Degrades Before the Fuel Compacts

This section presents the results of the calculation described in Section 5.5.1.2.

In the first results of this section, the assembly is broken into pieces and the separation between pieces is varied (shown in Table 19). The results show that as the pieces are moved apart, k_{eff} decreases.

In the last two cases, the C block and water that would be present in the block's voids and channels are homogenized together while leaving the fuel compacts in their intact positions. The assemblies are assumed to maintain their intact size and hexagonal shape. While unphysical since it is highly unlikely that the blocks would maintain their intact shape and size, this case is equivalent to the block being broken into many very small pieces.

Table 19. Intact Fuel Compacts with C Block Broken into Pieces

File Name	$k_{eff} \pm \sigma$	$k_{eff} + 2\sigma$	AENCF (keV)	H/X Ratio	Number of Pieces; Distance Moved in Radial Direction (cm)
hlfa.o	0.8994 ± 0.0009	0.9011	6.799	602.7	2; 0.5
hlfb.o	0.8767 ± 0.0009	0.8784	6.570	602.7	2; 1.0
qrta.o	0.8994 ± 0.0009	0.9011	6.540	602.7	4; 0.5
qrtb.o	0.8699 ± 0.0009	0.8718	6.511	602.7	4; 1.0
hxa.o	0.8984 ± 0.0008	0.9000	6.539	602.7	6; 0.5
hxb.o	0.8771 ± 0.0008	0.8788	6.297	602.7	6; 1.0
Npsa.o	0.9253 ± 0.0009	0.9271	6.526	577.5	Many; 0.0
Npsarf.o	0.9245 ± 0.0009	0.9262	6.670	577.5	(Previous case, but reflective BC)

The logical continuation of the last case in Table 19 would be for the completely degraded C block to fill the bottom of the canister as shown in Figures 10 and 11. Results for these cases with different configurations, pitches, water volume percent in the C rubble and axial separation are given in Table 20. Note that due to the curvature of the canister, the pins are in an irregular array, being neither completely triangular nor square. As such the values of H/X listed in the table are an average of the values for square and triangular lattices. Configurations listed in the comment section of the table refer to Figure 19. (Note that the pin configurations in Configurations h and i are the same as in Figures 10 and 11, respectively, but the material levels are different.

Table 20. Fuel Compacts form "Fuel Pins" in Rubble from Degraded C Blocks

File Name	$k_{eff} \pm \sigma$	$k_{eff} + 2\sigma$	AENCF (keV)	H/X Ratio	% Additional Water in C Rubble	Pitch (cm) / Axial Separation (cm)	Comment
No Axial Separation Between Compacts							
tcha.o	0.8446 ± 0.0011	0.8468	15.593	202.1	0	1.27/ 0.0	Pins touching, configuration "a", see Figure 19

File Name	$k_{eff} \pm \sigma$	$k_{eff} + 2\sigma$	AENCF (keV)	H/X Ratio	% Additional Water in C Rubble	Pitch (cm) / Axial Separation (cm)	Comment
tchb.o	0.7633 ± 0.0010	0.7654	15.740	202.1	0	1.27/ 0.0	Similar to above, but configuration "b",
tchc.o	0.7846 ± 0.0011	0.7868	15.624	202.1	0	1.27/ 0.0	Similar to above, but configuration "c",
tcha+.2.o	0.8467 ± 0.0011	0.8489	14.799	213.5	20	1.27/ 0.0	Configuration "a"
tcha+.4.o	0.8453 ± 0.0011	0.8475	14.659	224.9	40	1.27/ 0.0	Configuration "a"
tcha+.5.o	0.8411 ± 0.0010	0.8431	14.351	230.3	49.4	1.27/ 0.0	Configuration "a" (full canister)
tcha+1.o	0.8372 ± 0.0011	0.8394	13.908	259.2	100	1.27/ 0.0	Configuration "a" all C in rubble is neglected
p1.50a.o	0.8458 ± 0.0011	0.8480	12.983	233.6	0	1.50/ 0.0	Configuration "d", see Figure 19
p1.50a+.5.o	0.8941 ± 0.0010	0.8960	11.176	332.2	49.4	1.50/ 0.0	Configuration "d" (full canister)
p1.75+.3.o	0.9110 ± 0.0010	0.9130	9.289	388.1	30	1.75/ 0.0	Configuration "e", see Figure 19
p1.75+.4.o	0.9179 ± 0.0010	0.9198	8.927	426.2	40	1.75/ 0.0	Configuration "e"
p1.75+.5.o	0.9225 ± 0.0010	0.9245	8.807	462.1	49.4	1.75/ 0.0	Configuration "e" (full canister)
pact+.2.o	0.9013 ± 0.0010	0.9033	9.062	394.3	20	1.8796/ 0.0	Configuration "f"
pact+.4.o	0.9248 ± 0.0010	0.9267	8.027	491.6	40	1.8796/ 0.0	Configuration "f"
pact+.4rf.o	0.9254 ± 0.0009	0.9273	8.256	491.6	40	1.8796/ 0.0	Previous case, but reflective BC
pact+.5.o	0.9274 ± 0.0009	0.9293	7.660	537.4	49.4	1.8796/ 0.0	Configuration "f" (full canister)
pacta+.5.o	0.9032 ± 0.0010	0.9052	8.066	537.4	49.4	1.8796/ 0.0	Similar to above, but configuration "g" (more plausible configuration)
p2.00a.o	0.8174 ± 0.0010	0.8195	9.590	320.1	0	2.0/ 0.0	Configuration "h"
p2.00b.o	0.8445 ± 0.0011	0.8466	8.960	320.1	0	2.0/ 0.0	Configuration "i"
p2.00a+.1.o	0.8549 ± 0.0010	0.8569	9.073	379.2	10	2.0/ 0.0	Configuration "h"
p2.00a+.2.o	0.8817 ± 0.0010	0.8838	8.606	438.3	20	2.0/ 0.0	Configuration "h"
p2.00a+.4.o	0.9007 ± 0.0009	0.9026	7.425	556.5	40	2.0/ 0.0	Configuration "h"
p2.00a+.5.o	0.8994 ± 0.0010	0.9014	7.573	612.1	49.4	2.0/ 0.0	Configuration "h" (full canister)
p2.00b+.1.o	0.8763 ± 0.0010	0.8784	8.652	379.2	10	2.0/ 0.0	Configuration "i"
p2.00b+.2.o	0.8990 ± 0.0010	0.9010	8.337	438.3	20	2.0/ 0.0	Configuration "i"
p2.00b+.4.o	0.9238 ± 0.0009	0.9256	7.524	556.5	40	2.0/ 0.0	Configuration "i"
p2.00b+.5.o	0.9276 ± 0.0009	0.9294	7.353	612.1	49.4	2.0/ 0.0	Configuration "i" (full canister)
Non-zero Axial Separation Between Compacts							
tla_0a.o	0.8485 ± 0.0010	0.8505	14.822	213.5	20	1.27/ 0.0004	Similar to tcha+.2
tla_.05.o	0.8448 ± 0.0011	0.8471	14.835	215.0	20	1.27/ 0.050	Similar to tcha+.2
tla_.1.o	0.8405 ± 0.0010	0.8425	14.659	216.6	20	1.27/ 0.10	Similar to tcha+.2
p2l_.05.o	0.9187 ± 0.0009	0.9206	7.176	618.5	49.4	2.0/ 0.050	Similar to p2.00b+.5
p2l_.1.o	0.9161 ± 0.0009	0.9178	7.062	625.0	49.4	2.0/ 0.10	Similar to p2.00b+.5

Values of pitch for the cases in the table range from that for touching pins, 1.27 cm, to a value of 2.0 cm which is greater than that for the intact fuel assembly, 1.9796 cm. The pins are covered with C rubble that generally contains some volume percent of additional water. This layer is in turn covered by water for all cases except those where the volume percent of water in the rubble mixture is sufficient for the rubble mixture to completely fill the canister. In one case with the pins touching, tcha+1.o, the carbon rubble is neglected and the pins are completely surrounded by water.

Examination of the results in Table 20 shows that k_{eff} increases for increasing pitch and volume fraction of water in the carbon rubble, but decreases for increasing axial separation between fuel compacts, though not significantly. For a given pitch, volume fraction of water in the rubble, and axial separation, reactivity changes occurs for configurations that form different cross-sectional profiles, e.g., Configuration i as compared to Configuration h in Figure 19. These various geometries shown in Figure 19 reflect changing surface to volume (S/V) ratios in which the larger S/V ratios promote more neutron leakage and a decreased k_{eff}. Fortunately, these smaller S/V ratio configurations would appear to be less probable since any disturbance of the WP would tend to spread out the pins and could also decrease their separation (pitch), thereby promoting decreased k_{eff}'s.

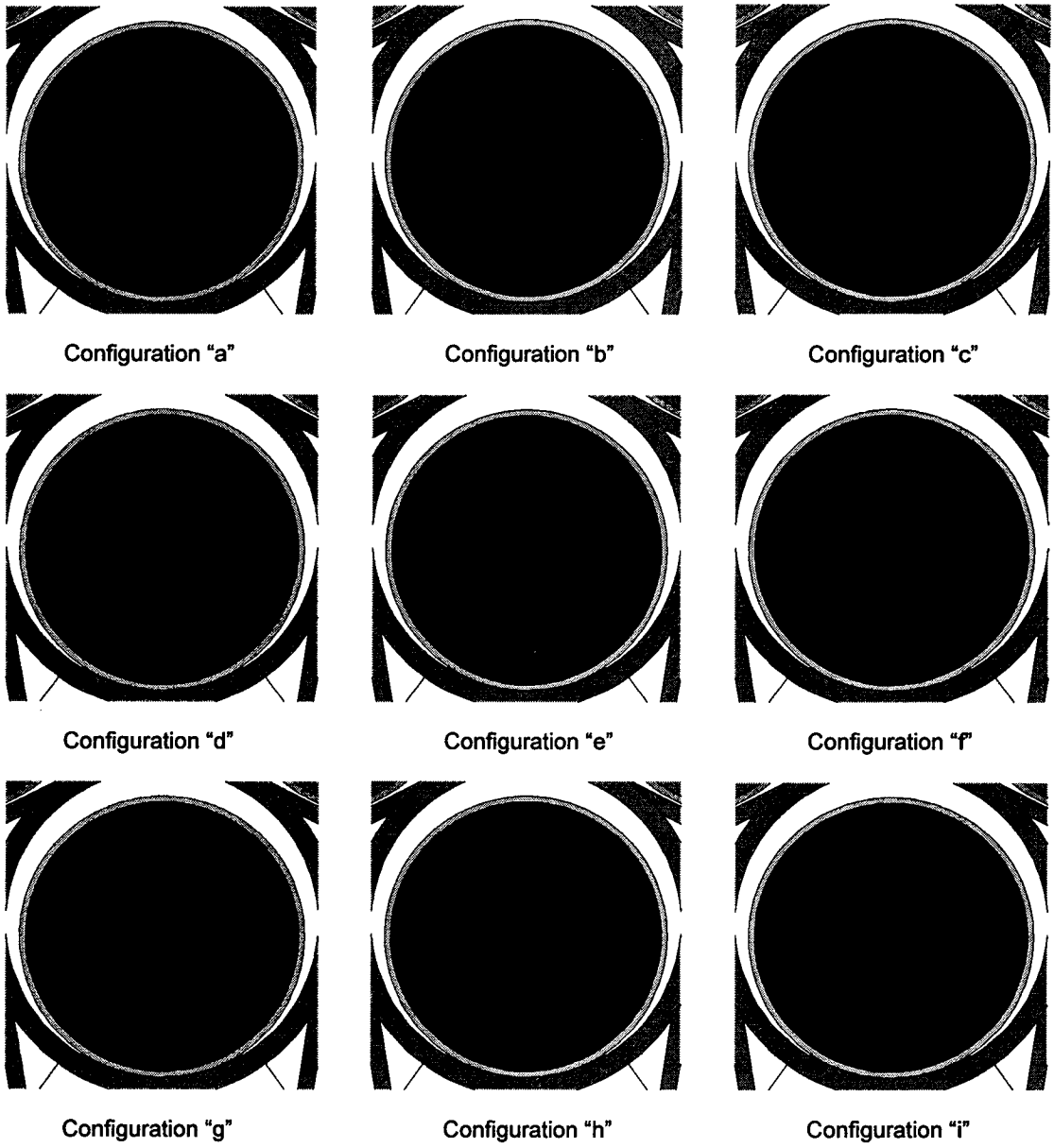

Figure 19. "Fuel Pin" Configurations Investigated in Table 20

6.2.1.3 C Blocks and Fuel Compacts Degrade Before SNF Canister

The results in this section are for configurations where the fuel compacts and C blocks are fully degraded (see Section 5.5.1.3). The first seven cases presented in Table 21 indicate the C rubble from the assemblies is neglected. Next, cases where the degradation products from the fuel compacts and the C blocks do not mix together, i.e. each material mixed only with water forms its own layer, are investigated.

Table 21. Results for Completely Degraded Fuel Assemblies with no Mixing of Degraded Materials in Intact SNF Canister

File Name	$k_{eff} \pm \sigma$	$k_{eff} + 2\sigma$	AENCF (keV)	H/X Ratio in Fuel	Bottom Layer Contents by Volume (%)	Next Layer Contents by Volume (%)
Mixture of Degraded Fuel Compacts and Water (C Neglected)						
[a] f_w.o	0.6994 ± 0.0010	0.7014	18.898	189.5	Fuel 100	—
[a] f.8_w.o	0.7860 ± 0.0011	0.7883	13.927	282.2	Fuel 80 Water 20	—
[a] f.6_w.o	0.8646 ± 0.0010	0.8667	10.212	436.6	Fuel 60 Water 40	—
[a] f.4_w.o	0.9105 ± 0.0009	0.9123	6.894	745.6	Fuel 40 Water 60	—
[a] f.3_w.o	0.9012 ± 0.0008	0.9028	5.501	1054.6	Fuel 30 Water 70	—
[a] f.2_w.o	0.8385 ± 0.0006	0.8398	4.300	1672.6	Fuel 20 Water 80	—
[a] f.176.o	0.8078 ± 0.0006	0.8089	3.793	1920.2	Fuel 17.6 Water 82.4	(canister is full)
Mixture of Degraded Fuel Compacts and Water with a Layer of C)						
f.2_c.o	0.8464 ± 0.0006	0.8476	4.194	1672.6	Fuel 20 Water 80	Carbon 100
f.3_c.o	0.9343 ± 0.0007	0.9357	5.255	1054.6	Fuel 30 Water 70	Carbon 100
c_f.3.o	0.9293 ± 0.0007	0.9308	5.358	1054.6	Carbon 100	Fuel 30 Water 70
f.4_c.o	0.9582 ± 0.0009	0.9600	6.556	745.6	Fuel 40 Water 60	Carbon 100
c_f.4.o	0.9348 ± 0.0008	0.9364	6.543	745.6	Carbon 100	Fuel 40 Water 60
f.6_c.o	0.9347 ± 0.0010	0.9366	9.430	436.6	Fuel 60 Water 40	Carbon 100
[c] f.6_crf.o	0.9360 ± 0.0010	0.9380	9.560	436.6	Fuel 60 Water 40	Carbon 100
[b] f.6_ca.o	0.9328 ± 0.0010	0.9348	9.513	436.6	Fuel 60 Water 40	Carbon 100
f.3_c.8.o	0.9262 ± 0.0008	0.9279	5.469	1054.6	Fuel 30 Water 70	Carbon 80 Water 20
f.3_c.6.o	0.9163 ± 0.0007	0.9178	5.476	1054.6	Fuel 30	Carbon 60 Water 40

File Name	$k_{eff} \pm \sigma$	$k_{eff} + 2\sigma$	AENCF (keV)	H/X Ratio in Fuel	Bottom Layer Contents by Volume (%)	Next Layer Contents by Volume (%)
Mixture of Degraded Fuel Compacts and Water (C Neglected)						
					Water 70	
f.3_c.4.o	0.9123 ± 0.0008	0.9139	5.358	1054.6	Fuel 30 Water 70	Carbon 40 Water 60
f.4_c.8.o	0.9463 ± 0.0008	0.9480	6.823	745.6	Fuel 40 Water 60	Carbon 80 Water 20
f.4_c.6.o	0.9332 ± 0.0009	0.9349	6.747	745.6	Fuel 40 Water 60	Carbon 60 Water 40
f.4_c.4.o	0.9238 ± 0.0009	0.9255	6.833	745.6	Fuel 40 Water 60	Carbon 40 Water 60

NOTES: [a] Carbon from C blocks is neglected.
[b] Different type of Carbon block (type H-327) is used (see Table 3).
[c] WP uses reflective BC on outside surface.

Results from this table show that the most reactive cases, i.e., highest values of k_{eff}, occur when the fuel mixture layer is at the bottom of the canister covered by carbon rubble that contains no additional water. The most reactive fuel mixture shown contains a 60% volume fraction of water.

In the next set of cases some portion of the carbon from the degraded assembly blocks is mixed with the fuel layer. The remaining carbon is in a layer above the fuel mixture. These cases consider varying amounts of carbon, expressed as a volume percent, and use a water volume percent that gives the same H/X ratio as some of the most reactive cases of Table 21. The results for these cases are shown in Table 22, which also shows 4 cases (the last 4) where all of the degraded carbon and fuel are mixed together with varying amounts of water. The cases in this table are more realistic than those in Table 21, since it is more probable that the degradation products would mix together rather than separate in layers.

Table 22. Results for Completely Degraded Fuel Assemblies with Mixed Degraded Materials in Intact SNF Canister

File Name	$k_{eff} \pm \sigma$	$k_{eff} + 2\sigma$	AENCF (keV)	H/X Ratio in Fuel	Case from Table 21 with Same H/X, / % water / and Volume of C (%) (or Comment)	Water Content in C Layer Above Fuel Layer by Volume (%)
f.3+c.1_c.4.o	0.9110 ± 0.0008	0.9125	5.494	1054.6	f.3_c.o / 62.5 / 10	60
f.3+c.1_c.6.o	0.9142 ± 0.0008	0.9157	5.228	1054.6	f.3_c.o / 62.5 /10	40
f.3+c.1_c.8.o	0.9249 ± 0.0008	0.9264	5.374	1054.6	f.3_c.o / 62.5 /10	20
f.3+c.1_c.o	0.9300 ± 0.0008	0.9315	5.314	1054.6	f.3_c.o / 62.5 /10	0
f.3+c.2_c.4.o	0.9077 ± 0.0008	0.9092	4.947	1054.6	f.3_c.o / 55.0 /20	60
f.3+c.2_c.6.o	0.9168 ± 0.0007	0.9182	5.080	1054.6	f.3_c.o / 55.0 /20	40
f.3+c.2_c.8.o	0.9194 ± 0.0008	0.9209	4.946	1054.6	f.3_c.o / 55.0 /20	20
f.3+c.2_c.o	0.9263 ± 0.0007	0.9277	4.993	1054.6	f.3_c.o / 55.0 /20	0
f.3+c.4_c.4.o	0.9062 ± 0.0007	0.9077	4.583	1054.6	f.3_c.o / 40.0 /40	60
f.3+c.4_c.6.o	0.9099 ± 0.0007	0.9113	4.693	1054.6	f.3_c.o / 40.0 /40	40

File Name	$k_{eff} \pm \sigma$	$k_{eff} + 2\sigma$	AENCF (keV)	H/X Ratio in Fuel	Case from Table 21 with Same H/X, / % water / and Volume of C (%) (or Comment)	Water Content in C Layer Above Fuel Layer by Volume (%)
f.3+c.4_c.8.o	0.9108 ± 0.0008	0.9123	4.706	1054.6	f.3_c.o / 40.0 /40	20
f.3+c.4_c.o	0.9107 ± 0.0008	0.9123	4.839	1054.6	f.3_c.o / 40.0 /40	0
f.4+c.1_c.4.o	0.9208 ± 0.0009	0.9225	6.381	745.6	f.4_c.o / 53.3 /10	60
f.4+c.1_c.6.o	0.9318 ± 0.0008	0.9335	6.643	745.6	f.4_c.o / 53.3 /10	40
f.4+c.1_c.8.o	0.9439 ± 0.0008	0.9456	6.509	745.6	f.4_c.o / 53.3 /10	20
f.4+c.1_c.o	0.9550 ± 0.0008	0.9567	6.422	745.6	f.4_c.o / 53.3 /10	0
f.4+c.2_c.4.o	0.9207 ± 0.0009	0.9225	6.367	745.6	f.4_c.o / 46.7 /20	60
f.4+c.2_c.6.o	0.9288 ± 0.0009	0.9305	6.576	745.6	f.4_c.o / 46.7 /20	40
f.4+c.2_c.8.o	0.9394 ± 0.0009	0.9413	6.289	745.6	f.4_c.o / 46.7 /20	20
f.4+c.2_c.o	0.9497 ± 0.0009	0.9515	6.207	745.6	f.4_c.o / 46.7 /20	0
f.4+c.4_c.4.o	0.9176 ± 0.0008	0.9193	5.764	745.6	f.4_c.o / 33.3 /40	60
f.4+c.4_c.6.o	0.9257 ± 0.0009	0.9274	5.786	745.6	f.4_c.o / 33.3 /40	40
f.4+c.4_c.8.o	0.9316 ± 0.0008	0.9333	5.692	745.6	f.4_c.o / 33.3 /40	20
f.4+c.4_c.o	0.9318 ± 0.0008	0.9335	5.702	745.6	f.4_c.o / 33.3 /40	0
f.4+c.5_c.o	0.9173 ± 0.0009	0.9192	5.568	745.6	f.4_c.o / 26.7 /50	0
f.6+c.1_c.o	0.9308 ± 0.0010	0.9328	9.339	436.6	f.6_c.o / 35.0 /10	0
f.6+c.2_c.o	0.9241 ± 0.0010	0.9261	9.053	436.6	f.6_c.o / 30.0 /20	0
f.6+c.4_c.o	0.9087 ± 0.0009	0.9106	8.314	436.6	f.6_c.o / 20.0 /40	0
f+c_w.o	0.8045 ± 0.0010	0.8065	8.551	335.4	(all of C mixed in and no additional water)	—
f+c+w.2_w.o	0.8999 ± 0.0010	0.9018	5.828	647.0	(all of C mixed in and 20% additional water)	—
fcw.2_wrf.o	0.9020 ± 0.0009	0.9039	5.767	647.0	(Previous case, but reflective BC)	—
f+c+w.4061.o	0.8896 ± 0.0007	0.8911	4.428	1190.6	(all of C mixed in and 40.69% additional water; canister is full)	—

6.2.2 Outer Components of the WP Degrade (Outside SNF Canister)

This section gives the results of the calculations described in Section 5.5.2. In the configurations studied in this section, the high-level waste canisters and the waste package basket degrade before the inner component (fuel assembly) of the SNF canister. The results in this section are divided depending upon whether the SNF canister is intact, results given in Section 6.2.2.1, or degraded, results in Section 6.2.2.2.

6.2.2.1 Intact SNF Canister with Contents Either Intact or Degraded Surrounded by Pre-breach Clay in the WP

The results in this section are for an intact SNF canister and are described in Section 5.5.2.1. Table 23 gives values of k_{eff} for waste packages containing an intact SNF canister surrounded by pre-breach clay. The volume percent of water in the pre-breach clay is varied as shown in Table

23. The cases in Table 23 are taken from the previous results in this report, but replace the intact outer contents of the WP with pre-breach clay.

The first two sets of results in Table 23 are for a canister containing intact fuel positioned at different depths in either dry or water containing pre-breach clay. In the first set, the WP contains dry clay and the location of the canister is varied from being just under the surface of the clay to being at the bottom of the WP. Cases are investigated where the canister is at the bottom of the WP which is reflected by tuff and a reflective BC. In the second set, the canister is located at what is found to be a more reactive location in the WP by varying its height along a vertical centerline in the clay mixture, and the volume percent of water in the clay is increased until the WP is completely filled. Finally, the set of cases are for the canister containing degraded fuel, as noted in the table, that is positioned in the most reactive pre-breach clay configuration. The effect of replacing the water reflector with tuff is also investigated.

Table 23. Intact SNF Canister Surrounded by Pre-Breach Clay

File Name	$k_{eff} \pm \sigma$	$k_{eff} + 2\sigma$	AENCF (keV)	^{a}H/X Ratio	Comments
Canister (Containing Intact Assemblies) Positioned at Different Depths in Dry Pre-breach Clay					
cs1_prba.o	0.9140 ± 0.0010	0.9159	6.526	602.7	Top of SNF canister at top of dry pre-breach clay at 59473 years (case cs1.o, Table 14)
cs1_prbb.o	0.9167 ± 0.0009	0.9185	6.372	602.7	Canister positioned between top and center of dry pre-breach clay at 59473 years (case cs1.o, Table 14)
cs1_prbc.o	0.9168 ± 0.0009	0.9185	6.496	602.7	Canister positioned at center of dry pre-breach clay at 59473 years (case cs1.o, Table 14)
cs1_prbcrf.o	0.9171 ± 0.0009	0.9188	6.467	602.7	Previous case, but uses reflective BC
cs1_cal.o	0.9150 ± 0.0009	0.9169	6.567	602.7	Canister positioned at center of dry pre-breach clay at 53241 years (case cs1.o, Table 14) (alternative clay)
cs1_prbd.o	0.9175 ± 0.0009	0.9193	6.409	602.7	Canister positioned between bottom and center of dry pre-breach clay at 59473 years (case cs1.o, Table 14)
cs1_prbe.o	0.9161 ± 0.0009	0.9179	6.360	602.7	Canister at bottom of dry pre-breach clay at 59473 years (case cs1.o, Table 14)
cs1_prbetf.o	0.9192 ± 0.0009	0.9209	6.588	602.7	Previous case, but reflected by dry tuff
cs1_prberf.o	0.9265 ± 0.0009	0.9283	6.524	602.7	Previous case, but uses reflective BC
Canister (Containing Intact Assemblies) Centered in Pre-breach Clay Containing Water					
cs1_c+.9.o	0.9110 ± 0.0008	0.9127	6.492	602.7	Canister positioned at center of pre-breach clay with 10 vol. % of water at 59473 years (case cs1.o, Table 14)
cs1_c+.8.o	0.9073 ± 0.0010	0.9093	6.636	602.7	Canister positioned at center of pre-breach clay with 20 vol. % of water at 59473 years (case cs1.o, Table 14)
cs1_c+.714.o	0.9038 ± 0.0009	0.9056	6.537	602.7	Canister positioned at center of pre-breach clay containing 28.6% water which fills WP at 59473 years (case cs1.o, Table 14)
Canister (Containing Partially or Completely Degraded Fuel Components) Centered in Dry Pre-breach Clay					
fl_2%pc.o	0.9264 ± 0.0009	0.9281	6.251	591.9	Canister positioned at center of dry pre-breach clay at 59473 years (case fl_2%.o, Table 15)
fl_3%pc.o	0.9303 ± 0.0009	0.9321	6.480	586.7	Canister positioned at center of dry pre-breach clay at 59473 years (case fl_3%.o, Table 15)
bd.1w.4pc.o	0.9300 ± 0.0009	0.9317	6.573	317.9	Canister positioned at center of dry pre-breach clay at 59473 years (case bd.1+w.4.o, Table 16)
a.1w.4pc.o	0.9065 ± 0.0009	0.9083	6.117	689.8 / 317.9	Canister positioned at center of dry pre-breach clay at 59473 years (case alt.1+w.4h.o, Table 17)
t1a_.4pbc.o	0.9137 ± 0.0009	0.9156	6.423	436.6	Canister positioned at center of dry pre-breach clay at 59473 years (case tlt1a_.4.o, Table 18)

File Name	$k_{eff} \pm \sigma$	$k_{eff} + 2\sigma$	AENCF (keV)	[a]H/X Ratio	Comments
t2b_.4pbc.o	0.9149 ± 0.0009	0.9166	6.303	436.6 / 2074.7	Canister positioned at center of dry pre-breach clay at 59473 years (case tlt2b_.4.o, Table 18)
Npsapc.o	0.9273 ± 0.0009	0.9291	6.451	577.5	Canister positioned at center of dry pre-breach clay at 59473 years (case Npsa.o, Table 19)
pa.5pc.o	0.9368 ± 0.0010	0.9387	7.577	394.8	Canister positioned at center of dry pre-breach clay at 59473 years (case pact+.5.o, Table 20)
paa.5pc.o	0.9154 ± 0.0009	0.9173	7.706	394.8	Canister positioned at center of dry pre-breach clay at 59473 years (case pacta+.5.o, Table 20)
f.6_cpc.o	0.9495 ± 0.0009	0.9513	9.046	436.6	Canister positioned at center of dry pre-breach clay at 59473 years (case f.6_c.o, Table 21)
f.3c.4cpc.o	0.9156 ± 0.0008	0.9172	4.260	1054.6	Canister positioned at center of dry pre-breach clay at 59473 years (case f.3+c.4_c.o, Table 22)
f.4c.5cpc.o	0.9241 ± 0.0009	0.9259	5.229	745.6	Canister positioned at center of dry pre-breach clay at 59473 years (case f.4+c.5_c.o, Table 22)
f.6c.2cltf.o	0.9402 ± 0.0010	0.9422	8.449	436.6	Canister at bottom of dry pre-breach clay at 59473 years, WP reflected by tuff (case: f.6+c.2_c.o, Table 22)
f.6c.4cltf.o	0.9244 ± 0.0010	0.9264	7.973	436.6	Canister at bottom of dry pre-breach clay at 59473 years, WP reflected by tuff (case: f.6+c.4_c.o, Table 22)

NOTE: [a] If two values of H/X are given, the first is for the fuel assembly while the second is for the displaced fuel.

The results show that k_{eff} for the canister containing intact fuel does not (statistically) change as the position of the canister is varied in the dry pre-breach clay (at 59473 years). For the canister containing intact fuel, k_{eff} decreases as the volume percent of water in the clay increases. This occurs because the water 'thermalizes' neutrons away from the canister, making them more prone to capture rather than reflection. For the degraded cases, the canister is centered in dry clay, which is the most reactive configuration for the clay because of its reflective properties.

6.2.2.2 Intact and Degraded Fuel Components Surrounded by Products of Degraded SNF Canister with Non-reacted Pre-breach Clay

The results in this section are for a degraded SNF canister that has mixed, but not chemically reacted, with the pre-breach clay formed from the degradation of the outer components of the WP. These results are described in Section 5.5.2.2 and are presented in Sections 6.2.2.2.1 (intact assemblies), 6.2.2.2.2 (intact fuel compacts with degraded C blocks) and 6.2.2.2.3 (completely degraded fuel assemblies).

6.2.2.2.1 Intact Assemblies Surrounded by Degradation Products of the SNF Canister and Pre-breach Clay

The results in this section are for cases described in Section 5.5.2.2.1. The results for these cases are given in Table 24.

In the first set of results, the goethite and clay form separate layers with varying amounts of water as indicated in the table. In the next set of results the goethite mixed with various volume percentages of water forms either a cylinder or hexagon that surrounds the assemblies. The assemblies are centered in the dry pre-breach clay layer that was shown, in the first set of results,

to be the most reactive configuration. The c/v channels of the assemblies contain water, unless noted otherwise, in which case they contain water and/or pre-breach clay or goethite.

Table 24. Intact Assemblies Surrounded by Goethite and Pre-Breach Clay in the WP

File Name	$k_{eff} \pm \sigma$	$k_{eff} + 2\sigma$	AENCF (keV)	H/X Ratio	Bottom (or Surrounding) Layer Contents by Volume (%)	Next Layer Contents by Volume (%)	Comment
Goethite and Clay Form Separate Layers in WP							
in_cla.o	0.9085 ± 0.0009	0.9103	6.761	602.7	Goethite 100	Clay 100	assembly just under top of clay layer
in_clc.o	0.9129 ± 0.0009	0.9146	6.645	602.7	Goethite 100	Clay 100	assembly centered in clay layer
in_cle.o	0.9039 ± 0.0009	0.9057	6.760	602.7	Goethite 100	Clay 100	assembly just above top of goethite
in_clerf.o	0.9110 ± 0.0009	0.9128	6.860	602.7	Goethite 100	Clay 100	previous case, but reflective BC
in_cl.9c.o	0.9032 ± 0.0009	0.9051	6.876	602.7	Goethite 100	Clay 90 Water 10	assembly centered in clay layer
in_cl.8c.o	0.8941 ± 0.0009	0.8959	6.687	602.7	Goethite 100	Clay 90 Water 20	assembly centered in clay layer
in_cl.714c.o	0.8889 ± 0.0009	0.8907	6.846	602.7	Goethite 100	Clay 71.4 Water 28.6	assembly centered in clay layer (canister full)
in_clc-w.9.o	0.8835 ± 0.0009	0.8852	7.180	575.8	Goethite 100	Clay 100	Assembly centered in clay layer; 10% vf clay in c/v channels
in_clc-w.8.o	0.8534 ± 0.0009	0.8552	7.501	548.9	Goethite 100	Clay 100	Assembly centered in clay layer; 20% vf clay in c/v channels
in_clc-w.o	0.6545 ± 0.0008	0.6561	10.509	333.6	Goethite 100	Clay 100	assembly centered in clay layer; 100% vf clay in c/v channels
Goethite Mixture Forms Layer Around Assemblies							
cyl_clc.o	0.9011 ± 0.0008	0.9028	6.746	602.7	(Goethite 100)	Clay 100	goethite cylinder surrounds assembly centered in clay layer
cyl.9_clc.o	0.9081 ± 0.0009	0.9099	6.819	602.7	(Goethite 90 Water 10)	Clay 100	goethite cylinder surrounds assembly centered in clay layer
cyl.9_clerf.o	0.9189 ± 0.0009	0.9207	6.612	602.7	(Goethite 90 Water 10)	Clay 100	assembly at bottom of WP, reflective BC
cyl.6_clc.o	0.9000 ± 0.0010	0.9019	6.807	602.7	(Goethite 60 Water 40)	Clay 100	goethite cylinder surrounds assembly centered in clay layer
hex_clc.o	0.9000 ± 0.0009	0.9018	6.815	602.7	(Goethite 100)	Clay 100	goethite hexagon surrounds assembly centered in clay layer
hex.9_clc.o	0.9052 ± 0.0009	0.9069	6.864	602.7	(Goethite 90 Water 10)	Clay 100	goethite hexagon surrounds assembly centered in clay layer
hex.6_clc.o	0.8998 ± 0.0009	0.9016	6.558	602.7	(Goethite 60 Water 40)	Clay 100	goethite hexagon surrounds assembly centered in clay layer

File Name	$k_{eff} \pm \sigma$	$k_{eff} + 2\sigma$	AENCF (keV)	H/X Ratio	Bottom (or Surrounding) Layer Contents by Volume (%)	Next Layer Contents by Volume (%)	Comment
cyl.9_clc-w.9.o	0.8746 ± 0.0009	0.8763	6.947	586.3	(Goethite 90 Water 10)	Clay 100	goethite cylinder surrounds assembly centered in clay layer; 10% vf goethite in c/v channels
cyl.9_clc-w.8.o	0.8447 ± 0.0009	0.8465	7.252	569.9	(Goethite 90 Water 10)	Clay 100	goethite cylinder surrounds assembly centered in clay layer; 20% vf goethite in c/v channels
cyl.9_clc-w.6.o	0.7942 ± 0.0009	0.7959	7.581	537.0	(Goethite 90 Water 10)	Clay 100	goethite cylinder surrounds assembly centered in clay layer; 40% vf goethite in c/v channels
cyl.9_clc-w0.o	0.6725 ± 0.0008	0.6740	9.694	438.4	(Goethite 90 Water 10)	Clay 100	goethite cylinder surrounds assembly centered in clay layer; 100% vf goethite in c/v channels

6.2.2.2.2 Intact Fuel Compacts Surrounded by Degradation Products of the SNF Canister and Pre-breach Clay

The results in this section are for cases described in Section 5.5.2.2.2 where the C assembly blocks have degraded and the fuel compacts remain intact. In this section, the values of H/X listed in the table are an average of the values for square and triangular lattices and are also weighted by the number of "fuel pins" in each layer (for those cases where the fuel pins are in different layers).

The first set of results in Table 25 is for pins collected at the bottom of the WP surrounded by degradation products that form separate layers. In general, some of the pins are in each of the different layers depending on the volume of each material, the order in which the materials are layered and the height of the pin stack. The composition of each layer is given in the table as well as the volume fraction of water in the materials. These cases all use the same pitch as the intact fuel assembly, 1.8796 cm. In the next set of results in the table, the goethite and C rubble are mixed together with various volume percentages of water. The pitch for these cases is the same as that for the intact assembly, except for the last two cases of the second set where the pitch is 1.27 cm, (touching pins; case ptag+C.4_cl.o), and 1.575 cm, (the average of the pitches for the intact assembly and touching pins; case p.5ag+C.4_cl.o). In the final set of cases in the table, a small amount of clay is mixed in with the goethite and C rubble layer at the bottom of the WP. The pitch for these cases is also the same as that for the intact assembly.

Table 25. Fuel Compacts Form "Pins" Piled at the Bottom of the WP Surrounded by Layers of C Rubble, Goethite and Pre-breach Clay

File Name	$k_{eff} \pm \sigma$	$k_{eff} + 2\sigma$	AENCF (keV)	H/X Ratio	Bottom Layer Contents by Volume (%)	Next Layer Contents by Volume (%)	Top Layer Contents by Volume (%)	Pitch (cm)/ Comment
Goethite, C Rubble and Clay Form Separate Layers in WP								
p0ag_C_cl.o	0.6232 ± 0.0008	0.6247	12.936	330.5	Goethite 100	C 100	Clay 100	1.8796
p0ag.8_C_cl.o	0.6430 ± 0.0007	0.6445	12.165	366.7	Goethite 80 Water 20	C 100	Clay 100	1.8796
p0ag.6_C_cl.o	0.6702 ± 0.0008	0.6717	11.479	417.1	Goethite 60 Water 40	C 100	Clay 100	1.8796
p0ag.4_C_cl.o	0.7183 ± 0.0008	0.7199	10.340	494.4	Goethite 40 Water 60	C 100	Clay 100	1.8796
p0ag_C.8_cl.o	0.6916 ± 0.0008	0.6932	11.420	372.7	Goethite 100	C 80 Water 20	Clay 100	1.8796
p0ag_C.6_cl.o	0.7638 ± 0.0009	0.7655	9.768	435.9	Goethite 100	C 60 Water 40	Clay 100	1.8796
p0ag_C.4_cl.o	0.8328 ± 0.0010	0.8347	8.486	527.8	Goethite 100	C 40 Water 60	Clay 100	1.8796
p0ag_C_cl.8.o	0.6357 ± 0.0009	0.6376	12.605	364.1	Goethite 100	C 100	Clay 80 Water 20	1.8796
p0ag_C_cl.714.o	0.6443 ± 0.0008	0.6460	11.803	364.1	Goethite 100	C 100	Clay 71.4 Water 28.6	1.8796 / nearly full canister
p0ag.4_C.4_cl.o	0.8153 ± 0.0009	0.8171	8.250	624.2	Goethite 40 Water 60	C 40 Water 60	Clay 100	1.8796
p0ag.4_C.4_cl.74.o	0.8081 ± 0.0008	0.8098	8.236	624.2	Goethite 40 Water 60	C 40 Water 60	Clay 74 Water 26	1.8796
Goethite and C Rubble Mixed Together Form Bottom Layer								
p0ag+C_cl.o	0.6202 ± 0.0008	0.6219	13.086	307.5	Goethite 29.3 C 70.7	Clay 100	Water 100	1.8796
p0ag+C.8_cl.o	0.6974 ± 0.0008	0.6991	11.296	387.9	Goethite 23.4 C 56.6 Water 20	Clay 100	Water 100	1.8796
p0ag+C.6_cl.o	0.7725 ± 0.0008	0.7742	9.703	489.2	Goethite 17.6 C 42.4 Water 40	Clay 100	Water 100	1.8796
p0ag+C.4_cl.o	0.8318 ± 0.0009	0.8336	8.013	606.4	Goethite 11.7 C 28.3 Water 60	Clay 100	Water 100	1.8796
p.5ag+C.4_cl.o	0.8387 ± 0.0009	0.8406	10.324	404.7	Goethite 11.7 C 28.3 Water 60	Clay 100	Water 100	1.575
ptag+C.4_cl.o	0.7832 ± 0.0010	0.7852	14.953	238.4	Goethite 11.7 C 28.3 Water 60	Clay 100	Water 100	1.27
Goethite, C Rubble and Clay Mixed Together Form Bottom Layer								
p0acl.05+g+C.4_cl.o	0.8115 ± 0.0008	0.8131	8.509	600.9	Goethite 10.2 C 24.8 Water 60 Clay 5	Clay 100	Water 100	1.8796

File Name	$k_{eff} \pm \sigma$	$k_{eff} + 2\sigma$	AENCF (keV)	H/X Ratio	Bottom Layer Contents by Volume (%)	Next Layer Contents by Volume (%)	Top Layer Contents by Volume (%)	Pitch (cm)/ Comment
p0acl.1+g+C.4_cl.o	0.7858 ± 0.0009	0.7875	8.836	595.5	Goethite 8.8 C 21.2 Water 60 Clay 10	Clay 100	Water 100	1.8796

The results in Table 26 are for cases where the pins remain clumped together in either a circular or hexagonal array rather than forming a pile at the bottom of the WP. Unless indicated otherwise, the array of pins is approximately centered in the clay.

For the first set of results in the table, the fuel pins are assumed to remain in their intact positions and thus remain in a hexagonal array. The volume percentage of additional water in the C rubble is varied as indicated in the table. For example in the first case of the set, the volume of water is equal to the volume of the c/v channels and is homogenized with the C rubble so that the volume and shape of the mixture surrounding the fuel pins are exactly the same as for the intact assembly.

For the remaining cases in the table the "fuel pins" are arranged so as to form a circular array or a cylinder of fuel pins. In the first set of cases for this type of array, the pins are surrounded by C rubble with varying amounts of water, which in turn are surrounded by an annulus of goethite and finally by pre-breach clay. The pitch of the pins is varied from that of the intact assembly, 1.8796 cm, to that for touching pins, 1.27 cm. The configurations for the cases with the pins touching include 3 additional fuel pins to fill the void at the center of the array, i.e., more fuel is modeled than is actually in the 5 assemblies. The void is a consequence of the outermost pins being at the same distance from the array's center, i.e., the array is filled from the outside towards the center.

For a given set of degradation product compositions, reducing the pitch reduces the reactivity of the system. Also, three variations of cases cytcC.4_g_cl.o are presented where some or all of the C rubble is replaced by water. The results in this set of cases show the two opposing roles that the C from the graphite block can play. First, if the carbon displaces water, i.e., it plays the role of a moderator displacer, the system becomes less reactive. On the other hand, if its presence separates the "fuel pins" the system is more reactive than if the fuel is touching. A greater water content in the C would decrease the density of the mixture, and make it less likely to support (and separate) the "fuel pins". Conversely, less water in the C would allow it to physically support (and separate) the fuel pins, but would also displace water which plays a much greater role in moderation than does the C.

In the next to the last set of cases a small amount of goethite is mixed in with the C rubble and water that directly surrounds the fuel pins. These cases are variations of case cy0cC.6_g_cl.o, having the same percent of additional water (40%). A small addition of even 5% goethite by

volume reduces k_{eff} by over 4%. Finally, in the last set of cases a homogeneous mixture of C rubble with varied amounts of goethite and water surrounds the pins. The pitch for these cases is the same as for the intact assembly and the array of pins is positioned near the center of the pre-breach clay layer.

Table 26. Fuel Compacts Form Circular or Hexagonal Array of "Pins" Surrounded by Layers of C Rubble, Goethite and Pre-breach Clay in the WP

File Name	$k_{eff} \pm \sigma$	$k_{eff} + 2\sigma$	AENCF (keV)	H/X Ratio	Contents of First Layer Around Fuel by Volume (%)	Contents of Next Layer by Volume (%)	Contents of Outermost Layer by Volume (%)	Pitch (cm)/ Comment
Fuel Pins and Layers of C Rubble and Goethite Form Hexagonal Array								
hexc_g_cl.o	0.9147 ± 0.0009	0.9165	6.640	577.5	C 73.4 Water 26.6	Goethite 100	Clay 100	1.8796
hexc.7_g_cl.o	0.9173 ± 0.0010	0.9193	6.385	604.4	C 70 Water 30	Goethite 100	Clay 100	1.8796
hexc.6_g_cl.o	0.9268 ± 0.0009	0.9286	6.217	684.1	C 60 Water 40	Goethite 100	Clay 100	1.8796
hx.6_g_cltf.o	0.9256 ± 0.0009	0.9274	6.171	684.1	C 60 Water 40	Goethite 100	Clay 100	1.8796/ fuel at bottom of WP reflected by dry tuff
hx.6_g_clrf.o	0.9333 ± 0.0008	0.9349	6.356	684.1	C 60 Water 40	Goethite 100	Clay 100	previous case, but reflective BC
hexc.5_g_cl.o	0.9227 ± 0.0008	0.9244	5.932	763.7	C 50 Water 50	Goethite 100	Clay 100	1.8796
hexc.4_g_cl.o	0.9123 ± 0.0009	0.9141	5.876	843.4	C 40 Water 60	Goethite 100	Clay 100	1.8796
Fuel Pins and Separate Layers of C Rubble and Goethite Form Circular Array								
cy0aC_g_cl.o	0.8637 ± 0.0010	0.8657	9.411	297.0	C 100	Goethite 100	Clay 100	1.8796/ fuel at bottom of WP
cy0aC_g_clrf.o	0.8906 ± 0.0010	0.8927	9.009	297.0	C 100	Goethite 100	Clay 100	previous case, but reflective BC
cy0cC_g_cl.o	0.8695 ± 0.0011	0.8716	9.214	297.0	C 100	Goethite 100	Clay 100	1.8796/ fuel centered in clay
cy0eC_g_cl.o	0.8629 ± 0.0010	0.8649	9.492	297.0	C 100	Goethite 100	Clay 100	1.8796/ fuel just under top of clay
cy0cC.8_g_cl.o	0.9312 ± 0.0009	0.9331	8.077	394.3	C 80 Water 20	Goethite 100	Clay 100	1.8796/ fuel centered in clay
cy0cC.6_g_cl.o	0.9574 ± 0.0009	0.9592	7.454	491.6	C 60 Water 40	Goethite 100	Clay 100	1.8796/ fuel centered in clay
cy0cC.4_g_cl.o	0.9515 ± 0.0009	0.9534	6.805	588.9	C 40 Water 60	Goethite 100	Clay 100	1.8796/ fuel centered in clay

File Name	$k_{eff} \pm \sigma$	$k_{eff} + 2\sigma$	AENCF (keV)	H/X Ratio	Contents of First Layer Around Fuel by Volume (%)	Contents of Next Layer by Volume (%)	Contents of Outermost Layer by Volume (%)	Pitch (cm)/ Comment
	Variations of Fuel Pin Pitch							
cy.75cC.6_g_cl.o	0.9532 ± 0.0010	0.9552	8.217	416.6	C 60 Water 40	Goethite 100	Clay 100	1.73/ fuel centered in clay
cy.5cC.6_g_cl.o	0.9435 ± 0.0010	0.9455	9.374	345.4	C 60 Water 40	Goethite 100	Clay 100	1.575/ fuel centered in clay
cy.25cC.6_g_cl.o	0.9267 ± 0.0010	0.9288	10.790	281.0	C 60 Water 40	Goethite 100	Clay 100	1.42/ fuel centered in clay
[a] cytcC_g_cl.o	0.8941 ± 0.0011	0.8963	14.090	202.1	C 100	Goethite 100	Clay 100	1.27/ fuel centered in clay
[a] cytcC.8_g_cl.o	0.9078 ± 0.0010	0.9098	13.422	213.5	C 80 Water 20	Goethite 100	Clay 100	1.27/ fuel centered in clay
[a] cytcC.6_g_cl.o	0.9055 ± 0.0011	0.9076	13.183	224.9	C 60 Water 40	Goethite 100	Clay 100	1.27/ fuel centered in clay
[a] cytcC.4_g_cl.o	0.8894 ± 0.0010	0.8915	13.094	236.3	C 40 Water 60	Goethite 100	Clay 100	1.27/ fuel centered in clay
[a] cytcC0_g_cl.o	0.8654 ± 0.0011	0.8676	12.885	259.2	Water 100	Goethite 100	Clay 100	previous case, but water replaces C
[a] cytcC0p_g_cl.o	0.8725 ± 0.0010	0.8746	13.423	259.2	Water 100 (amount of water reduced around assembly)	Goethite 100	Clay 100	previous case, but goethite directly surrounds fuel
cytcC0pm_g_cl.o	0.8694 ± 0.0011	0.8716	13.338	259.2	Water 100	Goethite 100	Clay 100	previous case, but 210 pins/ element
Fuel Pins and Separate Layers of C Rubble (Mixed with Some Goethite) and Goethite Form Circular Array								
cy0cC.6+g.05_g_cl.o	0.9177 ± 0.0009	0.9195	7.619	499.1	C 55 Water 40 Goethite 5	Goethite 100	Clay 100	1.8796/ variation of cy0cC.6_g_cl.o
cC.6+g.05_g_clrf.o	0.9211 ± 0.0009	0.9229	7.550	499.1	C 55 Water 40 Goethite 5	Goethite 100	Clay 100	Previous case, but reflective BC
cy0cC.6+g.1_g_cl.o	0.8789 ± 0.0008	0.8806	7.758	506.5	C 50 Water 40 Goethite 10	Goethite 100	Clay 100	1.8796/ variation of cy0cC.6_g_cl.o
All of C Rubble and Goethite Mixed Together Form Layer Around Fuel Pins in Circular Array								
cy0cC+g.8_cl.o	0.7943 ± 0.0009	0.7960	9.060	429.3	C 56.6 Water 20 Goethite 23.4	Clay 100	Water 100	1.8796

File Name	$k_{eff} \pm \sigma$	$k_{eff} + 2\sigma$	AENCF (keV)	H/X Ratio	Contents of First Layer Around Fuel by Volume (%)	Contents of Next Layer by Volume (%)	Contents of Outermost Layer by Volume (%)	Pitch (cm)/ Comment
cy0cC+g.6_cl.o	0.8266 ± 0.0009	0.8283	8.356	517.9	C 42.4 Water 40 Goethite 17.6	Clay 100	Water 100	1.8796
cy0cC+g.4_cl.o	0.8587 ± 0.0008	0.8603	7.729	606.4	C 28.3 Water 60 Goethite 11.7	Clay 100	Water 100	1.8796
cy0cC+g.3_cl.o	0.8755 ± 0.0009	0.8774	7.495	650.7	C 21.2 Water 70 Goethite 8.8	Clay 100	Water 100	1.8796
cy0cC+g.2_cl.o	0.8905 ± 0.0009	0.8923	7.129	694.9	C 14.1 Water 80 Goethite 5.9	Clay 100	Water 100	1.8796
cy0cC+g.2_clp.o	0.8907 ± 0.0009	0.8924	7.091	694.9	C 14.1 Water 80 Goethite 5.9	Clay 100	Water 100	1.8796/ above case, but pins more centered in clay

NOTE: [a] Three additional fuel pins are added at center of circular array to fill center void (213 pins/assembly).

6.2.2.2.3 Completely Degraded Fuel Compacts, SNF Canister Degradation Products and Pre-breach Clay in the WP

The results in this section are for cases described in Section 5.5.2.2.3 where the C assembly blocks and the fuel compacts have fully degraded and are in the WP with pre-breach clay. These results are shown in Table 27.

Table 27. Completely Degraded Fuel Compacts, C Rubble, Goethite and Pre-breach Clay Form Layers in the WP

File Name	$k_{eff} \pm \sigma$	$k_{eff} + 2\sigma$	AENCF (keV)	H/X Ratio	Contents of Bottom Layer by Volume (%)	Contents of Next Layer by Volume (%)	Contents of Next Layer by Volume (%)	Contents of Top Layer by Volume (%)
Separate Layers for Each Degradation Product								
f_C_g_cl.o	0.5464 ± 0.0009	0.5482	19.520	189.5	Fuel 100	C 100	Goethite 100	Clay 100
f.8_C_g_cl.o	0.6217 ± 0.0009	0.6236	14.545	282.2	Fuel 80 Water 20	C 100	Goethite 100	Clay 100
f.6_C_g_cl.o	0.6981 ± 0.0010	0.7000	10.377	436.6	Fuel 60 Water 40	C 100	Goethite 100	Clay 100
f.5_C_g_cl.o	0.7304 ± 0.0009	0.7322	8.638	560.2	Fuel 50 Water 50	C 100	Goethite 100	Clay 100
f.4_C_g_cl.o	0.7523 ± 0.0009	0.7541	6.894	745.6	Fuel 40 Water 60	C 100	Goethite 100	Clay 100
g_f.4_C_cl.o	0.6934 ± 0.0009	0.6951	6.968	745.6	Goethite 100	Fuel 40 Water 60	C 100	Clay 100

File Name	$k_{eff} \pm \sigma$	$k_{eff} + 2\sigma$	AENCF (keV)	H/X Ratio	Contents of Bottom Layer by Volume (%)	Contents of Next Layer by Volume (%)	Contents of Next Layer by Volume (%)	Contents of Top Layer by Volume (%)
f.2_C_g_cl.o	0.7236 ± 0.0006	0.7248	3.942	1672.6	Fuel 20 Water 80	C 100	Goethite 100	Clay 100
Separate Layers for Each Degradation Product Except Some C Mixed in with Fuel								
[a] f.4+C.2_C_g_cl.o	0.7327 ± 0.0008	0.7344	6.764	745.6	Fuel 33.4 Water 46.6 C 20	C 100	Goethite 100	Clay 100
[a] f.4+C.4_C_g_cl.o	0.7010 ± 0.0009	0.7027	6.399	745.6	Fuel 26.9 Water 33.1 C 40	C 100	Goethite 100	Clay 100
Separate Layer of Fuel Mixed with C and Remaining Degradation Products in Separate Layers								
f+C_g_cl.o	0.5419 ± 0.0009	0.5436	10.270	347.9	Fuel 29.7 C 70.3	Goethite 100	Clay 100	—
f+C.8_g_cl.o	0.6519 ± 0.0009	0.6537	6.776	659.5	Fuel 23.8 C 56.2 Water 20	Goethite 100	Clay 100	—
f+C.6_g_cl.o	0.6999 ± 0.0008	0.7015	4.588	1178.9	Fuel 17.8 C 42.2 Water 40	Goethite 100	Clay 100	—
f+C.4_g_cl.o	0.6546 ± 0.0006	0.6557	3.242	2217.5	Fuel 11.9 C 28.1 Water 60	Goethite 100	Clay 100	—
Some Goethite Mixed with Fuel and C in Bottom Layer								
f+C+g.05+.4_g_cl.o	0.6441 ± 0.0007	0.6455	4.567	1303.4	Fuel 16.4 C 38.6 Water 40 Goethite 5	Goethite 100	Clay 100	—
f+C+g.1+.4_g_cl.o	0.5888 ± 0.0006	0.5899	4.434	1452.9	Fuel 14.9 C 35.1 Water 40 Goethite 10	Goethite 100	Clay 100	—
Fuel, C and Goethite in Bottom Layer with Layer of Pre-breach Clay Above								
f+C+g_cl.o	0.4686 ± 0.0007	0.4699	9.497	504.8	Fuel 23.1 C 54.4 Goethite 22.5	Clay 100	—	—
f+C+g.9_cl.o	0.5064 ± 0.0007	0.5077	7.995	683.6	Fuel 20.7 C 49.0 Goethite 20.3 Water 10	Clay 100	—	—
f+C+g.8_cl.o	0.5354 ± 0.0006	0.5366	6.669	907.0	Fuel 18.5 C 43.5 Goethite 18.0 Water 20	Clay 100	—	—
f+C+g.7_cl.o	0.5486 ± 0.0006	0.5498	5.645	1194.3	Fuel 16.1 C 38.1 Goethite 15.8 Water 30	Clay 100	—	—
f+C+g.6_cl.o	0.5504 ± 0.0005	0.5514	4.567	1577.4	Fuel 13.8 C 32.7 Goethite 13.5 Water 40	Clay 100	—	—

File Name	$k_{eff} \pm \sigma$	$k_{eff} + 2\sigma$	AENCF (keV)	H/X Ratio	Contents of Bottom Layer by Volume (%)	Contents of Next Layer by Volume (%)	Contents of Next Layer by Volume (%)	Contents of Top Layer by Volume (%)
f+C+g.4_cl.o	0.5032 ± 0.0004	0.5040	3.317	2918.1	Fuel 9.2 C 21.8 Goethite 9.0 Water 60	Clay 100	—	—

The results show that the most reactive cases occur for the fuel and water mixtures, and k_{eff} decreases as greater amounts of other degradation products are mixed in with this layer.

6.2.3 Waste Package Components Degrade at the Same Time

This section presents the results of the calculations described in Section 5.5.3. Table 28 presents the results for the calculation where the fuel compacts are only partially degraded (the post-breach composition given in Table 10 at 72689 years). Table 29 gives the values of k_{eff} for the waste package containing post-breach clay where all of the fuel compacts are degraded and have become part of the post-breach clay.

The results in Table 28 are divided into three sets, in the first set the remains of the fuel compacts mixed with varying amounts of water are covered by dry post-breach clay. For the most reactive case of this set the water reflector around the WP is replaced by tuff and by a reflective boundary condition on the outer surfaces of the WP. The tuff is a better reflector than the water, but both are less effective than a perfect reflector. In the second set of results, the amount of water is varied in the post-breach clay covering the fuel mixture for the most reactive composition identified in the first set. The volume fraction of water is increased until the WP is completely filled with degradation products. Finally, in the last set of cases the remaining fuel is mixed with varying amounts of clay and water as indicated in the table. A layer of dry clay that is shown to be most reactive in the second set of results covers the fuel mixture layer.

Table 28. A Portion of the Fuel Compacts Remain with the Post-breach Clay

(Clay Composition is for 72689 years after emplacement, see Table 10)

File Name	$k_{eff} \pm \sigma$	$k_{eff} + 2\sigma$	AENCF (keV)	H/X Ratio	Contents of Fuel Layer by Volume (%)	Contents of Top Layer by Volume (%)	Comment
Separate Layers for Fuel and (Dry) Clay							
f_psta.o	0.4363 ± 0.0008	0.4379	24.502	189.5	Fuel 100	Clay 100	
f.8_psta.o	0.5195 ± 0.0009	0.5213	17.467	282.2	Fuel 80 Water 20	Clay 100	
f.6_psta.o	0.6083 ± 0.0010	0.6102	11.937	436.6	Fuel 60 Water 40	Clay 100	
f.4_psta.o	0.6843 ± 0.0008	0.6860	7.640	745.6	Fuel 40 Water 60	Clay 100	

File Name	$k_{eff} \pm \sigma$	$k_{eff} + 2\sigma$	AENCF (keV)	H/X Ratio	Contents of Fuel Layer by Volume (%)	Contents of Top Layer by Volume (%)	Comment
f.2_psta.o	0.6867 ± 0.0007	0.6880	4.351	1672.6	Fuel 20 Water 80	Clay 100	
f.2_pstatf.o	0.7138 ± 0.0006	0.71492	4.083	1672.6	Fuel 20 Water 80	Clay 100	Previous case, but reflected by dry tuff
f.2_pstarf.o	0.7532 ± 0.0006	0.7543	4.305	1672.6	Fuel 20 Water 80	Clay 100	Previous case, but reflective BC
Separate Layers for Fuel and (Wet) Clay							
f.2_pst.8a.o	0.6787 ± 0.0007	0.6801	4.266	1672.6	Fuel 20 Water 80	Clay 80 Water 20	
f.2_pst.6a.o	0.6751 ± 0.0006	0.6764	4.464	1672.6	Fuel 20 Water 80	Clay 60 Water 40	
f.2_pst.45a.o	0.6728 ± 0.0006	0.6741	4.166	1672.6	Fuel 20 Water 80	Clay 45 Water 55	WP is full
Fuel, Clay and Water Form Separate Layer Below Dry Clay							
f.15+c.05_psta.o	0.6144 ± 0.0005	0.6154	4.155	2178.0	Fuel 15 Water 80 Clay 5	Clay 100	
f.1+c.1_psta.o	0.5061 ± 0.0004	0.5068	3.599	3187.9	Fuel 10 Water 80 Clay 10	Clay 100	
f.1+c.2_psta.o	0.4555 ± 0.0004	0.4562	4.197	2850.1	Fuel 10 Water 70 Clay 20	Clay 100	
f.1+c.4_psta.o	0.3759 ± 0.0003	0.3766	5.678	2176.3	Fuel 10 Water 50 Clay 40	Clay 100	
f.1+c.6_psta.o	0.3086 ± 0.0003	0.3092	7.827	1505.2	Fuel 10 Water 30 Clay 60	Clay 100	

The highest values of k_{eff} occur when the fuel is mixed with water (80%) in the bottom layer below the dry clay. A volume percentage of 80% water in the fuel seems larger than what would be physically reasonable since gravity would not allow it to support the clay without mixing the two layers together.

In Table 29, the next two post-breach clays are investigated. There is no remaining fuel for these compositions, i.e., the entire contents of the WP are mixed together and have reacted (time after emplacement is given in the table). The dry clay compositions are given in Table 10 at 378240 years and in Table 11 except the amounts of U-235 are increased from the amount given in the tables to be the same as the amount initially in the FSV fuel (7.425 kg). For all cases in this table, a reflective boundary condition is used on the outer surface of the WP.

Table 29. Results for Post-breach Clay where the Contents of the WP are Completely Degraded and Mixed.

File Name	$k_{eff} \pm \sigma$	$k_{eff} + 2\sigma$	AENCF (keV)	H/X Ratio	Contents of Fuel Layer by Volume (%)	Comment
Clay Composition is for 378240 years after emplacement (see Table 10)						
pstb.o	0.0694 ± 0.0000	0.0694	9.876	2230.7	Clay 100	
pst.9b.o	0.0684 ± 0.0000	0.0684	7.866	5418.7	Clay 90 Water 10	
pst.8b.o	0.0653 ± 0.0000	0.0654	5.632	9403.8	Clay 80 Water 20	
pst.6b.o	0.0583 ± 0.0000	0.0583	4.433	21359.1	Clay 60 Water 40	
pst.55b.o	0.0558 ± 0.0000	0.0559	4.038	26108.9	Clay 55 Water 45	WP is full
Clay Composition is for 74818 years after emplacement (see Table 11)						
pstc.o	0.0936 ± 0.0001	0.09374	9.0417	2180.1	Clay 100	
pst.9c.o	0.0927 ± 0.0001	0.09283	7.013	4763.0	Clay 90 Water 10	
pst.8c.o	0.0891 ± 0.0001	0.08922	5.1598	7991.7	Clay 80 Water 20	
pst.6c.o	0.0789 ± 0.0001	0.07903	3.9653	17677.7	Clay 60 Water 40	
pst.44c.o	0.0678 ± 0.0000	0.06784	2.5113	31504.5	Clay 44 Water 56	WP is full

7. REFERENCES

7.1 DOCUMENTS CITED

Audi, G. and Wapstra, A.H. 1995. *Atomic Mass Adjustment, Mass List for Analysis.* [Upton, New York: Brookhaven National Laboratory, National Nuclear Data Center]. TIC: 242718.

Beyer, W.H., ed. 1987. *CRC Standard Mathematical Tables.* 28th Edition. 3rd Printing 1988. Boca Raton, Florida: CRC Press. TIC: 240507.

BSC (Bechtel SAIC Company) 2001. *EQ6 Calculation for Chemical Degradation of Fort St. Vrain (Th/U Carbide) Waste Packages.* CAL-EDC-MD-000011 REV 00. Las Vegas, Nevada: Bechtel SAIC Company. ACC: MOL.20010831.0300.

CRWMS M&O 1998a. *Software Qualification Report for MCNP Version 4B2, A General Monte Carlo N-Particle Transport Code.* CSCI: 30033 V4B2LV. DI: 30033-2003, Rev. 01. Las Vegas, Nevada: CRWMS M&O. ACC: MOL.19980622.0637.

CRWMS M&O 1998b. *Software Code: MCNP.* 4B2LV. HP. 30033 V4B2LV.

CRWMS M&O 1999a. *DOE SRS HLW Glass Chemical Composition.* BBA000000-01717-0210-00038 REV 00. Las Vegas, Nevada: CRWMS M&O. ACC: MOL.19990215.0397.

CRWMS M&O 1999b. *Generic Degradation Scenario and Configuration Analysis for DOE Codisposal Waste Package.* BBA000000-01717-0200-00071 REV 00. Las Vegas, Nevada: CRWMS M&O. ACC: MOL.19991118.0180.

CRWMS M&O 2000a. *Technical Work Plan for: Department of Energy Spent Nuclear Fuel Work Packages.* TWP-MGR-MD-000010 REV 00. Las Vegas, Nevada: CRWMS M&O. ACC: MOL.20001107.0305.

CRWMS M&O 2000b. *EQ6 Calculation for Chemical Degradation of Shippingport LWBR (Th/U Oxide) Spent Nuclear Fuel Waste Packages.* CAL-EDC-MD-000008 REV 00. Las Vegas, Nevada: CRWMS M&O. ACC: MOL.20000926.0295.

CRWMS M&O 2000c. *Design Analysis for the Defense High-Level Waste Disposal Container.* ANL-DDC-ME-000001 REV 00. Las Vegas, Nevada: CRWMS M&O. ACC: MOL.20000627.0254.

CRWMS M&O 2001. *Intact and Degraded Component Criticality Calculations of N Reactor Spent Nuclear Fuel.* CAL-EDU-NU-000003 REV 00. Las Vegas, Nevada: CRWMS M&O. ACC: MOL.20010223.0060.

DOE (U.S. Department of Energy) 1999. "Design Specification." Volume 1 of *Preliminary Design Specification for Department of Energy Standardized Spent Nuclear Fuel Canisters.* DOE/SNF/REP-011, Rev. 3. Washington, D.C.: U.S. Department of Energy, Office of Spent Fuel Management and Special Projects. TIC: 246602.

Fowler, J.R.; Edwards, R.E.; Marra, S.L.; and Plodinec, M.J. 1995. *Chemical Composition Projections for the DWPF Product (U).* WSRC-IM-91-116-1, Rev. 1. Aiken, South Carolina: Westinghouse Savannah River Company. TIC: 232731.

Parrington, J.R.; Knox, H.D.; Breneman, S.L.; Baum, E.M.; and Feiner, F. 1996. *Nuclides and Isotopes, Chart of the Nuclides.* 15th Edition. San Jose, California: General Electric Company and KAPL, Inc. TIC: 233705.

Plodinec, M.J. and Marra, S.L. 1994. *Projected Radionuclide Inventories and Radiogenic Properties of the DWPF Product (U).* WSRC-IM-91-116-3, Rev. 0. Aiken, South Carolina: Westinghouse Savannah River Company. TIC: 242337.

Stout, R.B. and Leider, H.R., eds. 1991. *Preliminary Waste Form Characteristics Report.* Version 1.0. Livermore, California: Lawrence Livermore National Laboratory. ACC: MOL.19940726.0118.

Taylor, L.L. 2001. *Fort Saint Vrain HTGR (Th/U Carbide) Fuel Characteristics for Disposal Criticality Analysis.* DOE/SNF/REP-060, Rev. 0. [Washington, D.C.]: U.S. Department of Energy, Office of Environmental Management. TIC: 249783.

Taylor, W.J. 1997. "Incorporating Hanford 15 Foot (4.5 Meter) Canister into Civilian Radioactive Waste Management System (CRWMS) Baseline." Memorandum from W.J. Taylor (DOE) to J. Williams (Office of Waste Acceptance Storage and Transportation), April 2, 1997. ACC: HQP.19970609.0014.

YMP (Yucca Mountain Site Characterization Project) 2000. *Disposal Criticality Analysis Methodology Topical Report.* YMP/TR-004Q, REV 01. Las Vegas, Nevada: Yucca Mountain Site Characterization Office. ACC: MOL.20001214.0001.

7.2 CODES, STANDARDS, REGULATIONS, AND PROCEDURES

AP-3.12Q, Rev. 0, ICN 4. *Calculations.* Washington, D.C.: U.S. Department of Energy, Office of Civilian Radioactive Waste Management. ACC: MOL.20010404.0008.

AP-3.15Q, Rev. 3. *Managing Technical Product Inputs.* Washington, D.C.: U.S. Department of Energy, Office of Civilian Radioactive Waste Management. ACC: MOL.20010801.0318.

ASTM A 240/ A 240M-99b. 2000. *Standard Specification for Heat-Resisting Chromium and Chromium-Nickel Stainless Steel Plate, Sheet, and Strip for Pressure Vessels.* West Conshohocken, Pennsylvania: American Society for Testing and Materials. TIC: 248529.

ASTM A 276-91a. 1991. *Standard Specification for Stainless and Heat-Resisting Steel Bars and Shapes.* Philadelphia, Pennsylvania: American Society for Testing and Materials. TIC: 240022.

ASTM G 1-90 (Reapproved 1999). 1990. *Standard Practice for Preparing, Cleaning, and Evaluating Corrosion Test Specimens.* West Conshohocken, Pennsylvania: American Society for Testing and Materials. TIC: 238771.

7.3 SOURCE DATA

MO0003RIB00071.000. Physical and Chemical Characteristics of Alloy 22. Submittal date: 03/13/2000.

MO0003RIB00072.000. Physical and Chemical Characteristics of Steel, A 516. Submittal date: 03/13/2000.

8. ATTACHMENTS

Attachment I: One Compact disc (CD) containing the MCNP input and output files and the Excel spreadsheet.

Attachment II: List of the electronic files located in Attachment I, 14 pages.

OFFICE OF CIVILIAN RADIOACTIVE WASTE MANAGEMENT
SPECIAL INSTRUCTION SHEET

file last 10-15-01 nfc

1. QA: QA
Page: 1 of: 1

Complete Only Applicable Items

This is a placeholder page for records that cannot be scanned.

2. Record Date	3. Accession Number
09/28/2001	ATT-TO MOL. 20011015.0020
4. Author Name(s)	**5. Author Organization**
LELAND MONTIERTH	N/A

6. Title/Description
INTACT AND DEGRADED MODE CRITICALITY CALCULATIONS FOR THE CODISPOSAL OF FORT SAINT VRAIN HTGR SPENT NUCLEAR FUEL IN A WASTE PACKAGE

7. Document Number(s)	8. Version Designator
CAL-EDC-NU-000007	REV. 00
9. Document Type	**10. Medium**
DATA	CD-ROM

11. Access Control Code
PUB

12. Traceability Designator
DC# 28746

(AB) 10/15/01

13. Comments
THIS IS A SPECIAL PROCESS CD-ROM AS PART OF ATTACHMENT I

~~RPC~~

THIS DATA SUBMITTAL TO THE RECORDS PROCESSING CENTER IS FOR ARCHIVE PURPOSES ONLY, AND IS NOT AVAILABLE FOR VIEWING OR REPRODUCTION

182

OFFICE OF CIVILIAN RADIOACTIVE WASTE MANAGEMENT
ELECTRONIC FILE CERTIFICATION

QA: N/A

1. DOCUMENT TITLE:

Intact and Degraded Mode Criticality Calculations for the Codisposal of Fort Saint Vrain HTGR Spent Nuclear Fuel in a Waste Package

2. IDENTIFIER (e.g., DI OR PI):	3. REVISION DESIGNATOR:
CAL-EDC-NU-000007	Rev. 00

ATTACHED SOFTWARE FILE INFORMATION

4. PDF FILE SUBMITTED: ☐ YES ☑ NO

5. FILE NAMES(S) WITH FILE EXTENSION(S) PROVIDED BY THE SOFTWARE:

See Attached

6. DATE LAST MODIFIED:	7. NATIVE APPLICATION: (i.e., EXCEL, WORD, CORELDRAW)	8. FILE SIZE IN KILOBYTES:
See Attached	Word	See Attached

9. FILE LINKAGE INSTRUCTIONS/INFORMATION:

Standard

10. PRINTER SPECIFICATION (I.E., HP4SI) INCLUDING POSTSCRIPT INFORMATION (i.e., PRINTER DRIVER) AND PRINTING PAGE SETUP: (i.e., LANDSCAPE, 11 X 17 PAPER)

8 1/2 x 11(portrait)=T1024AHP5si

11. COMPUTING PLATFORM USED: (i.e., PC, SUN, WIN 95, NT, HP)	12. OPERATING SYSTEM AND VERSION: (i.e., WINDOWS UNIX, SOLARIS)
PC#113594	Wiondows 95

13. ADDITIONAL HARDWARE/SOFTWARE REQUIREMENT USED TO CREATE FILE(S):	14. ACCESS RESTRICTIONS: (COPYRIGHT OR LICENSE ISSUES)
None	None

COMMENTS/SPECIAL INSTRUCTIONS

15. IS SOFTWARE AVAILABLE FROM SOFTWARE CONFIGURATION MANAGEMENT? ☑ YES ☐ NO
SOFTWARE MEDIA TRACKING NUMBER N/A.

NOTE: The software product(s) to develop this document are Commercial-Off-The-Shelf (COTS) software products which require no Software Media Number (SMN). The COTS software products are under Sofware Configuration Management (SCM) control.

CERTIFICATION

16. DOCUMENT OWNER (Print and Sign):			17. DATE:
Leland Montierth for L. Montierth			10/02/2001
18. ORGANIZATION:	**19. DEPARTMENT:**	**20. LOCATION/MAIL STOP:**	**21. PHONE:**
BSC	Criticality	MS423/1000E	295-3437
22. SUBMITTED BY (Print and Sign):			**23. DATE:**
Daynett D. Vosicky Daynett D. Vosicky			10/02/2001

DC USE ONLY

24. DATE RECEIVED:	25. DATE FILES TRANSFERRED:	26. DC NO.:
10/2/01	N/A	28746
27. NAME (Print and Sign):		**28. DATE:**
N/A		10-3-01

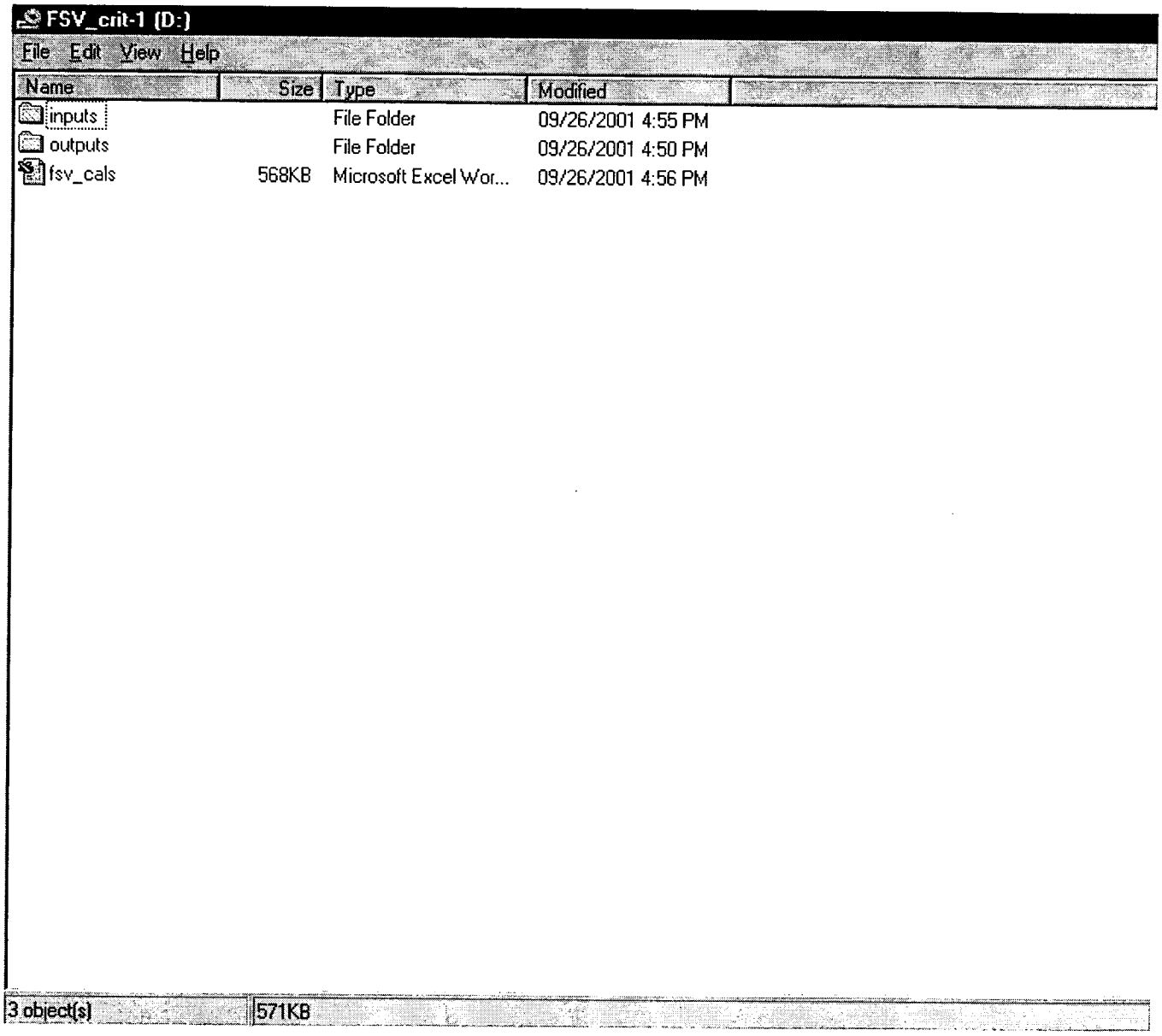
FSV_crit-1 (D:)
File Edit View Help
Name
Size
Type
Modified
inputs
File Folder
09/26/2001 4:55 PM
outputs
File Folder
09/26/2001 4:50 PM
fsv_cals
568KB
Microsoft Excel Wor...
09/26/2001 4:56 PM
3 object(s)
571KB

Attachment II

Table II-1. List of Computer Files Contained on Compact Disk (Attachment I)

File Name /Directory Name	Size (bytes)	Date of Last Access	Time of Last Access	Table Used
Directory of d:				
fsv_cals.xls	581,120	9/26/2001	04:56p	N/A
inputs	N/A	9/26/2001	04:55p	N/A
outputs	N/A	9/26/2001	04:50p	N/A
Directory of d:\inputs\Table_12				
cmp1	19,765	1/26/2001	02:49p	Table 12
cmp2	19,765	1/26/2001	02:49p	Table 12
cmp3	19,765	1/26/2001	02:50p	Table 12
cs1	19,686	1/29/2001	08:36a	Table 12
cs1-ph	19,704	1/29/2001	08:52a	Table 12
cs1-ph_ref	19,418	5/16/2001	03:41p	Table 12
cs1-th.05	19,686	7/17/2001	02:57p	Table 12
cs1_ref	19,461	3/27/2001	05:51p	Table 12
cs1aL	19,693	1/29/2001	09:07a	Table 12
cs1noPu	19,687	1/29/2001	09:15a	Table 12
cs1othrC	19,751	1/29/2001	09:12a	Table 12
Directory of d:\inputs\Table_13				
cs1+a	19,696	1/29/2001	08:49a	Table 13
cs1+b	19,696	1/29/2001	08:49a	Table 13
cs1+c	19,696	1/29/2001	08:50a	Table 13
cs1+Ca	19,700	1/26/2001	03:48p	Table 13
cs1+Cb	19,700	1/29/2001	08:38a	Table 13
cs1+Cc	19,700	1/29/2001	08:39a	Table 13
cs1a	19,701	1/29/2001	09:07a	Table 13
cs1c	19,701	1/29/2001	09:08a	Table 13
cs1Ca	19,700	1/29/2001	08:53a	Table 13
cs1Cb	19,700	1/29/2001	08:54a	Table 13
cs1Cc	19,762	2/5/2001	02:58p	Table 13
cs1drya	19,724	1/29/2001	09:09a	Table 13
cs1e	19,701	1/29/2001	09:14a	Table 13
Directory of d:\inputs\Table_14				
cs1+wa	19,686	1/29/2001	08:45a	Table 14
cs1+wb	19,764	1/29/2001	08:45a	Table 14
cs1-1	19,686	6/19/2001	08:34a	Table 14
cs1-2	19,686	6/19/2001	08:33a	Table 14
cs1-3	19,686	6/19/2001	08:32a	Table 14
cs1-4	19,686	6/19/2001	08:31a	Table 14
cs1_a	19,683	1/29/2001	08:57a	Table 14
cs1_b	19,751	1/29/2001	08:57a	Table 14
cs1_c	19,753	1/29/2001	08:58a	Table 14
cs1_c_ref	19,467	5/16/2001	05:36p	Table 14
cs2	17,830	1/29/2001	09:13a	Table 14
Directory of d:\inputs\Table_15				
fal1_10%	20,262	9/12/2001	02:46p	Table 15
fal1_10%a	20,262	9/12/2001	02:47p	Table 15
fal2_10%	20,262	9/12/2001	02:47p	Table 15
fal2_10%a	20,262	9/12/2001	02:47p	Table 15
fal3_10%	20,262	9/12/2001	02:47p	Table 15

File Name /Directory Name	Size (bytes)	Date of Last Access	Time of Last Access	Table Used
fal3_10%a	20,262	9/12/2001	02:47p	Table 15
fl_10%	19,844	1/29/2001	10:58a	Table 15
fl_10%a	19,844	1/29/2001	11:20a	Table 15
fl_2%	20,046	2/6/2001	08:13a	Table 15
fl_2%a	19,844	1/29/2001	11:20a	Table 15
fl_3%	19,844	1/29/2001	11:04a	Table 15
fl_3%a	19,844	1/29/2001	11:21a	Table 15
fl_3%rf	19,619	7/25/2001	09:48a	Table 15
fl_4%	19,844	1/29/2001	10:59a	Table 15
fl_4%a	20,046	2/5/2001	03:11p	Table 15
fl_5%	19,844	1/29/2001	11:02a	Table 15
fl_5%a	20,046	2/5/2001	03:11p	Table 15
fl_5%arf	19,821	7/25/2001	09:51a	Table 15
hlf_10%	20,789	1/29/2001	11:10a	Table 15
hlf_10%+w	20,791	1/29/2001	11:11a	Table 15
thq+10%	20,843	1/29/2001	11:11a	Table 15
thq+10%+w	20,843	1/29/2001	11:12a	Table 15
Directory of d:\inputs\Table_16				
bd.1	20,153	3/14/2001	12:50p	Table 16
bd.1+w.1	20,153	3/15/2001	12:40p	Table 16
bd.1+w.2	20,153	3/15/2001	12:40p	Table 16
bd.1+w.3	20,153	3/15/2001	12:40p	Table 16
bd.1+w.4	20,153	3/15/2001	12:41p	Table 16
bd.1+w.4rf	19,928	7/26/2001	03:37p	Table 16
bd.15	20,153	3/14/2001	04:59p	Table 16
bd.15+w.1	20,153	3/19/2001	09:00a	Table 16
bd.15+w.2	20,153	3/19/2001	09:03a	Table 16
bd.15+w.24	20,153	3/20/2001	08:53a	Table 16
bd.15+w.24p	19,835	3/21/2001	11:55a	Table 16
bd.15rf	19,928	7/26/2001	03:37p	Table 16
bd.197	20,153	3/15/2001	09:16a	Table 16
bd.2	20,153	3/14/2001	12:53p	Table 16
bdq	20,153	3/14/2001	08:41a	Table 16
bdqp	19,828	3/23/2001	11:07a	Table 16
Directory of d:\inputs\Table_17				
alt.1+w.4h	17,946	3/20/2001	01:33p	Table 17
alt.1+w.4h+g.02	17,980	5/16/2001	02:39p	Table 17
alt.1+w.4h+g.04	17,980	5/16/2001	02:40p	Table 17
alt.1+w.4h+g.1	17,761	5/16/2001	02:54p	Table 17
alt.1+w.4h+g.2	17,761	5/16/2001	03:03p	Table 17
alt.1+w.4hrf	17,721	7/26/2001	03:53p	Table 17
alt.15+w.24h	17,946	3/20/2001	01:02p	Table 17
alt.197	19,206	3/20/2001	10:47a	Table 17
alt.197h	18,013	3/20/2001	12:52p	Table 17
alt.25+w.2h	17,946	3/20/2001	02:44p	Table 17
alt.25h	17,946	3/20/2001	02:43p	Table 17
alt.5	19,206	3/20/2001	03:07p	Table 17
alt.5h	17,946	5/8/2001	03:03p	Table 17
Directory of d:\inputs\Table_18				
tlt1a	20,031	5/10/2001	09:56a	Table 18
tlt1a_.2	20,037	5/10/2001	11:51a	Table 18
tlt1a_.3	20,037	5/10/2001	11:51a	Table 18
tlt1a_.4	20,037	5/10/2001	11:52a	Table 18

File Name /Directory Name	Size (bytes)	Date of Last Access	Time of Last Access	Table Used
tlt1a_.4rf	19,956	7/26/2001	12:19a	Table 18
tlt1a_.5	20,037	5/10/2001	11:52a	Table 18
tlt1a_.6	20,037	5/10/2001	11:52a	Table 18
tlt1b_.2	20,334	5/10/2001	04:24p	Table 18
tlt1b_.4	20,365	5/14/2001	08:40a	Table 18
tlt1sh_.4	21,022	9/21/2001	03:33p	Table 18
tlt2a	19,827	5/14/2001	09:14a	Table 18
tlt2a_.4	19,778	5/14/2001	09:56a	Table 18
tlt2b_.4	20,022	5/14/2001	10:21a	Table 18
tlt2sh_.4	20,169	5/14/2001	11:44a	Table 18
Directory of d:\inputs\Table_19				
hlfa	20,398	1/29/2001	05:29p	Table 19
hlfb	19,958	1/29/2001	10:15a	Table 19
hxa	20,566	1/29/2001	10:16a	Table 19
hxb	20,566	1/29/2001	10:17a	Table 19
Npsa	20,170	3/12/2001	05:27p	Table 19
Npsarf	19,945	7/26/2001	03:55p	Table 19
qrta	20,308	1/29/2001	10:17a	Table 19
qrtb	20,308	1/29/2001	10:18a	Table 19
Directory of d:\inputs\Table_20				
p1.50a	25,641	1/29/2001	10:21a	Table 20
p1.50a+.5	25,637	2/7/2001	12:14p	Table 20
p1.75+.3	25,632	1/29/2001	10:21a	Table 20
p1.75+.4	25,632	1/29/2001	10:22a	Table 20
p1.75+.5	25,634	1/29/2001	10:22a	Table 20
p2.00a	25,792	1/29/2001	10:24a	Table 20
p2.00a+.1	25,791	1/29/2001	10:25a	Table 20
p2.00a+.2	25,791	1/29/2001	10:25a	Table 20
p2.00a+.4	25,845	2/5/2001	01:02p	Table 20
p2.00a+.5	25,788	1/29/2001	10:26a	Table 20
p2.00b	25,740	2/5/2001	01:06p	Table 20
p2.00b+.1	25,661	1/29/2001	10:26a	Table 20
p2.00b+.2	25,644	1/29/2001	10:27a	Table 20
p2.00b+.4	26,056	1/29/2001	10:27a	Table 20
p2.00b+.5	25,621	1/29/2001	10:27a	Table 20
p2l_.05	26,262	1/29/2001	10:41a	Table 20
p2l_.1	26,261	1/29/2001	10:41a	Table 20
pact+.2	25,676	2/7/2001	12:29p	Table 20
pact+.4	25,677	1/29/2001	10:31a	Table 20
pact+.4rf	25,452	7/26/2001	12:21a	Table 20
pact+.5	25,679	1/29/2001	10:31a	Table 20
pacta+.5	26,035	2/7/2001	07:56a	Table 20
tcha	25,576	1/29/2001	10:31a	Table 20
tcha+.2	25,576	1/29/2001	10:32a	Table 20
tcha+.4	25,658	2/5/2001	12:44p	Table 20
tcha+.5	25,644	1/29/2001	10:32a	Table 20
tcha+1	25,578	1/29/2001	10:32a	Table 20
tchb	25,480	1/29/2001	10:32a	Table 20
tchc	25,523	1/29/2001	10:32a	Table 20
tla_.05	26,180	1/29/2001	10:43a	Table 20
tla_.1	26,180	1/29/2001	10:43a	Table 20
tla_0a	26,180	1/29/2001	10:43a	Table 20
Directory of d:\inputs\Table_21				

File Name /Directory Name	Size (bytes)	Date of Last Access	Time of Last Access	Table Used
c_f.3	11,853	1/29/2001	01:50p	Table 21
c_f.4	12,022	2/5/2001	04:50p	Table 21
f.176	11,667	1/29/2001	01:41p	Table 21
f.2_c	11,877	2/5/2001	04:37p	Table 21
f.2_w	11,719	2/5/2001	04:38p	Table 21
f.3_c	11,853	1/29/2001	01:50p	Table 21
f.3_c.4	11,853	1/29/2001	01:53p	Table 21
f.3_c.6	11,853	1/29/2001	01:53p	Table 21
f.3_c.8	11,867	1/29/2001	01:54p	Table 21
f.3_w	11,719	1/29/2001	01:39p	Table 21
f.4_c	12,012	2/5/2001	04:44p	Table 21
f.4_c.4	11,934	2/6/2001	10:11a	Table 21
f.4_c.6	11,934	2/6/2001	10:09a	Table 21
f.4_c.8	12,020	2/6/2001	10:06a	Table 21
f.4_w	11,719	1/29/2001	01:39p	Table 21
f.6_c	12,648	2/5/2001	04:45p	Table 21
f.6_ca	12,012	2/5/2001	04:46p	Table 21
f.6_crf	12,423	7/26/2001	04:02p	Table 21
f.6_w	11,719	1/29/2001	01:43p	Table 21
f.8_w	11,869	2/27/2001	02:26p	Table 21
f_w	11,774	1/29/2001	01:39p	Table 21
Directory of d:\inputs\Table_22				
f+c+w.2_w	11,744	1/29/2001	02:28p	Table 22
f+c+w.4061	11,642	1/29/2001	02:28p	Table 22
f+c_w	11,733	1/29/2001	02:29p	Table 22
f.3+c.1_c	11,956	1/29/2001	02:00p	Table 22
f.3+c.1_c.4	11,852	1/29/2001	02:00p	Table 22
f.3+c.1_c.6	11,852	1/29/2001	02:00p	Table 22
f.3+c.1_c.8	11,852	1/29/2001	02:00p	Table 22
f.3+c.2_c	11,953	1/29/2001	02:08p	Table 22
f.3+c.2_c.4	11,867	1/29/2001	02:08p	Table 22
f.3+c.2_c.6	11,852	1/29/2001	02:08p	Table 22
f.3+c.2_c.8	11,852	1/29/2001	02:08p	Table 22
f.3+c.4_c	11,953	1/29/2001	02:22p	Table 22
f.3+c.4_c.4	11,852	1/29/2001	02:22p	Table 22
f.3+c.4_c.6	11,953	1/29/2001	02:22p	Table 22
f.3+c.4_c.8	11,956	1/29/2001	02:22p	Table 22
f.4+c.1_c	12,011	2/6/2001	11:12a	Table 22
f.4+c.1_c.4	11,925	2/6/2001	11:25a	Table 22
f.4+c.1_c.6	11,925	2/6/2001	11:23a	Table 22
f.4+c.1_c.8	12,011	2/6/2001	11:16a	Table 22
f.4+c.2_c	12,011	2/6/2001	11:42a	Table 22
f.4+c.2_c.4	11,925	2/6/2001	12:58p	Table 22
f.4+c.2_c.6	11,925	2/6/2001	12:54p	Table 22
f.4+c.2_c.8	12,011	2/6/2001	11:46a	Table 22
f.4+c.4_c	12,012	2/6/2001	12:00p	Table 22
f.4+c.4_c.4	11,924	2/6/2001	01:03p	Table 22
f.4+c.4_c.6	12,294	2/7/2001	08:08a	Table 22
f.4+c.4_c.8	12,012	2/6/2001	12:04p	Table 22
f.4+c.5_c	12,012	2/7/2001	11:05a	Table 22
f.6+c.1_c	12,011	7/26/2001	05:10p	Table 22
f.6+c.2_c	12,011	7/26/2001	05:15p	Table 22
f.6+c.4_c	12,011	7/26/2001	05:19p	Table 22
fcw.2_wrf	11,550	7/26/2001	05:20p	Table 22

File Name /Directory Name	Size (bytes)	Date of Last Access	Time of Last Access	Table Used
Directory of d:\inputs\Table_23				
a.1w.4pc	12,783	6/25/2001	08:46a	Table 23
bd.1w.4pc	14,951	6/25/2001	08:45a	Table 23
cs1_c+.714	14,790	2/8/2001	08:41a	Table 23
cs1_c+.8	14,821	2/8/2001	08:42a	Table 23
cs1_c+.9	14,821	2/8/2001	08:43a	Table 23
cs1_cal	15,044	8/29/2001	03:25p	Table 23
cs1_prba	14,796	2/7/2001	03:31p	Table 23
cs1_prbb	14,817	2/7/2001	04:01p	Table 23
cs1_prbc	14,827	2/7/2001	04:06p	Table 23
cs1_prbcrf	14,750	7/26/2001	05:34p	Table 23
cs1_prbd	14,829	2/7/2001	04:09p	Table 23
cs1_prbe	14,828	2/7/2001	04:11p	Table 23
cs1_prberf	14,751	7/26/2001	05:34p	Table 23
cs1_prbetf	15,224	7/26/2001	05:52p	Table 23
f.3c.4cpc	6,822	6/25/2001	08:34a	Table 23
f.4c.5cpc	6,881	6/25/2001	08:34a	Table 23
f.6_cpc	7,481	6/25/2001	08:34a	Table 23
f.6c.2cltf	7,287	7/27/2001	04:48p	Table 23
f.6c.4cltf	7,287	7/31/2001	08:20a	Table 23
fl_2%pc	17,017	6/25/2001	08:18a	Table 23
fl_3%pc	14,679	6/22/2001	05:21p	Table 23
Npsapc	15,043	6/22/2001	05:41p	Table 23
pa.5pc	20,830	6/22/2001	06:08p	Table 23
paa.5pc	20,873	6/22/2001	06:10p	Table 23
t1a_.4pbc	15,572	5/15/2001	09:21a	Table 23
t2b_.4pbc	15,527	5/15/2001	09:21a	Table 23
Directory of d:\inputs\Table_24				
cyl.6_clc	13,871	2/12/2001	04:16p	Table 24
cyl.9_clc	13,871	2/12/2001	04:16p	Table 24
cyl.9_clc-w.6	14,129	2/13/2001	03:39p	Table 24
cyl.9_clc-w.8	14,133	2/13/2001	03:43p	Table 24
cyl.9_clc-w.9	14,133	2/13/2001	03:43p	Table 24
cyl.9_clc-w0	14,115	2/13/2001	03:43p	Table 24
cyl.9_clerf	13,794	7/30/2001	04:43p	Table 24
cyl_clc	13,856	2/9/2001	03:49p	Table 24
hex.6_clc	14,250	2/12/2001	04:10p	Table 24
hex.9_clc	14,250	2/12/2001	04:11p	Table 24
hex_clc	14,236	2/12/2001	01:05p	Table 24
in_cl.714c	13,771	2/9/2001	11:30a	Table 24
in_cl.8c	13,801	2/9/2001	11:23a	Table 24
in_cl.9c	13,801	2/9/2001	11:13a	Table 24
in_cla	13,786	2/8/2001	01:44p	Table 24
in_clc	13,807	2/8/2001	01:47p	Table 24
in_clc-w	13,787	2/8/2001	02:20p	Table 24
in_clc-w.8	14,449	2/9/2001	02:00p	Table 24
in_clc-w.9	14,449	2/9/2001	01:50p	Table 24
in_cle	13,807	2/8/2001	01:49p	Table 24
in_clerf	13,730	7/30/2001	04:28p	Table 24
Directory of d:\inputs\Table_25				
p.5ag+C.4_cl	19,238	2/26/2001	04:16p	Table 25
p0acl.05+g+C.4_cl	19,605	2/20/2001	10:21a	Table 25
p0acl.1+g+C.4_cl	19,605	2/20/2001	10:33a	Table 25

File Name /Directory Name	Size (bytes)	Date of Last Access	Time of Last Access	Table Used
p0ag+C.4_cl	19,238	2/19/2001	02:58p	Table 25
p0ag+C.6_cl	19,370	2/19/2001	02:51p	Table 25
p0ag+C.8_cl	19,346	2/19/2001	02:40p	Table 25
p0ag+C_cl	19,328	2/19/2001	02:26p	Table 25
p0ag.4_C.4_cl	19,472	2/19/2001	12:58p	Table 25
p0ag.4_C.4_cl.74	19,470	2/19/2001	01:24p	Table 25
p0ag.4_C_cl	19,597	2/15/2001	02:50p	Table 25
p0ag.6_C_cl	19,610	2/15/2001	02:50p	Table 25
p0ag.8_C_cl	19,884	2/20/2001	08:33a	Table 25
p0ag_C.4_cl	19,611	2/15/2001	02:50p	Table 25
p0ag_C.6_cl	19,670	2/15/2001	02:50p	Table 25
p0ag_C.8_cl	19,659	2/15/2001	02:50p	Table 25
p0ag_C_cl	19,641	2/15/2001	02:50p	Table 25
p0ag_C_cl.714	19,637	2/15/2001	02:50p	Table 25
p0ag_C_cl.8	19,635	2/15/2001	02:51p	Table 25
ptag+C.4_cl	19,221	2/26/2001	04:28p	Table 25
Directory of d:\inputs\Table_26				
cC.6+g.05_g_clrf	19,050	7/27/2001	05:53p	Table 26
cy.25cC.6_g_cl	19,007	2/26/2001	02:36p	Table 26
cy.5cC.6_g_cl	18,986	2/22/2001	09:09a	Table 26
cy.75cC.6_g_cl	19,005	2/22/2001	08:48a	Table 26
cy0aC_g_cl	19,058	2/19/2001	11:56a	Table 26
cy0aC_g_clrf	18,981	7/27/2001	05:42p	Table 26
cy0cC+g.2_cl	19,032	3/5/2001	12:43p	Table 26
cy0cC+g.2_clp	19,032	3/5/2001	12:43p	Table 26
cy0cC+g.3_cl	19,032	3/5/2001	12:45p	Table 26
cy0cC+g.4_cl	19,032	3/1/2001	01:16p	Table 26
cy0cC+g.6_cl	19,032	3/1/2001	01:16p	Table 26
cy0cC+g.8_cl	19,032	3/1/2001	01:16p	Table 26
cy0cC.4_g_cl	19,038	2/19/2001	05:02p	Table 26
cy0cC.6+g.05_g_cl	19,092	3/1/2001	01:02p	Table 26
cy0cC.6+g.1_g_cl	19,092	3/1/2001	01:02p	Table 26
cy0cC.6_g_cl	19,058	2/19/2001	05:04p	Table 26
cy0cC.8_g_cl	19,048	2/19/2001	05:06p	Table 26
cy0cC_g_cl	19,058	2/19/2001	11:52a	Table 26
cy0eC_g_cl	19,013	2/19/2001	12:00p	Table 26
cytcC.4_g_cl	19,179	2/22/2001	09:32a	Table 26
cytcC.6_g_cl	19,179	2/26/2001	01:22p	Table 26
cytcC.8_g_cl	19,179	2/26/2001	01:28p	Table 26
cytcC0_g_cl	19,194	2/22/2001	10:09a	Table 26
cytcC0p_g_cl	19,194	2/22/2001	10:13a	Table 26
cytcC0pm_g_cl	19,202	2/27/2001	09:25a	Table 26
cytcC_g_cl	19,179	2/26/2001	01:32p	Table 26
hexc.4_g_cl	14,145	3/8/2001	05:16p	Table 26
hexc.5_g_cl	14,145	3/9/2001	10:49a	Table 26
hexc.6_g_cl	14,145	3/8/2001	05:07p	Table 26
hexc.7_g_cl	14,145	3/9/2001	10:42a	Table 26
hexc_g_cl	14,143	3/8/2001	04:54p	Table 26
hx.6_g_clrf	14,456	7/31/2001	08:49a	Table 26
hx.6_g_cltf	14,540	7/27/2001	05:42p	Table 26
Directory of d:\inputs\Table_27				
f+C+g.05+.4_g_cl	5,237	3/1/2001	08:36a	Table 27
f+C+g.1+.4_g_cl	5,237	3/1/2001	08:37a	Table 27
f+C+g.4_cl	5,176	3/1/2001	08:12a	Table 27

File Name /Directory Name	Size (bytes)	Date of Last Access	Time of Last Access	Table Used
f+C+g.6_cl	5,176	3/1/2001	08:12a	Table 27
f+C+g.7_cl	5,176	3/1/2001	08:05a	Table 27
f+C+g.8_cl	5,176	3/1/2001	08:05a	Table 27
f+C+g.9_cl	5,176	3/1/2001	08:05a	Table 27
f+C+g_cl	5,176	3/1/2001	08:05a	Table 27
f+C.4_g_cl	5,209	2/28/2001	11:28a	Table 27
f+C.6_g_cl	5,209	2/28/2001	11:23a	Table 27
f+C.8_g_cl	5,209	2/28/2001	11:01a	Table 27
f+C_g_cl	5,209	2/28/2001	10:55a	Table 27
f.2_C_g_cl	5,278	2/27/2001	02:17p	Table 27
f.4+C.2_C_g_cl	5,278	2/27/2001	05:54p	Table 27
f.4+C.4_C_g_cl	5,278	2/27/2001	05:58p	Table 27
f.4_C_g_cl	5,278	2/27/2001	02:17p	Table 27
f.5_C_g_cl	5,278	2/27/2001	02:17p	Table 27
f.6_C_g_cl	5,278	2/27/2001	02:18p	Table 27
f.8_C_g_cl	5,330	2/27/2001	02:23p	Table 27
f_C_g_cl	5,348	2/27/2001	01:18p	Table 27
g_f.4_C_cl	5,384	3/1/2001	09:03a	Table 27
Directory of d:\inputs\Table_28				
f.1+c.1_psta	4,363	7/5/2001	12:25p	Table 28
f.1+c.2_psta	4,363	7/5/2001	12:29p	Table 28
f.1+c.4_psta	4,363	7/5/2001	12:34p	Table 28
f.1+c.6_psta	4,363	7/5/2001	12:37p	Table 28
f.15+c.05_psta	4,365	7/5/2001	12:22p	Table 28
f.2_pst.45a	3,893	7/5/2001	09:35a	Table 28
f.2_pst.6a	3,880	7/5/2001	09:00a	Table 28
f.2_pst.8a	3,880	7/5/2001	08:57a	Table 28
f.2_psta	3,882	7/3/2001	04:37p	Table 28
f.2_pstarf	3,805	7/6/2001	10:35a	Table 28
f.2_pstatf	4,278	7/23/2001	02:16p	Table 28
f.4_psta	3,882	7/3/2001	04:09p	Table 28
f.6_psta	3,882	7/3/2001	04:01p	Table 28
f.8_psta	3,934	7/3/2001	03:59p	Table 28
f_psta	3,952	7/3/2001	03:55p	Table 28
Directory of d:\inputs\Table_29				
pst.44c	3,078	7/9/2001	12:09p	Table 29
pst.55b	3,051	7/6/2001	01:14p	Table 29
pst.6b	3,040	7/6/2001	01:10p	Table 29
pst.6c	3,066	7/9/2001	12:06p	Table 29
pst.8b	3,040	7/6/2001	01:07p	Table 29
pst.8c	3,066	7/9/2001	12:03p	Table 29
pst.9b	3,040	7/6/2001	01:03p	Table 29
pst.9c	3,066	7/9/2001	12:00p	Table 29
pstb	3,042	7/6/2001	11:42a	Table 29
pstc	3,070	7/9/2001	11:57a	Table 29
Directory of d:\outputs\Table_12				
cmp1.o	610,407	1/29/2001	02:23p	Table 12
cmp2.o	610,916	1/29/2001	07:44p	Table 12
cmp3.o	611,060	1/30/2001	12:59a	Table 12
cs1-ph.o	608,068	2/1/2001	11:30a	Table 12
cs1-ph_ref.o	605,781	5/16/2001	08:42p	Table 12
cs1-th.05.o	608,769	7/17/2001	07:55p	Table 12
cs1.o	608,770	1/30/2001	05:54a	Table 12

File Name /Directory Name	Size (bytes)	Date of Last Access	Time of Last Access	Table Used
cs1_ref.o	605,801	3/27/2001	10:52p	Table 12
cs1aL.o	607,540	2/3/2001	07:59a	Table 12
cs1noPu.o	603,800	1/31/2001	11:49p	Table 12
cs1othrC.o	605,168	2/1/2001	02:08a	Table 12
Directory of d:\outputs\Table_13				
cs1+a.o	608,630	1/31/2001	09:11a	Table 13
cs1+b.o	608,601	1/31/2001	03:49p	Table 13
cs1+c.o	608,314	1/31/2001	08:45p	Table 13
cs1+Ca.o	608,601	1/30/2001	10:54a	Table 13
cs1+Cb.o	608,621	1/30/2001	05:41p	Table 13
cs1+Cc.o	608,818	1/31/2001	01:40a	Table 13
cs1a.o	608,404	2/3/2001	03:06a	Table 13
cs1c.o	608,341	2/3/2001	12:51p	Table 13
cs1Ca.o	608,701	2/1/2001	04:27p	Table 13
cs1Cb.o	608,605	2/1/2001	09:25p	Table 13
cs1Cc.o	607,520	2/5/2001	09:50p	Table 13
cs1drya.o	594,821	2/1/2001	04:23a	Table 13
cs1e.o	605,187	1/31/2001	09:33p	Table 13
Directory of d:\outputs\Table_14				
cs1+wa.o	609,264	2/1/2001	01:33a	Table 14
cs1+wb.o	609,765	2/1/2001	06:23a	Table 14
cs1-1.o	608,717	6/19/2001	01:35p	Table 14
cs1-2.o	608,097	6/19/2001	06:33p	Table 14
cs1-3.o	608,503	6/19/2001	01:33p	Table 14
cs1-4.o	608,195	6/19/2001	06:26p	Table 14
cs1_a.o	608,636	2/2/2001	12:26p	Table 14
cs1_b.o	608,664	2/2/2001	05:20p	Table 14
cs1_c.o	608,548	2/2/2001	10:14p	Table 14
cs1_c_ref.o	605,995	5/17/2001	03:09a	Table 14
cs2.o	581,751	1/31/2001	07:17p	Table 14
Directory of d:\outputs\Table_15				
fal1_10%.o	616,790	9/13/2001	08:29a	Table 15
fal1_10%a.o	617,043	9/13/2001	08:29a	Table 15
fal2_10%.o	619,681	9/13/2001	08:29a	Table 15
fal2_10%a.o	619,900	9/13/2001	08:29a	Table 15
fal3_10%.o	620,203	9/13/2001	08:29a	Table 15
fal3_10%a.o	619,217	9/13/2001	08:29a	Table 15
fl_10%.o	607,529	1/29/2001	06:03p	Table 15
fl_10%a.o	607,212	1/29/2001	08:19p	Table 15
fl_2%.o	609,448	2/6/2001	12:38p	Table 15
fl_2%a.o	607,385	1/30/2001	12:55a	Table 15
fl_3%.o	607,380	1/30/2001	10:49a	Table 15
fl_3%a.o	607,385	1/30/2001	01:07p	Table 15
fl_3%rf.o	607,880	7/25/2001	02:56p	Table 15
fl_4%.o	607,120	1/30/2001	03:27p	Table 15
fl_4%a.o	607,262	2/5/2001	06:08p	Table 15
fl_5%.o	607,269	1/30/2001	08:00p	Table 15
fl_5%a.o	607,479	2/5/2001	09:29p	Table 15
fl_5%arf.o	607,913	7/25/2001	08:02p	Table 15
hlf_10%+w.o	621,337	1/31/2001	02:40p	Table 15
hlf_10%.o	620,064	1/31/2001	12:30p	Table 15
thq+10%+w.o	623,783	1/31/2001	02:17a	Table 15
thq+10%.o	621,932	1/30/2001	10:00p	Table 15

File Name /Directory Name	Size (bytes)	Date of Last Access	Time of Last Access	Table Used
Directory of d:\outputs\Table_16				
bd.1+w.1.o	610,147	3/15/2001	05:37p	Table 16
bd.1+w.2.o	610,031	3/15/2001	10:29p	Table 16
bd.1+w.3.o	610,248	3/16/2001	03:24a	Table 16
bd.1+w.4.o	610,031	3/16/2001	08:15a	Table 16
bd.1+w.4rf.o	604,402	7/30/2001	08:49a	Table 16
bd.1.o	609,309	3/14/2001	05:01p	Table 16
bd.15+w.1.o	610,033	3/19/2001	02:02p	Table 16
bd.15+w.2.o	608,989	3/19/2001	06:57p	Table 16
bd.15+w.24.o	610,035	3/20/2001	01:59p	Table 16
bd.15+w.24p.o	602,189	3/21/2001	04:55p	Table 16
bd.15.o	609,236	3/14/2001	09:56p	Table 16
bd.15rf.o	604,280	7/30/2001	08:49a	Table 16
bd.197.o	610,246	3/15/2001	02:12p	Table 16
bd.2.o	610,455	3/14/2001	06:13p	Table 16
bdq.o	610,145	3/14/2001	02:18p	Table 16
bdqp.o	601,995	3/23/2001	04:05p	Table 16
Directory of d:\outputs\Table_17				
alt.1+w.4h+g.02.o	584,961	5/16/2001	08:40p	Table 17
alt.1+w.4h+g.04.o	584,961	5/17/2001	01:41a	Table 17
alt.1+w.4h+g.1.o	577,278	5/17/2001	06:46a	Table 17
alt.1+w.4h+g.2.o	576,103	5/17/2001	11:50a	Table 17
alt.1+w.4h.o	584,815	3/20/2001	07:03p	Table 17
alt.1+w.4hrf.o	578,969	7/30/2001	08:43a	Table 17
alt.15+w.24h.o	581,551	3/20/2001	03:33p	Table 17
alt.197.o	599,606	3/20/2001	04:31p	Table 17
alt.197h.o	583,760	3/20/2001	04:01p	Table 17
alt.25+w.2h.o	581,575	3/20/2001	05:12p	Table 17
alt.25h.o	581,683	3/20/2001	07:38p	Table 17
alt.5.o	600,112	3/20/2001	11:47p	Table 17
alt.5h.o	585,558	5/8/2001	09:05p	Table 17
Directory of d:\outputs\Table_18				
tlt1a.o	613,900	5/10/2001	12:14p	Table 18
tlt1a_.2.o	616,021	5/10/2001	04:12p	Table 18
tlt1a_.3.o	615,905	5/10/2001	08:21p	Table 18
tlt1a_.4.o	616,021	5/11/2001	12:28a	Table 18
tlt1a_.4rf.o	616,474	7/26/2001	05:27a	Table 18
tlt1a_.5.o	615,905	5/11/2001	04:38a	Table 18
tlt1a_.6.o	615,905	5/11/2001	08:45a	Table 18
tlt1b_.2.o	625,593	5/10/2001	09:06p	Table 18
tlt1b_.4.o	624,555	5/14/2001	12:50p	Table 18
tlt1sh_.4.o	640,715	9/21/2001	03:34p	Table 18
tlt2a.o	611,739	5/14/2001	11:34a	Table 18
tlt2a_.4.o	613,688	5/14/2001	02:39p	Table 18
tlt2b_.4.o	618,819	5/14/2001	12:41p	Table 18
tlt2sh_.4.o	619,365	5/14/2001	01:51p	Table 18
Directory of d:\outputs\Table_19				
hlfa.o	617,148	1/29/2001	09:40p	Table 19
hlfb.o	618,070	1/29/2001	08:30p	Table 19
hxa.o	624,078	1/30/2001	07:01a	Table 19
hxb.o	624,179	1/30/2001	12:16p	Table 19
Npsa.o	609,265	3/12/2001	09:30p	Table 19
Npsarf.o	604,035	7/30/2001	08:30a	Table 19

File Name /Directory Name	Size (bytes)	Date of Last Access	Time of Last Access	Table Used
qrta.o	621,022	1/30/2001	05:25p	Table 19
qrtb.o	620,883	1/30/2001	10:33p	Table 19
Directory of d:\outputs\Table_20				
p1.50a+.5.o	706,482	2/8/2001	04:54a	Table 20
p1.50a.o	703,487	1/29/2001	05:53p	Table 20
p1.75+.3.o	704,860	1/30/2001	02:23a	Table 20
p1.75+.4.o	705,796	1/30/2001	11:39a	Table 20
p1.75+.5.o	705,294	1/30/2001	09:17p	Table 20
p2.00a+.1.o	709,681	1/31/2001	10:46a	Table 20
p2.00a+.2.o	710,448	1/31/2001	06:20p	Table 20
p2.00a+.4.o	712,563	2/5/2001	11:02p	Table 20
p2.00a+.5.o	711,321	2/1/2001	01:26p	Table 20
p2.00a.o	709,051	1/31/2001	03:48a	Table 20
p2.00b+.1.o	742,311	2/2/2001	02:40a	Table 20
p2.00b+.2.o	709,775	2/2/2001	09:59a	Table 20
p2.00b+.4.o	712,173	2/2/2001	06:54p	Table 20
p2.00b+.5.o	711,005	2/3/2001	04:23a	Table 20
p2.00b.o	709,768	2/6/2001	06:03a	Table 20
p2l_.05.o	718,811	1/30/2001	06:09p	Table 20
p2l_.1.o	718,708	1/30/2001	10:56p	Table 20
pact+.2.o	710,857	2/8/2001	04:30p	Table 20
pact+.4.o	711,909	2/3/2001	01:28p	Table 20
pact+.4rf.o	709,601	7/27/2001	05:14a	Table 20
pact+.5.o	710,186	2/3/2001	10:59p	Table 20
pacta+.5.o	729,694	2/7/2001	05:02p	Table 20
tcha+.2.o	711,538	2/2/2001	11:12p	Table 20
tcha+.4.o	713,124	2/6/2001	04:40a	Table 20
tcha+.5.o	713,396	2/3/2001	10:45a	Table 20
tcha+1.o	713,016	2/3/2001	10:49p	Table 20
tcha.o	709,976	2/1/2001	09:03p	Table 20
tchb.o	709,913	2/2/2001	05:29a	Table 20
tchc.o	710,101	2/2/2001	01:46p	Table 20
tla_.05.o	718,486	1/29/2001	03:12p	Table 20
tla_.1.o	718,484	1/29/2001	07:38p	Table 20
tla_0a.o	718,383	1/30/2001	04:25a	Table 20
Directory of d:\outputs\Table_21				
c_f.3.o	499,534	1/29/2001	07:56p	Table 21
c_f.4.o	499,827	2/5/2001	07:53p	Table 21
f.176.o	498,610	1/30/2001	06:59a	Table 21
f.2_c.o	497,816	2/5/2001	10:32p	Table 21
f.2_w.o	499,519	2/5/2001	10:08p	Table 21
f.3_c.4.o	499,633	1/30/2001	10:25p	Table 21
f.3_c.6.o	499,850	1/31/2001	12:47a	Table 21
f.3_c.8.o	499,749	1/31/2001	03:11a	Table 21
f.3_c.o	499,536	1/30/2001	07:59p	Table 21
f.3_w.o	498,896	1/31/2001	05:42a	Table 21
f.4_c.4.o	500,415	2/6/2001	12:49p	Table 21
f.4_c.6.o	500,299	2/6/2001	03:25p	Table 21
f.4_c.8.o	501,011	2/6/2001	05:56p	Table 21
f.4_c.o	499,827	2/5/2001	11:53p	Table 21
f.4_w.o	499,401	1/31/2001	03:56p	Table 21
f.6_c.o	500,376	2/6/2001	01:12a	Table 21
f.6_ca.o	499,711	2/6/2001	02:32a	Table 21
f.6_crf.o	497,480	7/27/2001	04:04p	Table 21

File Name /Directory Name	Size (bytes)	Date of Last Access	Time of Last Access	Table Used
f.6_w.o	499,415	2/1/2001	12:08a	Table 21
f.8_w.o	498,966	2/27/2001	05:06p	Table 21
f_w.o	499,922	2/1/2001	06:24a	Table 21
Directory of d:\outputs\Table_22				
f+c+w.2_w.o	498,799	1/29/2001	10:35p	Table 22
f+c+w.4061.o	497,180	1/30/2001	01:22a	Table 22
f+c_w.o	498,737	1/30/2001	03:55a	Table 22
f.3+c.1_c.4.o	499,757	1/31/2001	09:37p	Table 22
f.3+c.1_c.6.o	499,857	1/31/2001	11:59p	Table 22
f.3+c.1_c.8.o	499,857	2/1/2001	02:22a	Table 22
f.3+c.1_c.o	500,916	1/31/2001	07:14p	Table 22
f.3+c.2_c.4.o	499,857	2/1/2001	07:04a	Table 22
f.3+c.2_c.6.o	499,741	2/1/2001	09:34a	Table 22
f.3+c.2_c.8.o	499,842	2/1/2001	12:20p	Table 22
f.3+c.2_c.o	500,704	2/1/2001	04:41a	Table 22
f.3+c.4_c.4.o	499,857	2/1/2001	07:44p	Table 22
f.3+c.4_c.6.o	501,020	2/1/2001	11:31p	Table 22
f.3+c.4_c.8.o	500,904	2/2/2001	03:16a	Table 22
f.3+c.4_c.o	500,799	2/1/2001	03:53p	Table 22
f.4+c.1_c.4.o	500,110	2/6/2001	06:33p	Table 22
f.4+c.1_c.6.o	499,798	2/6/2001	10:00p	Table 22
f.4+c.1_c.8.o	500,706	2/7/2001	01:29a	Table 22
f.4+c.1_c.o	500,702	2/6/2001	02:59p	Table 22
f.4+c.2_c.4.o	499,684	2/6/2001	03:40p	Table 22
f.4+c.2_c.6.o	499,996	2/6/2001	06:03p	Table 22
f.4+c.2_c.8.o	499,764	2/6/2001	05:40p	Table 22
f.4+c.2_c.o	499,760	2/6/2001	02:53p	Table 22
f.4+c.4_c.4.o	499,583	2/6/2001	08:21p	Table 22
f.4+c.4_c.6.o	499,714	2/7/2001	09:37a	Table 22
f.4+c.4_c.8.o	499,648	2/6/2001	11:07p	Table 22
f.4+c.4_c.o	499,659	2/6/2001	08:32p	Table 22
f.4+c.5_c.o	501,521	2/7/2001	01:59p	Table 22
f.6+c.1_c.o	500,914	7/26/2001	07:52p	Table 22
f.6+c.2_c.o	500,486	7/26/2001	10:19p	Table 22
f.6+c.4_c.o	500,914	7/27/2001	01:04a	Table 22
fcw.2_wrf.o	494,798	7/30/2001	09:00a	Table 22
Directory of d:\outputs\Table_23				
a.1w.4pc.o	516,953	6/25/2001	01:52p	Table 23
bd.1w.4pc.o	539,780	6/25/2001	11:13a	Table 23
cs1_c+.714.o	538,148	2/8/2001	11:01a	Table 23
cs1_c+.8.o	538,174	2/8/2001	01:14p	Table 23
cs1_c+.9.o	537,751	2/8/2001	03:27p	Table 23
cs1_cal.o	512,342	8/30/2001	09:34a	Table 23
cs1_prba.o	541,177	2/7/2001	09:04p	Table 23
cs1_prbb.o	541,224	2/8/2001	02:01a	Table 23
cs1_prbc.o	541,177	2/8/2001	06:52a	Table 23
cs1_prbcrf.o	537,338	7/27/2001	10:50a	Table 23
cs1_prbd.o	541,115	2/8/2001	11:51a	Table 23
cs1_prbe.o	539,996	2/8/2001	04:49p	Table 23
cs1_prberf.o	537,203	7/27/2001	10:50a	Table 23
cs1_prbetf.o	540,601	7/27/2001	03:52p	Table 23
f.3c.4cpc.o	434,572	6/25/2001	11:30a	Table 23
f.4c.5cpc.o	432,441	6/25/2001	09:57a	Table 23
f.6_cpc.o	434,088	6/25/2001	10:55a	Table 23

File Name /Directory Name	Size (bytes)	Date of Last Access	Time of Last Access	Table Used
f.6c.2cltf.o	437,115	7/30/2001	09:08a	Table 23
f.6c.4cltf.o	436,211	7/31/2001	08:19a	Table 23
fl_2%pc.o	550,413	6/25/2001	12:33p	Table 23
fl_3%pc.o	543,132	6/22/2001	11:40p	Table 23
Npsapc.o	543,448	6/22/2001	11:01p	Table 23
pa.5pc.o	644,704	6/23/2001	10:37a	Table 23
paa.5pc.o	643,279	6/24/2001	03:00a	Table 23
t1a_.4pbc.o	556,310	5/15/2001	11:39a	Table 23
t2b_.4pbc.o	564,296	5/15/2001	02:01p	Table 23
Directory of d:\outputs\Table_24				
cyl.6_clc.o	519,575	2/12/2001	08:50p	Table 24
cyl.9_clc-w.6.o	529,290	2/13/2001	06:03p	Table 24
cyl.9_clc-w.8.o	529,454	2/13/2001	08:23p	Table 24
cyl.9_clc-w.9.o	529,386	2/13/2001	10:46p	Table 24
cyl.9_clc-w0.o	529,031	2/14/2001	01:13a	Table 24
cyl.9_clc.o	519,623	2/13/2001	01:28a	Table 24
cyl.9_clerf.o	516,005	7/31/2001	08:32a	Table 24
cyl_clc.o	518,387	2/10/2001	06:18a	Table 24
hex.6_clc.o	522,162	2/13/2001	07:14a	Table 24
hex.9_clc.o	522,225	2/13/2001	01:09p	Table 24
hex_clc.o	521,916	2/12/2001	11:59p	Table 24
in_cl.714c.o	519,650	2/9/2001	06:49p	Table 24
in_cl.8c.o	519,621	2/10/2001	04:34a	Table 24
in_cl.9c.o	519,390	2/10/2001	09:17a	Table 24
in_cla.o	517,579	2/8/2001	04:18p	Table 24
in_clc-w.8.o	548,518	2/9/2001	08:03p	Table 24
in_clc-w.9.o	547,805	2/10/2001	01:50a	Table 24
in_clc-w.o	543,940	2/8/2001	08:10p	Table 24
in_clc.o	517,675	2/8/2001	06:42p	Table 24
in_cle.o	517,266	2/8/2001	08:59p	Table 24
in_clerf.o	519,314	7/31/2001	08:32a	Table 24
Directory of d:\outputs\Table_25				
p.5ag+C.4_cl.o	638,411	2/27/2001	12:41a	Table 25
p0acl.05+g+C.4_cl.o	655,055	2/20/2001	09:54p	Table 25
p0acl.1+g+C.4_cl.o	663,976	2/21/2001	09:10a	Table 25
p0ag+C.4_cl.o	640,188	2/19/2001	07:21p	Table 25
p0ag+C.6_cl.o	639,182	2/19/2001	10:50p	Table 25
p0ag+C.8_cl.o	638,558	2/20/2001	01:53a	Table 25
p0ag+C_cl.o	638,242	2/20/2001	04:42a	Table 25
p0ag.4_C.4_cl.74.o	646,440	2/20/2001	03:10a	Table 25
p0ag.4_C.4_cl.o	646,060	2/19/2001	08:15p	Table 25
p0ag.4_C_cl.o	644,996	2/15/2001	08:41p	Table 25
p0ag.6_C_cl.o	644,704	2/16/2001	02:05a	Table 25
p0ag.8_C_cl.o	732,963	2/20/2001	03:19p	Table 25
p0ag_C.4_cl.o	647,259	2/15/2001	10:22p	Table 25
p0ag_C.6_cl.o	645,448	2/16/2001	04:35a	Table 25
p0ag_C.8_cl.o	645,121	2/16/2001	10:29a	Table 25
p0ag_C_cl.714.o	643,500	2/15/2001	11:44p	Table 25
p0ag_C_cl.8.o	643,184	2/16/2001	04:06a	Table 25
p0ag_C_cl.o	643,281	2/15/2001	07:17p	Table 25
ptag+C.4_cl.o	644,953	2/27/2001	09:37a	Table 25
Directory of d:\outputs\Table_26				
cC.6+g.05_g_clrf.o	635,661	7/30/2001	09:35a	Table 26

File Name /Directory Name	Size (bytes)	Date of Last Access	Time of Last Access	Table Used
cy.25cC.6_g_cl.o	642,338	2/27/2001	12:39a	Table 26
cy.5cC.6_g_cl.o	642,356	2/22/2001	08:49p	Table 26
cy.75cC.6_g_cl.o	642,241	2/23/2001	06:46a	Table 26
cy0aC_g_cl.o	638,306	2/19/2001	06:44p	Table 26
cy0aC_g_clrf.o	636,381	7/30/2001	09:35a	Table 26
cy0cC+g.2_cl.o	647,637	3/6/2001	05:07a	Table 26
cy0cC+g.2_clp.o	647,641	3/6/2001	05:12a	Table 26
cy0cC+g.3_cl.o	646,771	3/6/2001	08:09p	Table 26
cy0cC+g.4_cl.o	641,604	3/2/2001	12:23a	Table 26
cy0cC+g.6_cl.o	639,488	3/2/2001	08:57a	Table 26
cy0cC+g.8_cl.o	637,895	3/2/2001	04:30p	Table 26
cy0cC.4_g_cl.o	642,646	2/20/2001	03:49a	Table 26
cy0cC.6+g.05_g_cl.o	642,906	3/1/2001	11:18p	Table 26
cy0cC.6+g.1_g_cl.o	642,788	3/2/2001	09:34a	Table 26
cy0cC.6_g_cl.o	639,906	2/20/2001	01:55p	Table 26
cy0cC.8_g_cl.o	638,102	2/20/2001	11:08p	Table 26
cy0cC_g_cl.o	638,502	2/20/2001	01:33a	Table 26
cy0eC_g_cl.o	631,458	2/20/2001	08:20a	Table 26
cytcC.4_g_cl.o	646,776	2/22/2001	11:04p	Table 26
cytcC.6_g_cl.o	640,560	2/27/2001	01:04a	Table 26
cytcC.8_g_cl.o	643,169	2/27/2001	09:31a	Table 26
cytcC0_g_cl.o	648,200	2/23/2001	12:54p	Table 26
cytcC0p_g_cl.o	638,029	2/23/2001	07:19p	Table 26
cytcC0pm_g_cl.o	637,021	2/27/2001	02:54p	Table 26
cytcC_g_cl.o	641,555	2/26/2001	08:28p	Table 26
hexc.4_g_cl.o	522,936	3/8/2001	09:31p	Table 26
hexc.5_g_cl.o	510,287	3/9/2001	03:45p	Table 26
hexc.6_g_cl.o	507,202	3/8/2001	07:24p	Table 26
hexc.7_g_cl.o	510,095	3/9/2001	08:30p	Table 26
hexc_g_cl.o	509,351	3/8/2001	09:12p	Table 26
hx.6_g_clrf.o	507,145	7/31/2001	08:49a	Table 26
hx.6_g_cltf.o	509,569	7/30/2001	12:50p	Table 26
Directory of d:\outputs\Table_27				
f+C+g.05+.4_g_cl.o	425,362	3/1/2001	10:13a	Table 27
f+C+g.1+.4_g_cl.o	424,398	3/1/2001	11:47a	Table 27
f+C+g.4_cl.o	426,784	3/1/2001	12:13p	Table 27
f+C+g.6_cl.o	425,976	3/1/2001	03:23p	Table 27
f+C+g.7_cl.o	425,664	3/1/2001	06:22p	Table 27
f+C+g.8_cl.o	424,219	3/1/2001	09:17p	Table 27
f+C+g.9_cl.o	425,563	3/2/2001	12:13a	Table 27
f+C+g_cl.o	424,812	3/2/2001	03:20a	Table 27
f+C.4_g_cl.o	427,600	2/28/2001	04:00p	Table 27
f+C.6_g_cl.o	426,732	2/28/2001	06:59p	Table 27
f+C.8_g_cl.o	426,420	2/28/2001	09:42p	Table 27
f+C_g_cl.o	426,679	3/1/2001	12:37a	Table 27
f.2_C_g_cl.o	426,091	2/27/2001	05:46p	Table 27
f.4+C.2_C_g_cl.o	427,254	2/27/2001	08:05p	Table 27
f.4+C.4_C_g_cl.o	427,206	2/27/2001	10:13p	Table 27
f.4_C_g_cl.o	427,340	2/27/2001	08:21p	Table 27
f.5_C_g_cl.o	427,557	2/27/2001	10:53p	Table 27
f.6_C_g_cl.o	427,557	2/28/2001	01:25a	Table 27
f.8_C_g_cl.o	427,746	2/28/2001	04:05a	Table 27
f_C_g_cl.o	428,147	2/28/2001	06:46a	Table 27
g_f.4_C_cl.o	433,438	3/1/2001	11:40a	Table 27

File Name /Directory Name	Size (bytes)	Date of Last Access	Time of Last Access	Table Used
Directory of d:\outputs\Table_28				
f.1+c.1_psta.o	433,622	7/5/2001	10:36p	Table 28
f.1+c.2_psta.o	431,775	7/6/2001	05:37a	Table 28
f.1+c.4_psta.o	430,120	7/6/2001	05:27a	Table 28
f.1+c.6_psta.o	429,259	7/6/2001	01:32a	Table 28
f.15+c.05_psta.o	431,067	7/5/2001	10:13p	Table 28
f.2_pst.45a.o	424,690	7/5/2001	11:29a	Table 28
f.2_pst.6a.o	425,936	7/5/2001	12:37p	Table 28
f.2_pst.8a.o	425,475	7/5/2001	03:29p	Table 28
f.2_psta.o	426,030	7/3/2001	07:52p	Table 28
f.2_pstarf.o	422,909	7/6/2001	01:06p	Table 28
f.2_pstatf.o	428,665	7/23/2001	05:15p	Table 28
f.4_psta.o	423,915	7/3/2001	05:35p	Table 28
f.6_psta.o	423,698	7/3/2001	06:59p	Table 28
f.8_psta.o	423,893	7/3/2001	08:28p	Table 28
f_psta.o	424,391	7/3/2001	10:05p	Table 28
Directory of d:\outputs\Table_29				
pst.44c.o	418,923	7/9/2001	08:47p	Table 29
pst.55b.o	416,516	7/6/2001	06:01p	Table 29
pst.6b.o	414,380	7/6/2001	10:17p	Table 29
pst.6c.o	414,281	7/9/2001	04:27p	Table 29
pst.8b.o	415,143	7/7/2001	01:52a	Table 29
pst.8c.o	412,265	7/9/2001	06:28p	Table 29
pst.9b.o	413,719	7/7/2001	05:31a	Table 29
pst.9c.o	413,657	7/9/2001	08:26p	Table 29
pstb.o	413,868	7/7/2001	10:21a	Table 29
pstc.o	412,414	7/9/2001	10:31p	Table 29